The role of p17 protein in development of HIV associated neurocognitive disorder

Y Zeinolabediny

PhD   2016

The role of p17 protein in development of HIV associated neurocognitive disorder

Yasmin Zeinolabediny

A Thesis submitted in partial fulfilment of the

requirements of the Manchester Metropolitan University

for the degree of Doctor of Philosophy

School of Healthcare Sciences

Manchester Metropolitan University

June 2016

Contents

List of figures

List of tables

Abstract

HIV-associated neurocognitive disorder in HIV patients substantially reduces their quality of life. We hypothesised that the HIV matrix protein, p17, already linked to tumour promotion and aberrant angiogenesis could contribute to neurological decline and cellular dysfunction within the brain and aimed here to confirm this. The experimental design was formulated to test the direct neurodegenerative capacity of p17 protein on relevant brain cells, both *in vitro* and *in vivo* to ascertain the potential of p17 within the brain to encourage neurodegenerative processes and to confirm that p17 was present in the brain of infected individuals.

In vitro cell culture experiments identified cellular signalling induced by p17 within brain cells. I characterised the effects of hippocampal CA1 injection of p17 on histological appearance of brain sections following the analysis of the animals by our collaborators- behaviour, cognitive function and memory. Histological expression of p17 in tissue from three HIV patients who died from stroke was determined. Cell signalling pathways potentially associated with neurodegenerative signalling or aberrant angiogenesis were studied by Western blotting.

p17 increased phosphorylation of ERK1/2, IRS-1 and EGFR in endothelial cells, blocking cell signalling and angiogenesis via an inhibitor peptide of EGFR. In neurons, p17 induced the phosphorylation of ERK1/2, Tau, FAK and IRS-1. Cognitive function and behavioural deficiencies after p17 injection were mimicked by demonstration that it localised in ventricular tracts, cortical microvessels and neurons. p17 formed β-amyloid/prion-like protein fibrillar aggregates, suggesting a pathogenic direct capability similar to that of β-amyloid. P17 was also identified in macrophages, microvessels, neurons and amyloid-beta (Aβ)-positive plaques in HIV-infected human brain sections. This work supports the involvement of p17 in initiating/perpetuating neurodegenerative pathophysiology associated with cognitive decline.

Key words: P17, HIV-associated neurocognitive decline, angiogenesis, fibrillary, signalling.

Declaration

I hereby declare that this work has been composed by myself, and has not been accepted for any degree before and is not currently being submitted in candidature for any degree other than the degree of Doctor of Philosophy of the Manchester Metropolitan University.

Yasmin Zeinolabediny

Acknowledgment

No project such this can be carried out by only one individual. This thesis appears in its current form due to the assistance and guidance of several people. I would therefore like to offer my sincere thanks to all of them. I would like to express my sincere appreciation and gratitude to director of studies Prof. Jurek Krupinski for the continuous support of my PhD study and research, for his patience, motivation, enthusiasm, constructive criticism, and immense knowledge. I fell highly privileged to express my heartiest gratitude to the worthy and kind supervisor, Prof. Mark Slevin for his kindness and guidance which helped me throughout my research and writing of this thesis. I would like to express my deep gratitude and respect to Mr. Glenn Ferris an excellent technical officer who helped me learn several laboratory techniques including; fluorescence microscopy, immunohistochemistry and providing quotes for ordering laboratory materials. His outstanding attitude and vast knowledge helped me to carry on my laboratory work. Dr. Ria Weston helped me with Western blotting and histology work, her advices were of a great assistance to me. Thanks to Dr. Donghui Lui for his support through three years of laboratory work.

Words cannot describe how much I appreciate the support I received from my family throughout this journey. Indeed, it has been difficult all these years away from home, but my family's support, has kept me going until the end, especially the encouragement which gave me strengths to never give up.

I would like to thank my colleagues at the School of Healthcare Science who shared great research ideas during my study at Manchester Metropolitan University. Finally, in my daily work I have been blessed with a friendly and cheerful group of fellow students. Kamela Ali, who helped in western blotting and wound healing assay. Stuart Fielding, who provided good arguments about western blotting techniques, buffers preparations and cell culture, Ali Shukur

Published/ submitted works:

- **Monomeric C-reactive protein--a key molecule driving development of Alzheimer's disease associated with brain ischaemia?**
  Slevin M, Matou S, Zeinolabediny Y, Corpas R, Weston R, Liu D, Boras E, Di Napoli M, Petcu E, Sarroca S, Popa-Wagner A, Love S, Font MA, Potempa LA, Al-Baradie R, Sanfeliu C, Revilla S, Badimon L, Krupinski J.
  Sci Rep. 2015 Sep 3;5:13281. doi: 10.1038/srep13281

- **The amyloid-prone HIV-1 matrix protein p17 forms aggregates in human brain and induces neurocognitive disorders in mice**
  Yasmin Zeinolabediny, Francesca Caccuri, Ria Weston, Donghui Liu , Jerzy Krupinski, Laura Colombo, Mario Salmona, Ruben Corpas, Sara Sarroca, Coral Sanfeliu, Arnaldo Caruso, Mark Slevin
  Submitted to eLife.

- Proceedings of The Physiological Society
  Cellular Neurophysiology Abstracts

  Physiology 2014 (London, UK) (2014) Proc Physiol Soc 31, PCA080
  Poster Communications

  The role of p17 protein from HIV in early onset of neurodegenerative disease

  Y. Zeinolabediny1, J. Krupinski1, M. Slevin

List of Abbreviations

α-Syn	Alpha-Synuclein
Aβ	Amyloid-β
Akt	protein kinase B
APP	Amyloid Precursor Protein
AP-1	Activator protein 1
AIDS	Acquired Immune Deficiency Syndrome
AD	Alzheimer's disease
ANI	Asymptomatic Neurocognitive Impairment
APS	Ammonium persulfate
BBB	Blood-Brain Barrier
BSA	Bovine serum albumin
CAA	Cerebral amyloid angiopathy
CAM	Chick chorioallantoic membrane
CBF	Cerebral blood flow
CD	Cluster of differentiation
Cdc42	Cell division control protein 42 homolog
CO2	Carbon dioxide
CSF	Cerebrospinal fluid
CNS	Central nervous system
CXCR	CXC chemokine receptors
dH2O	Distilled H2O
DAPI	4',6-diamidino-2-phenylindole
DLB	Dementia with Lewy bodies#

DMSO	Dimethyl sulfoxide
DNA	Deoxyribonucleic acid
EBM-2	Endothelial cell basal medium-2
ECL	Enhanced chemiluminescence
ECM	Extracellular matrix
ECs	Endothelial cells
EDTA	Ethylenediaminetetraacetic acid
EGFR	Epidermal growth factor receptor
ERK 1/2	Extracellular signal–regulated kinases 1/2
FAK	Focal adhesion kinase
FGF-2	Fibroblast growth factor
Flk1	Fetal Liver Kinase 1
FTLD	Frontotemporal lobar dementia
GA-100	Gentamicin sulphate Amphotericin-B
HAND	HIV-associated neurocognitive decline
HAART	Highly active antiretroviral therapy
HCL	Hydrochloric acid
HCMEC/D3	Human Cerebro-vascular Microvessel endothelial cell line
HGF	Hepatocyte growth factor
HIF-1-alpha	Hypoxia-inducible factor 1-alpha
HIV	Human immunodeficiency virus
HRP	Horseradish peroxidase
HUVECs	Human umbilical vein endothelial cells
IGF-1	Insulin-like growth factor 1

IHC	Immunohistochemistry
IF	Immunofluorescence
IL-4	Interleukin 4
IgG	Immunoglobulin G
IMS	Industrial Methylated Spirit
IRS1	Insulin receptor substrate 1
LOAD	Late-onset AD
Mab	Monoclonal antibody
MEK	Mitogen-activated protein kinase kinase
mmol/L	Millimoles per Liter
MMP-1	Matrix metalloproteinase-1
MND	Mild neurocognitive disorder
MWM	Morris Water Maze
NCM	Nitrocellulose membranes
NO	Nitric oxide
NMDAR	N-methyl-D-aspartate glutamate receptor
NTg	Non-transgenic
p-	Phosphorylated
pAb	Polyclonal antibody
Pak	Protein activated kinase
PBS	Phosphate-buffered saline
PCR	Polymerase chain reaction
PDGF	Platelet-derived growth factor
PFA	Paraformaldehyde

PH	Power of Hydrogen
PI3K	Phosphatidylinositol-4,5-bisphosphate 3-kinase
PKC	Protein kinase C
PLC-ɣ	Phospholipase C-ɣ
R3 IGF-1	Recombinant long Receptor Insulin-like Growth Factor-1
Rac1	Ras-related C3 botulinum toxin substrate 1
RCN	Rat Cortical Neurons
rhEGF	Recombinant human Epidermal Growth Factor
rhVEGF	Recombinant human Vascular Endothelial Growth Factor
RIPA	Radioimmuno precipitation buffer
RNA	Ribonucleic acid
ROS	Reactive oxygen species
SDS	Sodium dodecyl sulfate
SMCs	Smooth muscle cells
SPM	Serum poor medium
TBST	TBS Tween
TEMED	N,N,N",N"- tetramethylethylenediamine
Tg	Transgenic
TIE	Tyrosine kinase with immunoglobulin and EGF-like domains
TNF	Tumour necrosis factor
TOR	Target of rapamycin
WHO	World Health Organisation
VaD	Vascular dementia
VEGF	Vascular endothelial growth factor

List of Units

%	Percentage
µg	microgram
µL	microliter
µm	micrometer
cm	centimetre
Da	Dalton
g	gram
h	hour
k	kilo
min	minute
ml	millilitre
mm	millimetre
mM	millimolar
°C	degree Celsius
RPM	revolutions per minute
Sec	second

Chapter 1

Introduction

Human Immunodeficiency Virus (HIV)

In the early 1980s, the first acknowledged cases of the acquired immune deficiency syndrome (AIDS), a condition in humans in which progressive failure of the immune system allows life-threatening opportunistic infections, were found in homosexual men in the United States of America. By 1983 the human immunodeficiency virus (HIV) had been identified. Over 7500 more people become infected with HIV every day world-wide. According to the World Health Organisation (WHO) the global summary of the AIDS epidemic in 2014 was, 36.9 million of people living with HIV, and 1.2 million AIDS-related deaths. The HIV pandemic has remained one of the most serious infectious disease challenges facing public health in past three decades. HIV is a lentivirus, which carries viral RNA into the DNA of the host cell; this feature enables the virus to infect cells that are not dividing. Infection with HIV arises by the transfer of blood, semen, vaginal fluid, pre-ejaculate, or breast milk. HIV can occur in the form of free virus particles or virus within infected immune cells within body fluid (Douek et al., 2009).

The virus exists as two copies of positive single-stranded RNA that code for the virus's nine genes enclosed by a conical capsid. The single-stranded RNA is bound to nucleocapsid proteins, p7, and additional enzymes required for development of the virion. These include reverse transcriptase, proteases, ribonuclease and integrase. A matrix composed of the viral protein p17 surrounds the capsid ensuring the integrity of the virion particle.
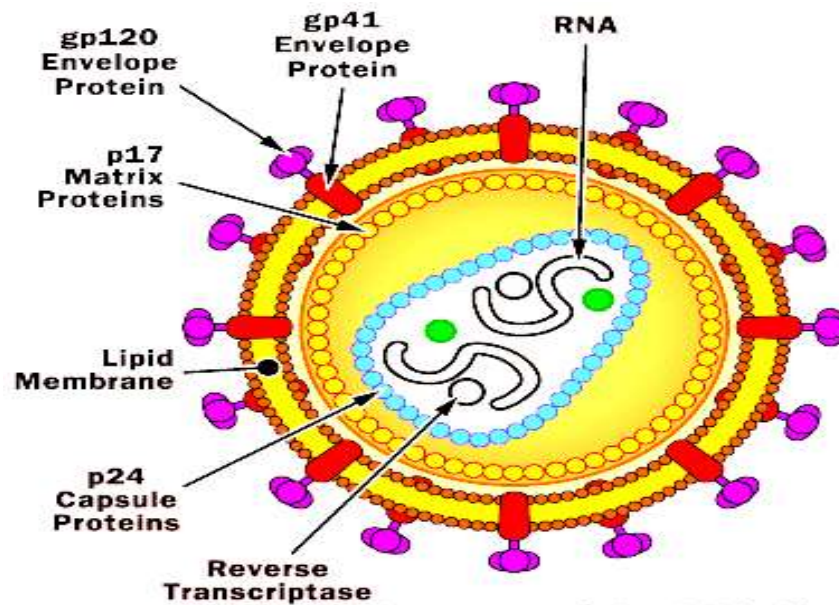
Figure 1. A diagram of the virus particle to show the internal structure and location of p17. (figure taken from (Bonsor and Curran, 2016)).

The late stages of viral assembly occur on the inner leaflet of the plasma membrane and virus is released by budding, thus obtaining a host-derived lipid envelope that is composed of two layers of fatty molecules called phospholipids. The possibility to inhibit the proliferation/integration of HIV-1 has brought great attention and hope, and with it opportunities for HIV-1 prevention and treatment. Primarily, the use of antiretroviral therapy has been reliably shown to prevent HIV-1 transmission over an extended period of time (Cohen et al., 2011).

The use of protease inhibitor drugs and combination therapies using nucleoside and non-nucleoside reverse transcriptase inhibitors in the treatment of HIV-infected patients via highly active antiretroviral therapy (HAART) procedures has resulted in almost complete inhibition of viral replication as well as CD4 (expressed on T lymphocytes that fight infection) cell repletion, and increased survival and decreased death rates (survivors into their 60-70 years).

Morbidity declined as a result, which is generally measured as the incidence of specific opportunistic infections, however, although clinical studies have in recent years investigated the effects of HAART in HIV infection they have not really addressed its influence on the quality of patient's life at the same time as medical variables (Brechtl et al., 2001).

Therefore, as patients with AIDS live longer because of HAART, the incidence of HIV related disorders in patients is increasing. As patients are known to develop drug-resistant mutations to antiretroviral drugs and with consequent decline in CD4 cell amounts, the incidence of HIV-associated neurological disease may also start to escalate soon (Sacktor, 2002).

Structure and function of p17 protein

The HIV-1 genome has nine genes. There are three coding regions - 5'-*gag-pol-env*-3' synthesized as a single precursor, and another six which act for accessory proteins connected with molecules linked to the pathogenesis of HIV-1 infection. The HIV-1 Gag protein is synthesized as a polyprotein precursor encoded by the HIV-1 *gag* gene. The HIV-1 protease cleaves the Gag precursor Pr55 (Pr55Gag) during virus budding (acquisition of a host-derived membrane vesicle) eventually forming into the mature proteins p17 matrix, p24 capsid, p7 nucleocapsid, p6 and two other 'spacer' peptides p1 and p2 (Bukrinskaya, 2007).

In the mature virus, p17 is a 132-amino acid polypeptide functioning as a protective shell and attached to the inner surface of the plasma membrane of the virus. The three-dimensional structure of p17 as determined by nuclear magnetic resonance and X-ray crystallography is shown in the Figure 2 below (Massiah et al., 1994). Individual p17 molecules are actually formed of five major α-helices and a basic platform of three beta strands.
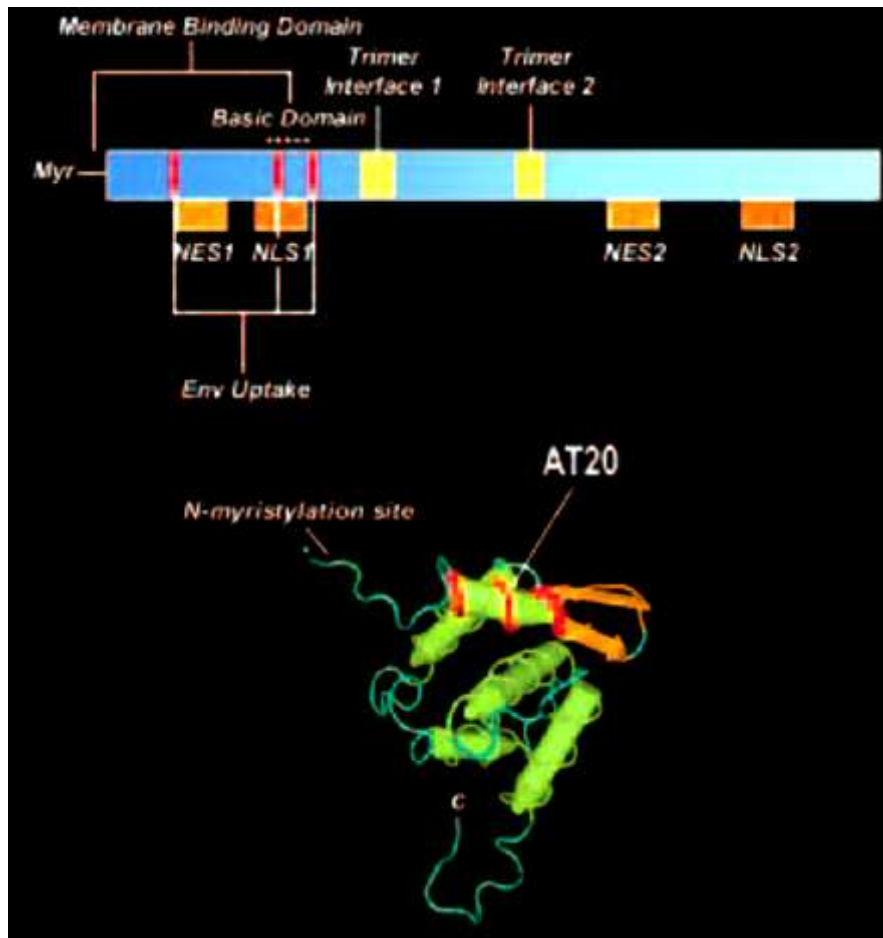
Figure 2. (A) Linear representation of the HIV-1 p17.Major functional domains are indicated. (B) Ribbon diagram of the matrix protein. The CXCR receptor binding region (AT20) is shown (Fiorentini et al., 2006).

Some of the major functions of p17 protein within the normal life cycle of HIV include:

- An important role in several steps of the virus replication, both in the early and late stages of the virus life cycle. During infection, p17, as part of Pr55Gag, directs unspliced viral RNA to the site of virus assembly. Here, a major function of the matrix protein is to direct binding to and assembly at the plasma membrane (Hermida-Matsumoto and Resh, 2000).

- Dong et al. showed that the amino-terminal α-helical segment of p17 interacts directly with the d subunit of the Adaptor Protein-3 complex (Dong et al., 2005). This is part of

a family of protein complexes that sort cargo proteins throughout membrane compartments of the secretory and endocytic pathways (Dong et al., 2005).

- P17 is essential for early post entry events of the virus life cycle. The ability of the virus to enter and replicate in non-dividing cells is critical to its survival and proliferation. The HIV proteins, p17, integrase and viral protein R, are probably the karyophilic agents that recruit the cellular nuclear import machinery to the viral pre-integration complex (PIC) (Bukrinsky, 2004).

- P17 has similar structure to IFN-ɣ, and it has been suggested it might act as a viral cytokine. Studies have shown that p17 binds to the p17-receptor (p17R) which is expressed on peripheral B cells but not on peripheral CD4+ and CD8+ T cells (De Francesco et al., 2002) suggesting this possibility.

- P17 favours HIV-1 replication *in vitro* by altering the cytokine production within the viral micro-environment. PBMCs infected with HIV- 1 and exposed in tissue culture to IL-2 and p17 release larger quantities of virus than other cells, at the same time inducing T lymphocytes activation and proliferation (De Francesco et al., 1998).

- P17 is found in large quantities in lymph nodes *in vivo* also suggesting it might exert biological activities (Popovic et al., 2005). P17 was retained in the tissue specimens during the 13 months of the study follow-up, also showing that it accumulated in the germinal centre light zone of lymph nodes of HAART treated patients in the absence of any – even in situ – HIV-1 replication.

Since one of the major issues for HIV patients is cognitive decline, or HIV-associated cognitive disorders (HAND), I decided to investigate the possible influence of the protein p17 on neurodegeneration and now follows a brief overview of the process and later a description of HIV-associated neurocognitive decline (HAND):

Overview of the pathophysiology of dementia

Dementia is a clinical diagnosis based on identification and interpretation of progressive cognitive decline. Approximately 1.3% of the UK population, and 7.1% of those aged 65 or over, have dementia (Cunningham et al., 2015). The clinical syndrome and features of dementia can be formed due to a variety of underlying and often mixed pathophysiological processes.

The most common form of dementia is Alzheimer's disease (AD; 50-75% of cases) then vascular dementia (VaD; 20% of cases), dementia with Lewy bodies (DLB; 5% of cases) and finally frontotemporal lobar dementia (FTLD; 5% of people) (Vieira et al., 2013). As stated before, the conditions are often mixed and difficult to decipher with clinical symptoms and pathophysiological processes overlapping significantly. There are no currently reliable biomarkers to aid diagnosis and prognosis although WHO drives are in process.

Cognitive impairment is a major consequence of dementia and for diagnostic purposes can be categorised into five areas those being: memory; executive function; language; visuospatial abilities; personality and behaviour (Budson and Solomon, 2012). As dementia, progresses, cognitive impairments become less specific and broader, involving multiple areas of the brain and increasing functional impairment. Latter stages are difficult to detail in type for this reason.

In the early stages key symptoms are critical in the identification and stratification of the most likely underlying disease process. Clinical criteria are closely linked to diagnosis of dementia

and symptom patterns are reviewed in keeping with specific types of dementias –on the presumption that cognitive impairments cannot be explained by a psychiatric illness or other cause (e.g. brain tumour etc.).

AD, the most common cause of dementia, appears with short-term memory deficits, e.g. appearing as repetitive questioning. Impairment in at least two cognitive domains is required for diagnosis of AD. Atypical presentations of AD are also possible and include behavioural/language deficits linked to frontal variants or even early visuospatial defects suggesting posterior cortical atrophy (Figure 3) (Warren et al., 2012). The most common feature of VaD is the temporal lobe-association of cognitive deficits with stroke (ischaemic or silent-lacunar) (Gottfries et al., 1994) and evidence of cerebrovascular disease on examination and PET/MRI imaging.
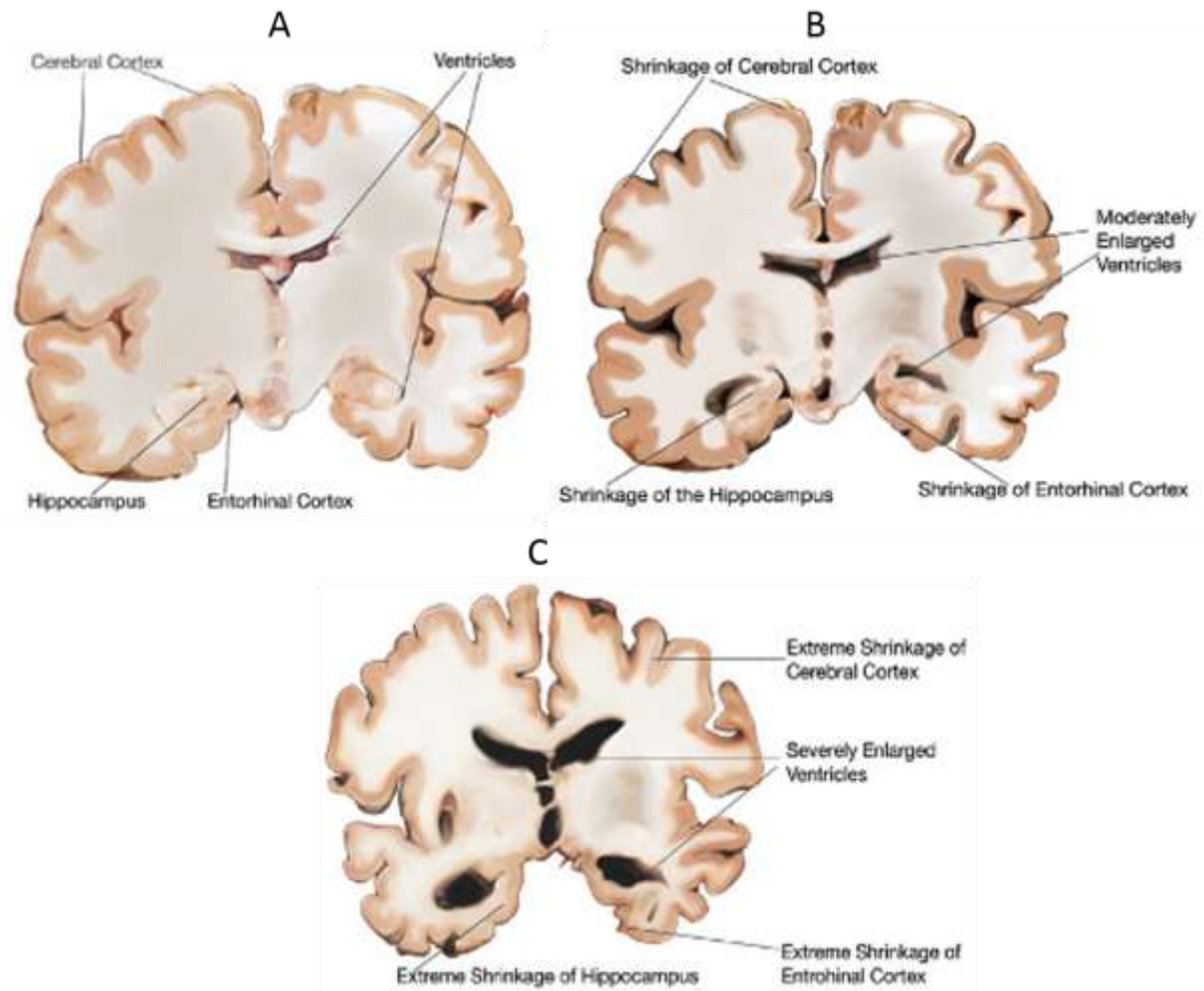
Figure 3. Images above show (A) Pre-clinical Alzheimer's Disease, (B) Mild Alzheimer's Disease and (C) Severe Alzheimer's disease (DEMENTIA-CARE-NOTES, 2016).

In AD, there is also evidence of dysfunctional and abnormal structure and function of cerebral blood vessels and other cells e.g. glia in the neurovascular unit. These effects may be perpetuated by vascular oxidative stress. Injury to the neurovascular unit alters cerebral blood flow and reduces vascular reserves, it can also disrupt the blood-brain barrier and reduce the brain's capacity to repair (Iadecola, 2004). For these reasons, brain injury such as this can further worsen cognitive dysfunction induced by stroke/ischemia and other coexisting neurodegeneration. Cardiovascular risk factors, genetic and other vascular abnormalities and brain endothelial damage in AD are described in detail by Kelleher and Soiza (2013).

All the dementia sub-types probably including VaD-involve abnormal accumulation of a native protein-for AD it is the plaques of amyloid forming within brain extra cellular matrix (ECM) and in addition, intracellular tangles of hyper-phosphorylated tau. Early onset AD, and late-onset AD (LOAD) are thought to be linked to abnormal clearance rates (slower) of amyloid from the brain (Tarasoff-Conway et al., 2015).

Biomarkers of disease particularly if sub-type specific, could improve our understanding of these disease processes and early identification of possible victims might allow better therapeutic or preventative treatment options in the future, prior to emergence of symptom. A biomarker should be measurable/quantifiable and associated strongly with the pathogenic process, or pharmacologic responses to a therapeutic intervention (Hu et al., 2010). So far, evidence of amyloid and tau accumulation measurements or neurodegeneration (e.g. markers of synapse/neuronal loss or atrophy) are the major options however, genetic and epigenetic markers may become available in the future (Wolfe, 2012).

Amyloid-β

During the 1980s-90s scientists found that amyloid-β protein was not only a pathological constituent but was also part of normal physiological cellular mechanisms of healthy people (van Norden et al., 2012). This 'amyloid hypothesis of AD was formulated and implies that the disease may be linked to abnormal cleavage of the amyloid precursor protein (APP) causing a long-term enhanced production and/or decreased clearance of soluble, diffusible amyloid-β. This may result in tissue 'precipitation' of aggregated and non-diffusible protein appearing as spherical plaques and vascular deposits in AD. Why this happens is not clear although factors involved may include genetic dominant mutations of the genes encoding APP and presenilin (Tanzi, 2012).

Tau protein

Tau is a microtubule-associated protein found mainly in neuronal axons, and key constituent of abnormal neurofibrillary tangles. Within the 'amyloid hypothesis' the imbalance between amyloid-β production and clearance may produce toxic concentrations of amyloid-β that are able to induce abnormal changes in tau causing tangle formation, although the mechanism for this is not yet determined (Prasansuklab and Tencomnao, 2013). Tau protein becomes hyper-phosphorylated and internally tangled in dementia and VaD.
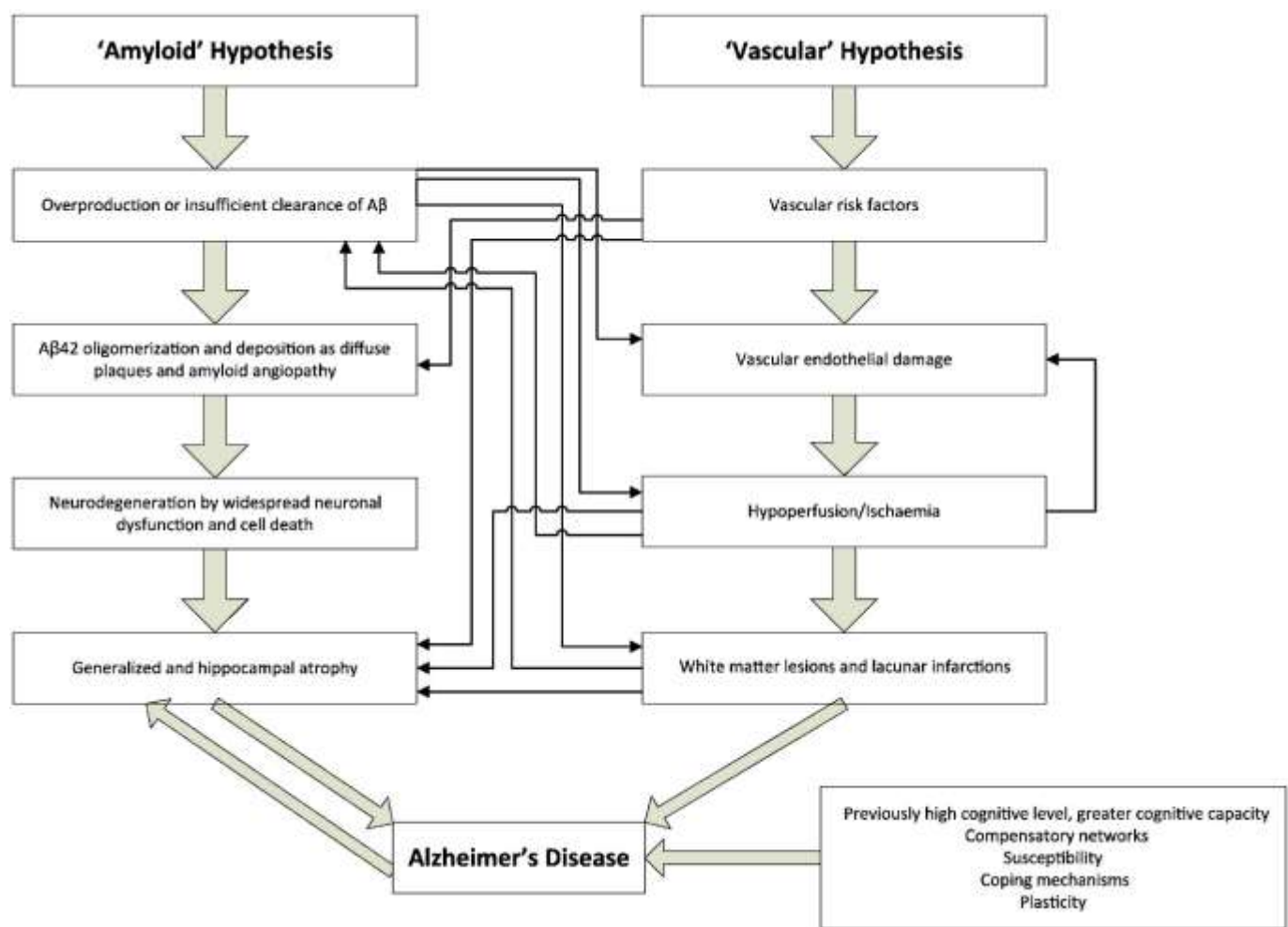
Figure 4. Above-Interaction between the amyloid hypothesis and the vascular hypothesis in the aetiology of Alzheimer's disease (van Norden et al., 2012).

Since we cannot directly follow the progress of dementia within the human brain we are currently reliant on the use of animal models to represent the developing stages of neurodegeneration-hence a description of the current models and their limitations is warranted here, one of which was used in this study.

Animal models of dementia

3xTg-AD mice

The ultimate diagnosis of AD has to come from post-mortem histological examination of tissues obtained to a certain neuropathological changes in the brain. Such analyses of clinical and pathological features, combined in correlation studies, have provided important information on how the pathology correlates with cognitive defects. There are of course what can be described loosely as preclinical model systems of AD pathology. The murine models, have been extremely useful to test mechanistic hypotheses linked to general AD pathophysiology and to predict outcomes from pharmacological interventions-albeit using generation of dementia-like symptoms and pathology over a period of months rather than years-decades as happens in humans. No animal model recapitulates in the entirety of AD in humans, with larger mammalian models e.g. canine, sheep and monkey being more closely related (but with ethical and cost issues), and so it is important to understand the limitations of particular animal models-and the reasons why translation of pre-clinical potential therapeutics normally fails in human clinical trials.

Some murine gene mutated models based around amyloid beta clearing and tau over-expression and hyper-activity are given here; (PDAPP, TG2576, APP23, TgCRND8, J20,

APP/PS1, TG2576 + PS1 (M146L), APP/PS1 KI, and 5×FAD) see Webster et al. (Webster et al., 2014) for details

One of the most commonly used model is the 3×Tg-AD mouse model, developed by Oddo et al. (Oddo et al., 2003). This 3xTg-AD mouse model has been genetically engineered at the University of California, Irvine to express the familial AD mutations PS1/M146V, APPswe and tauP301L (Revilla et al., 2014). These mice develop cognitive, motor and memory defects around 6 months of age and significant AD-like pathology as shown by histological and ICH analysis. Test materials can be implanted within the brain of rodents using stereotactic apparatus (see Figure 5 below).
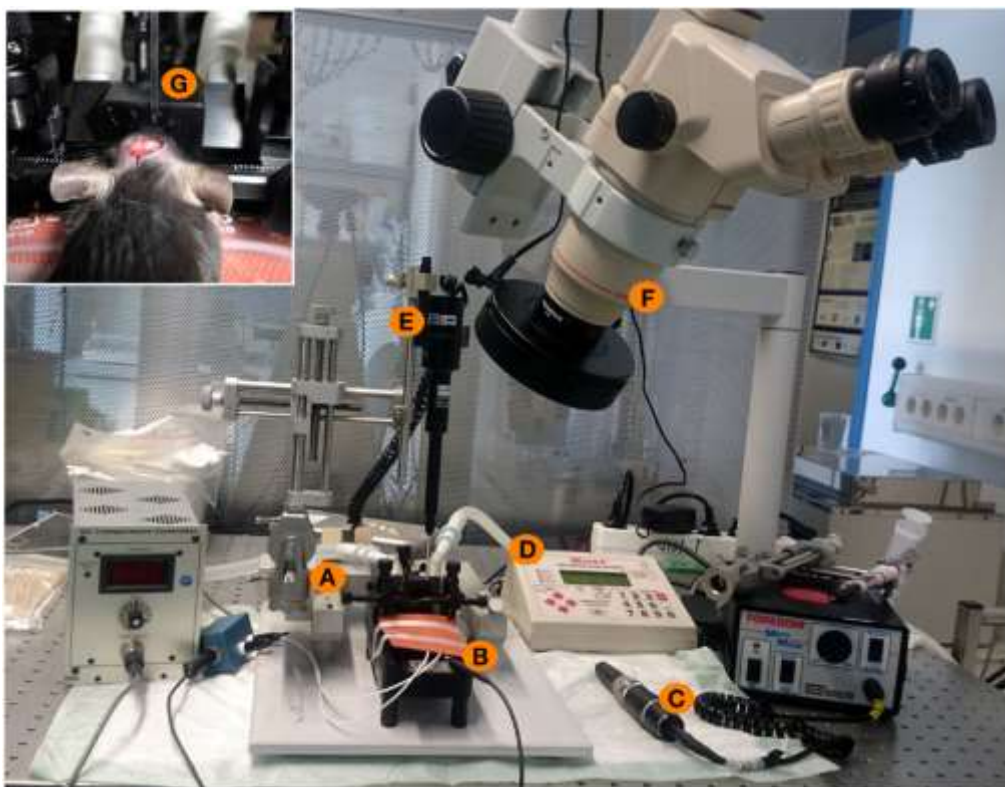
Figure 5. (A) Stereotactic frame with two arms (one fixing the injection pipette, one for fixation of a marker). (B) Heating pad to maintain the physiological temperature of 36°C of the mouse during surgery. (C) Drill head of 0.47 mm diameter. (D, E) Micro4-controller for injection of nL volumes with the injection pipette. (F) Binocular for optical control of experimental steps. (G) Inset shows the mouse skull during surgery. Intracranial holes have been drilled.

HIV-associated neurocognitive disorders

HIV-associated dementia (HAD), also recognized as the complex AIDS-Dementia, occurred at the start of the AIDS epidemic mostly in patients with advanced HIV disease and low CD4 cell counts (Baker et al., 2008). Patients with severe immune-depression, which has resulted in severe impairment of cognition, often accompanied by motor and behavioural changes, were the ones mostly affected. More recently, a further revised classification of HIV-associated neurocognitive disorders (HAND) was discovered. HAND, is divided into three sub-disorders also known as the Frascati criteria. Asymptomatic neurocognitive impairment (ANI) is recognised as occurrence of irregularity in two or more cognitive abilities (memory, attention, language, processing speed, sensory- perceptual, and motor skills) with no functional impairment but evidence of mild neurocognitive disorder; moderate neurocognitive decline (MND) which is defined as cognitive impairment with mild functional impairment, and HIV-associated dementia (HAD) is defined marked cognitive impairment involving at least two cognitive domains with No evidence of another previous cause for dementia (i.e. CNS infections or cerebrovascular disease), with marked functional impairment (Sanmarti et al., 2014).

It is difficult to evaluate the exact prevalence of HAND due to the large number of conditions covered by the definition of this disorder. Hence, understanding the incidence of HAND is established based on a relatively small number of basic and fundamental observational studies. The detailed pathogenesis of HAND is not known, however lately extensive research in this field has produced interesting data. It is believed the damage and death of neural cells in the brain is connected to the progression of neurocognitive impairment. It is also believed that secondary events following an HIV infection cause the damage which results in HAND. Initially, the virus enters the brain by monocytes and lymphocytes that cross the blood-brain barrier (BBB), next the monocytes infected with HIV change into perivascular macrophages

(Ivey et al., 2009). Because of HIV replication, activated macrophages and microglia express neurotoxic molecules, which are soluble immune mediators. Subsequent activation of astrocytes increase the BBB permeability and result in transfer of additional monocytes and lymphocytes (Elbirt et al., 2015).

There are two different explanations one direct and other indirect, used to describe the neurodegeneration and development of neurological symptoms in HAND. Implicit to both is that HIV primarily infects perivascular macrophages and other microglia within the brain (Spudich and Gonzalez-Scarano, 2012). The direct model then suggests that infected monocyte-derived cells release the viral proteins and that these can induce death of neuronal cells through direct interaction (i.e. gp 120, Tat and Vpr). The second, indirect model, explains that neuronal death is probably mediated via the inflammatory response against the virus and proteins it releases into the circulation (Lindl et al., 2010).

Macrophages and microglia activated because of HIV infection or exposure to viral particles secrete molecules including arachidonic acids, nitric oxide (NO), platelet activating factor, superoxide matrix metalloproteases, chemokines, growth factors, and pro-inflammatory cytokines including tumour necrosis factor (TNF). Some of these, e.g. brain-derived neurotrophic factor, have neuroprotective roles whilst others are neurotoxic (Elbirt et al., 2015).

Other material e.g. cytokines released during this process, including nitric oxide and TNF, impair the normally neuroprotective functions of astrocytes for example glutamate control and maintaining the blood brain barrier (BBB). In addition they can increase the rates of astrocytic/glial apoptosis (Heneka et al., 2015). The release of large quantities of excitatory amino acids e.g. glutamate and other N-methyl-D-aspartate glutamate receptor (NMDAR) agonists at the same time as a reduction in glutamate uptake –often seen in HIV infection, creates an environment that results in over- activation of NMDAR. Because of this, intra-

neuronal Ca^{2+} concentrations are high enough to become toxic and larger amounts of free radicals are produced, e.g. reactive oxygen species (ROS) and NO, eventually leading to neuronal death (Conant et al., 2004). Elevated systemic LPS levels and chronic immune cell activation in HIV can result in depletion of gut-associated lymphoid tissue following microbial translocation and in addition may have an impact on HAD. Similarly, individuals with HAD have higher levels of circulating and active CD14 and monocytes also expressing CD69, compared with none-HAD symptomatic individuals. Circulating raised levels of CD14 (sCD14) are also strongly linked with cognitive dysfunction in HIV infection (Ryan et al., 2001). All of this points to an important role for neuroinflammation – originating from systemic immune activation and/or inflammation and that this is strongly linked to onset or perpetuation of neurodegeneration observed in HAND.

Aberrant biological properties of p17

Since the HAART was introduced, HIV has changed significantly from an incurable disease to a chronic controllable disease. These days, the attention has been mostly on treating the acute complications of AIDS such as opportunistic infections, to managing enduring complications, including diseases of the cardiovascular, renal, osteological and central nervous systems, which could be a result of the long-lasting inflammatory response, the HIV infection itself, HAART-related adverse events, host genetics, socioeconomic factors, or the mixture of some of the above factors (Cockerham et al., 2010).

One of these factors which has been studied is p17, suggestions being that it could be the target of neutralizing antibodies against HIV-1 where high levels of p17 antibodies are correlated with slower progression to AIDS. The findings of a protective role of immunological response

against p17 and the presence of neutralizing epitopes on p17 are unusual and suggest an important role of p17 in perpetuating disease.

Immuno-electron microscopy and computer modelling studies of HIV-1 showed that p17 is located to the interior surface of the viral membrane, suggesting the possibility of activity of p17 during the budding process, external from the virus particle in supporting virus replication. HIV-1 matrix protein p17 increases the production of proinflammatory cytokines and counteracts IL-4 activity by binding to a cellular receptor (De Francesco et al., 2002).

AIDS-related lymphomas are usually high grade and aggressively metastatic with poor prognosis. Lymphangiogenesis is essential in supporting proliferation and survival of lymphoma, as well as tumour dissemination. Published work has shown that excessive lymphangiogenesis could be as a result of the action of HIV-1 proteins and not due to the direct viral efect. HIV-1 matrix protein p17 does accumulate and remain in lymph nodes of patients even when they are receiving HAART. Because p17 was recently found to exert a potent pro-angiogenic activity by interacting with chemokine (C-X-C motif) receptors 1 and 2, the authors tested the pro-lymphangiogenic activity of the viral protein. They showed that p17 was able to generate a pro-lymphangiogenic microenvironment and probably have a role in predisposing the lymph node to lymphoma growth and metastasis. These findings could help to identify treatment strategies in combating AIDS-related lymphomas (Caccuri et al., 2014).

Chemokines	Chemokine receptor	Location of receptor expression in brain	Effects in the brain
CXCL8 (IL-8)	CXCR1	Microglia, subsets of neurons, astrocytes and oligodendrocytes	Modulation of synaptic transmission and plasticity and inhibition of long-term potentiation in hippocampus
	CXCR2	Microglia, neurons, astrocytes and oligodendrocytes precusrsors	
CXCL10 (IP10)	CXCR3	Microglia, subsets of neurons and astrocytes	Alteration of synaptic plasticity in hippocampus and induction of leukocyte infiltration

Table 1. Role of selected chemokines and chemokine receptors in HIV-associated dementia (Zhou and Saksena, 2013).

p17 operates within an extracellular environment affecting the function of immune cells, -this is thought to happen via an interaction with its NH(2)-terminal region and a p17 receptor (none-designated). However, the intracellular events triggered by p17/p17R interaction are not known (Giagulli et al., 2011).

p17 up-regulates p-ERK1/2 and down-regulates p-Akt in human B cell lines, which are two of the major intracellular signalling components involved in AP-1 activation. Specifically, the COOH-terminal truncated form of p17 (p17Δ36) was able to induce activation of the PI3K/Akt pathway, and in addition it was shown that among different p17 variants, one derived from a Ugandan HIV-1 strain, (S75X), triggered an excessive activation of PI3K/Akt signalling pathway, increased B cell proliferation and malignant transformation.

The study demonstrated a role of the COOH-terminal region associated with p17 signalling modification demonstrating a level of complexity of p17 binding to and signalling through its receptor(s). The study in addition showed evidence that p17 natural variants mimicking the [p17Δ36] induced signalling in B cells and has the ability to promote B cell growth and tumourigenesis (Giagulli et al., 2011). The role of p17 in cognitive decline associated with HIV patients (HAND) has not been described and is the focus of this project.

Due to its strong potential pro-angiogenic qualities, this was also an element investigated here and hence it is important now to introduce the concept of angiogenesis and the main methods used for analysis:

The process of angiogenesis

The importance of angiogenesis was characterised originally by Folkman (1971) and after stroke or other brain injuries is well stablished by Krupinski (1993). Over the years the importance of vascular perturbation/damage with development of AD and dementia in general has been proven (Smith, 2016). In consideration of these facts and that p17 from HIV has been shown by my collaborators to be strongly pro-angiogenic particularly in relation to tumour angiogenesis and lymphatic endothelium (Caccuri et al., 2012), a description of the process of angiogenesis and the stages and mechanisms is warranted here, including techniques used to measure new blood vessel growth followed by a short section defining angiogenesis in vascular dementia.

Angiogenesis is the growth of blood vessels from the existing vasculature. It occurs throughout life mainly during disease but also e.g. during pregnancy and wound healing. All active tissue in the body is within about one hundred micrometers from a blood capillary, -these are formed by angiogenesis (originally during embryonic vascularization) and in all the human body contains approximately 100,000 Km of these. Changes in metabolic activity in health and disease lead to changes in the balance of secretion of pro and anti-angiogenic factors and, proportional changes in capillarity.

Modulation of angiogenesis has significant therapeutic value and in the 21st century, a thorough understanding of the mechanisms of its control have allowed us understanding the processes of tissue repair and regeneration. Stimulation of appropriate and controlled angiogenesis can be therapeutic in e.g. ischemic heart disease, stroke and other brain injury, and in diabetic or other wound healing. A reduction in angiogenesis is therapeutic in solid cancer inhibition of growth-a tumour can only grow to about the size of a pinhead (less than 2mm) without a blood supply, diabetic proliferative retinopathy, rheumatoid arthritis and other inflammatory

conditions (Goel et al., 2011). In athletes also for example, exercise increases blood flow and stimulates angiogenesis with new vessel formation in muscle and heart tissue. Similarly, a lack of exercise produces capillary regression

A summary of angiogenesis would be-, primary enzymatic degradation of capillary basement membrane, a stimulation of endothelial proliferation, directed migration resulting in tube-like structure formation, vessel fusion and pruning, and then pericyte/smooth muscle cell attraction, incorporation and final vessel stabilization. A major initiator of this 'sprouting' process is hypoxia, - a lack of oxygen causing oxygen sensing through HIF-1-alpha to activate early response genes and subsequently cell signalling linked to angiogenesis (figure 6) (Ke and Costa, 2006). Most cells (e.g. ECs, neurons, astrocytes, etc.) respond to hypoxia by secreting a proangiogenic growth factors e.g. FGF-2, PDGF and VEGF (VEGF-A).
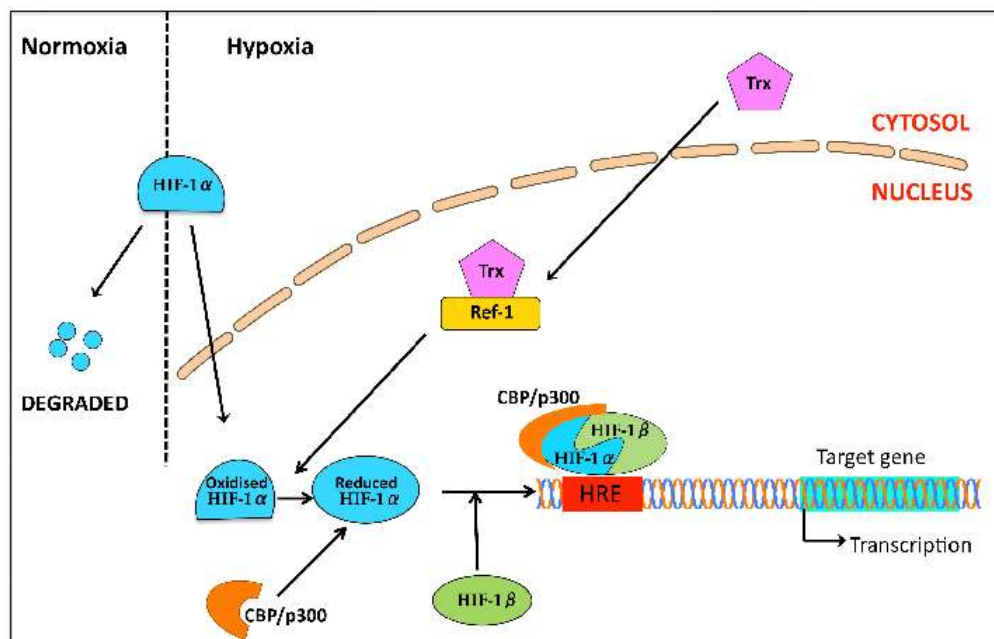
Figure 6. Regulation of the HIF-1 signalling pathway and the expression of its target genes (Bhatia et al., 2013).

Figure 6 above shows cytoplasmic stimulation of HIF-1α and translocation to the nucleus and stimulation of early response genes resulting in signal transduction activation and protein phosphorylation.

Growth factors induce signalling that leads to new vessel formation (figure 7):-example showing stimuli activating angiogenesis pathways through growth factors such as VEGF, FGF-2, HGF, PDGF and IGF-1.
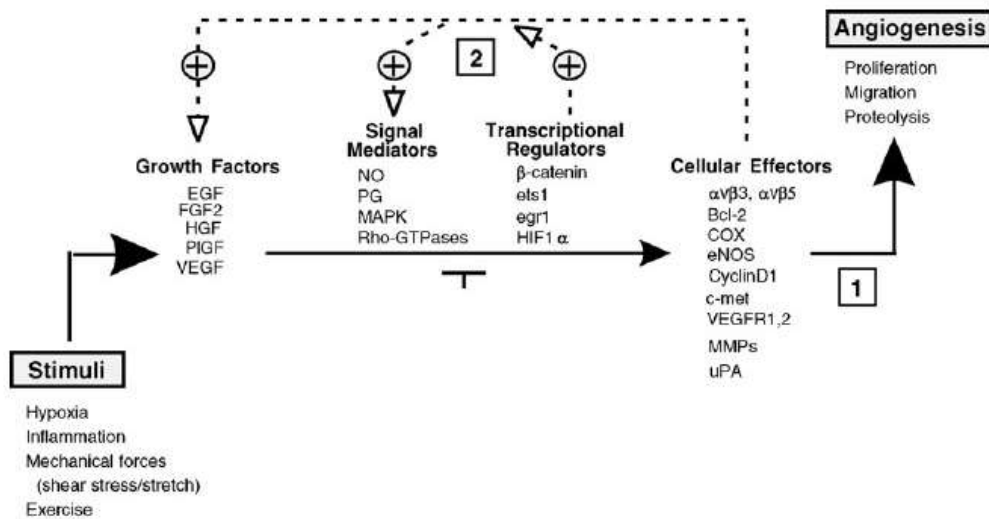
Figure 7. – Stimuli such as hypoxia and stress induce growth factor expression that cause cell signalling through NO/MAPK etc. Nuclear transcription perpetuates this with a feed-back loop to more growth factor production (Li and Li, 2014).

Angiogenic signalling pathways e.g. FGF-2/PDGF-R/VEGF (Fig. 8) operate through cytoplasmic stimulation of PI3K and RAF (Meadows et al., 2001). There is often cross-talk with one pathway stimulating another and often more than one receptor is activated -hence the detail of how local-environmental changes within ECM produce either normal-regular or aberrant angiogenesis are still not known.
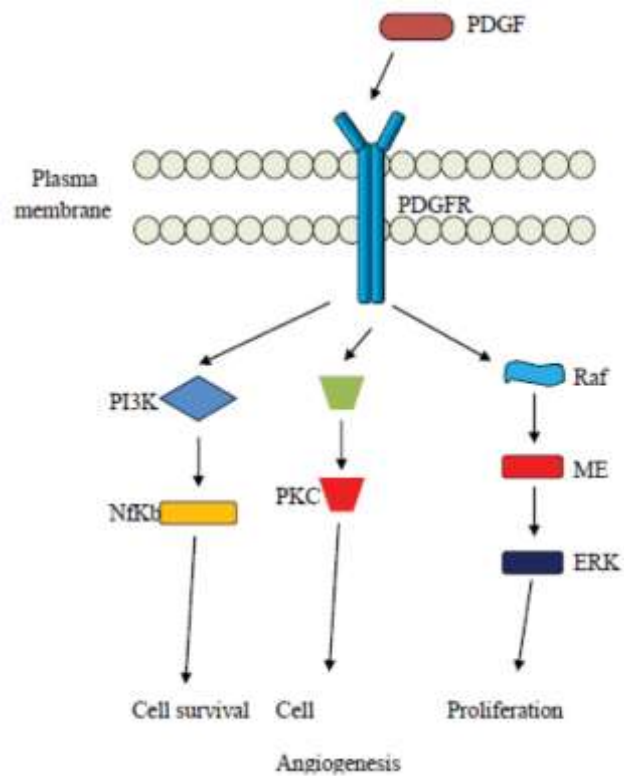
Figure 8. Schematic overview of the PDGF pathway (Gavalas et al., 2013).

Figure 8 shows PDGF signalling through its receptor and activation of down-stream cascade through RAF-MEK-ERK kinases to the nucleus where early response genes fos and jun undergo transcription and the result is cell proliferation. If these pathways described above are activated aberrantly, out of co-ordination or out of control, the resulting new vasculature may be pathological in nature, none functional and could contribute to tissue injury or neuropathological dementia.

Measurement of angiogenesis *in vitro* and *in vivo*

It is critical to be able to measure the effects of proteins such as p17 on regulation of angiogenesis. There are numerous methods describing individual elements of the process some of which are described below but not all of which have been used as techniques within the confines of this thesis.

Proliferation

Cell proliferation & viability analyses are crucial for cell growth and differentiation studies, and are used to test the effects of compounds such as p17 on cell replication and cell cycle parameters. Proliferation is determined using DNA content or on cellular metabolism (measuring the increase in labelled DNA on cell replication). Methods normally count total cell numbers/live cells, or measure average DNA synthesis per cell (Chan et al., 2013). Viability assays measure the relative numbers of dead and live cells from total cell numbers. Cell proliferation as stimulated via cell surface receptors is distinct from other processes such as migration even via the same receptor (figure 9).
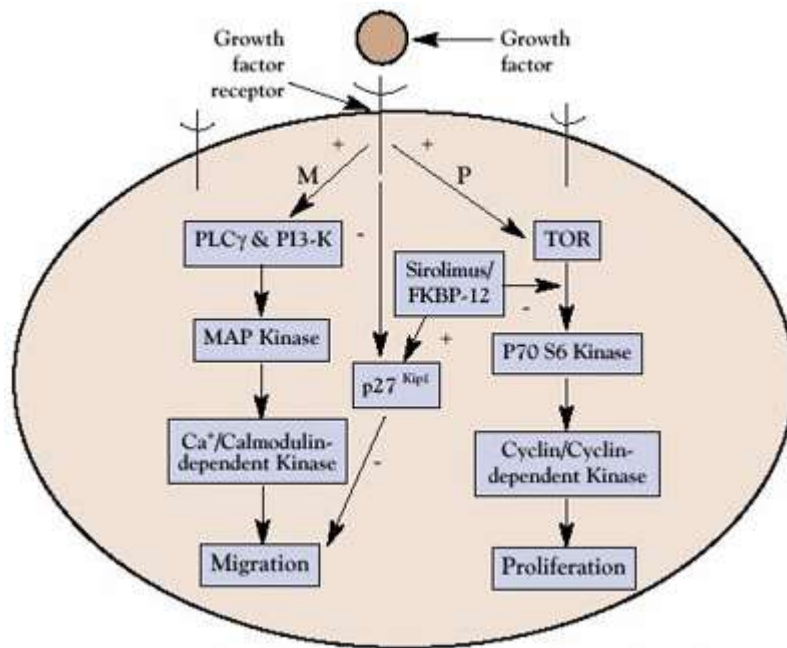
Figure 9. A simplified model showing growth factor induced vascular smooth muscle cell signal transduction pathways leading to cell proliferation (pathway P) and migration (pathway M) (Liuzzo et al., 2005).

This figure shows pathway specific signalling through membrane receptors upstream of cytoplasmic TOR (proliferation) and PLC-ɣ/PKC (resulting in migration).

Migration

Correct effective EC migration has three major components, 1) Directional migration toward chemoattractants (chemotaxis); 2) haptotaxis-similar but toward a gradient of immobilized ligands; and 3) mechanotaxis-linked to mechanical force stimuli (Munoz-Chapuli, 2011). Angiogenic growth factors such as VEGF and FGF-2, signalling is mainly associated with proliferation and directional migration whereas haptotaxis, is polarised directed migration and movement and operated signalling modified focal adhesion changes and integrins binding to ECM components.

ECs are in contact with variable shear stress produced from blood vessels, which activates surface cell adhesion molecules and migratory pathways. Fluid or dynamic shear stress initiates mechanotaxis resulting in leading edge extension, adhesion to the matrix, and release of adhesions behind the cells. It is therefore a mechanical and dynamic process that has to be co-ordinated (complex), through modulation of cell adhesion, appropriate signal transduction, and cytoskeletal dynamics and reorganisation (Versaevel et al., 2016).

Chemotactic Endothelial Cell Migration

The major promoters of actin-based motility are VEGF, FGF-2, angiopoietins, hepatocyte growth factor, PDGF, epidermal growth factor, transforming growth factor-β, and interleukins, tumor necrosis factor-α. In addition, endoglin (a specific marker of active and dividing ECs-otherwise known as CD105) is also activated and present in mainly activated ECs (Lamalice et al., 2007).
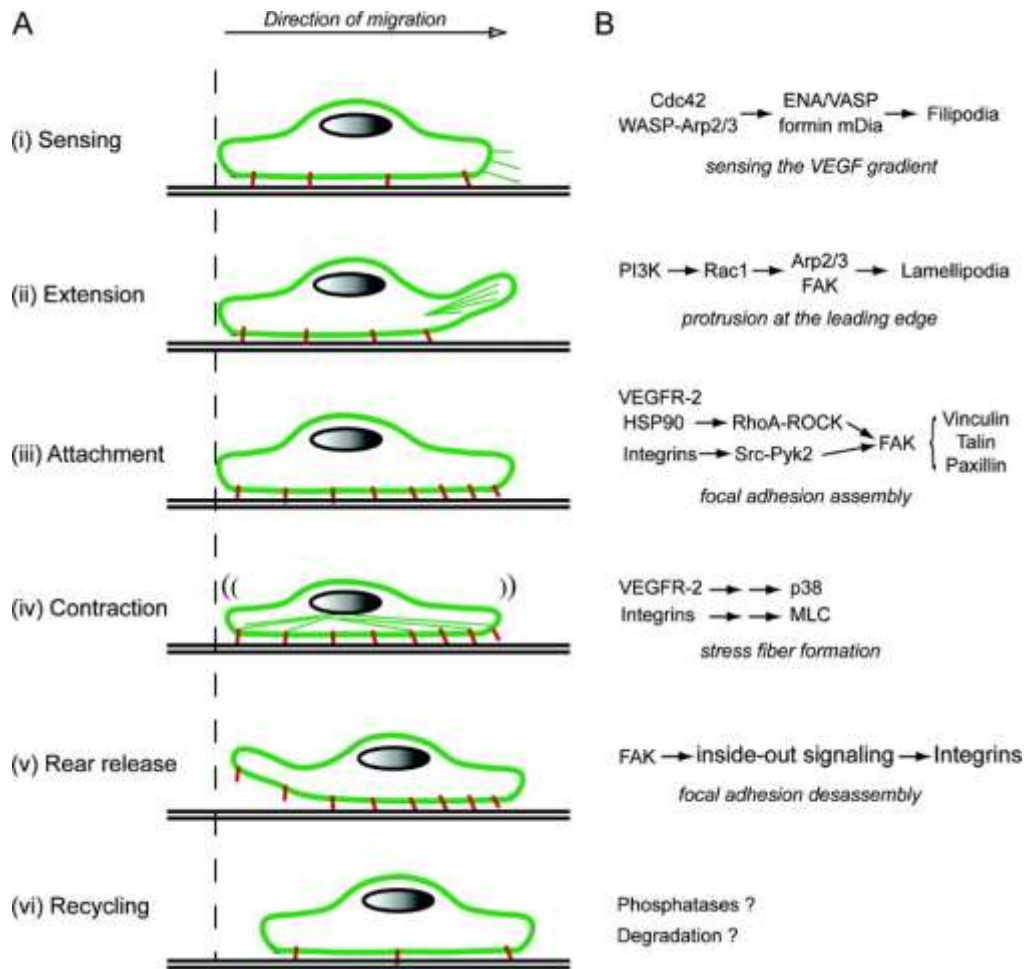
Figure 10. Major steps of endothelial cell migration. Endothelial cell migration divided in 6 sequential events (Lamalice et al., 2007).

The process of cell directed spreading and motility are shown above. Note the involvement of cell signalling intermediates such as FAK, PI-3K, activated through growth factor receptors and requiring basement membrane degradation by matrix metallo- proteinases for release and movement of the cells.

EC differentiation/tube-like structure formation

EC lumen formation is critical for the formation of patent vasculature during wound repair, and in other disease states. Signalling cascades downstream of integrin ligation cause activation of proteins including Rho GTPases, Cdc42 and Rac1, which are involved in lumen formation.

Intracellular vacuole formation and coalescence occur, which causes production of fluid-filled ECM-free regions which become connected together through EC-EC interactions to create multicellular tube structures. These tubes become polarised near to the centrosome whilst strongly accumulating Cdc42 protein. After CD-42, other molecules involved in processing for EC lumen formation are Pak2, Pak4, Par3, Par6, and PKC isoforms zeta and epsilon (Wonshill Koh et al., 2008). They coordinate critical 3-dimensional lumen formation in collagen matrices (Sacharidou et al., 2012).

Again, for effective tube production cell surface proteolysis via MMP1, is required and this helps in forming a guidance for the vasculature within a 3D matrix environment. Recruitment of pericytes (smooth muscle cells) are initiators of vascular tube maturation (via basement membrane matrix assembly) and stabilization-ensuring a working functional vessel. The absolute mechanisms are still not fully understood i.e. signalling integrin activation and concomitant lumen formation, with pericyte involvement, resulting in a stabilised 3D ECM environment (Davis et al., 2007).

The final result is production of a vascular basement membrane matrix assembly, - a critical

and key step in tube maturation and stabilization (Fig. 11).
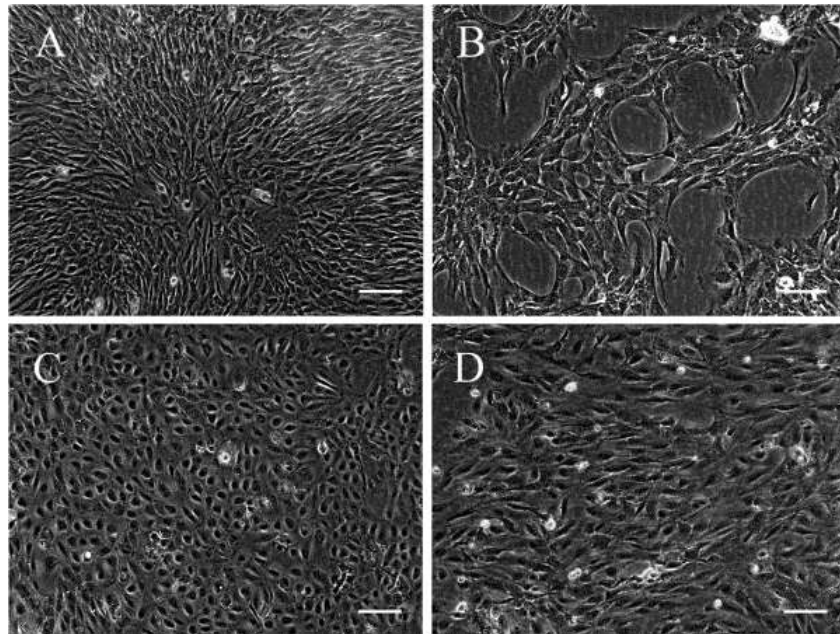
Figure 11. Shows confluent vascular EC cultured in 6-well plates with 'B' able to organize the cells into two dimensional tube-like-structures- in the presence of FGF-2 in the tissue culture media at 25ng/ml (Olyslaegers et al., 2013).
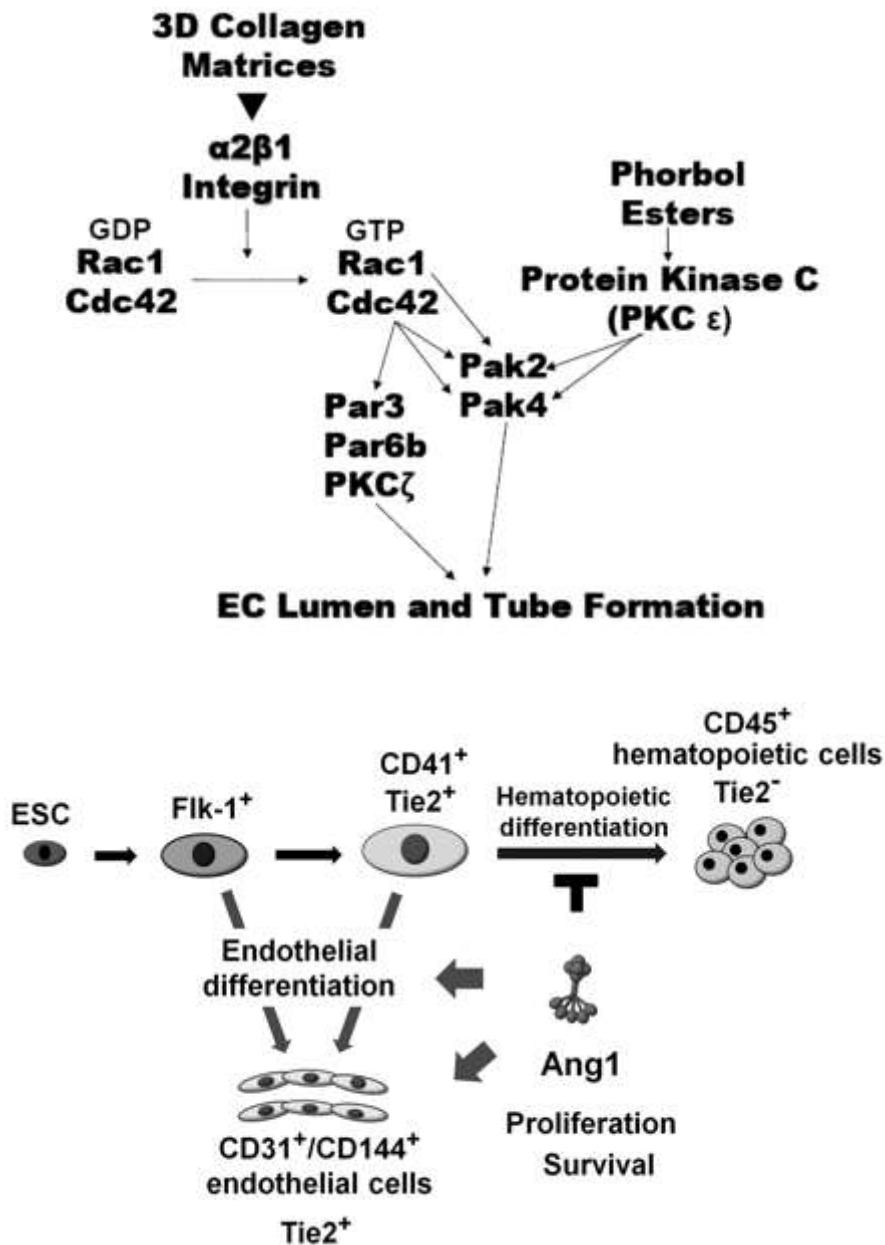
Figure 12. (top) gives an example of signaling through integrin activation, RAC1 and PKC induction of tube formation and (bottom) dynamics of stem cell differentiation following EC differentiation within a specific environment containing Flk-1, CD41, Tie2 and CD31 with increased expression of Ang1-a series of proteins that are secreted during new angiogenesis during remodeling (Koh et al., 2008).

Measurement of angiogenesis *in vivo*

In order to match more closely the physiological effects in humans the following techniques are used and form part of the requirement for early proof-of-concept to define the important role of a test substance on modulation of angiogenesis. Previous studies by our collaborators showed a strong proangiogenic effect of the HIV-1 matrix protein p17 both *in vitro* and *in vivo-* using the Aortic Ring Assay and Chick chorioallantoic membrane (CAM) assay. Hence, these assays provide stronger proof that p17 in ECs of HIV-1–infected patients may promote endothelial dysregulation, angiogenesis (CXCR1/2 receptors), and ultimately vascular diseases (Caccuri et al., 2012).

Some examples of *in vivo* methods are described briefly below:

Matrigel plug assay

The Matrigel plug assay is a rapid test used as a screening test for stimulators and inhibitors of angiogenesis with elements of inflammation included (Brown et al., 2016). Substances are added for example to a sponge or matrigel and the whole, injected subcutaneously into the ventral region of rodents usually mice. The angiogenic response within the matrigel provides evidence of the growth of new blood vessels- towards the plug or if mixed with an anti-angiogenic molecule then inhibition of vessel growth. Haemoglobin (estimating the amount of blood within the circulatory vessels) and an inflammatory response can also be measured. The experiment is terminated after 7-14 days, the plug removed, and new vessel formation observed in processed matrigel (Drabkin method) by histology and specific EC immunostaining (e.g. CD34, CD31, CD105). Since the native matrigel plug is avascular, any vessel that is formed in matrigel plug is easily distinguishable.
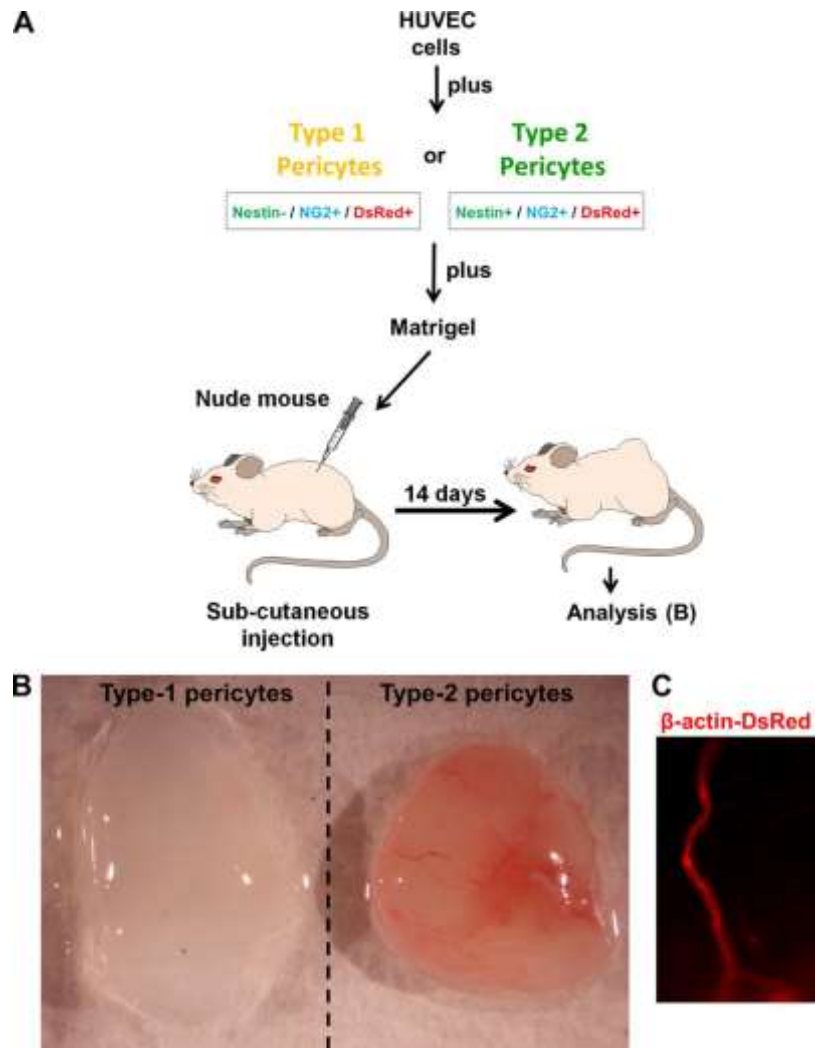
Figure 13. Matrigel plug assay shows that only type-2 pericytes are angiogenic in vivo. A: scheme of an in vivo Matrigel plug assay. A mixture of HUVECs and pericytes sorted from skeletal muscle are embedded in Matrigel and implanted subcutaneously into nude mice. The matrigel plug is recovered approximately 2 weeks later for analysis. B shows: gross anatomy of freshly removed Matrigel plug. C: β-actin-Red fluorescence around blood vessels in a Matrigel plug tracks type-2 pericytes in vivo (Birbrair et al., 2014).

Chick chorioallantoic membrane (CAM) assay

Here, the test substances are placed on the extra embryonic membrane through a 'window' created in the eggshell using a micro-saw-this is carried out around days 7-10 in the chick embryos. The test substances may be placed on filter paper or gelatin sponges within the embryo and the incubation period is 3 days-1 week. There can be problems in this assay where morphological change can mask new capillaries so they are difficult to distinguish from existing ones. The early stage CAM as stated before has an inflammatory response also, to various substances which can prevent the recognition of new vasculature. Quantification of the 'spoke wheel pattern of new vessels' is done by measuring the extent of vascularization manually or with a graphics package on a graded scale of 0-4.

i) Egg opened and CAM exposed.

ii) Test substance (liquid or solid) applied to the surface of the CAM.

iii) Test substance rinsed from CAM.

iv) CAM evaluated for signs of hemorrhage, coagulations and/or vessel lysis and scored.
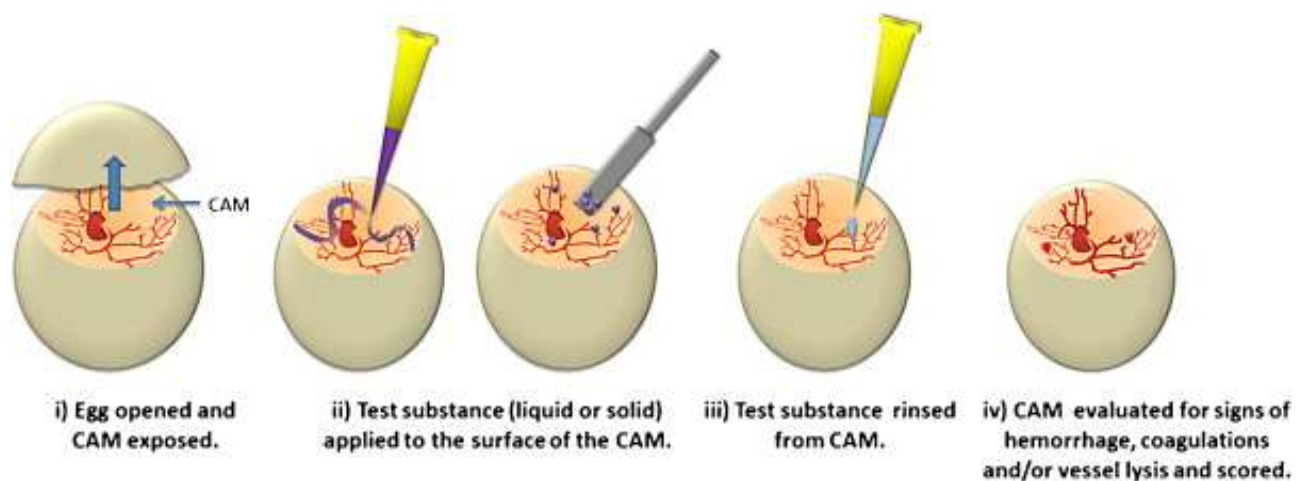
Figure 14. Representation of different phases of preparation of the CAM assay protocol from i) exposing the egg through to iv) evaluation (normally computer-aided-spoke wheel) (Wilson et al., 2015).

Details about our gifted human cortical brain endothelial cell line

Brain microvascular endothelial cell line hCMEC/D3 have been show to closely mimic the *in vivo* phenotype. These were derived from human temporal lobe microvessels isolated from tissue removed during surgery for control of epilepsy. The primary isolate was concentrated with cerebral endothelial cells. In the first passage, cells were immortalised by lentiviral vector transduction (hTERT telemorase) and SV40 large T antigen, followed by cloning, and clones were extensively characterised for the brain endothelial phenotype and provided to us as a gift (Weksler et al., 2013). hCMEC/D3 have many of the characteristics of primary brain EC such as the expression of markers, transporters, and tight junctional proteins even without co-culturing with glial cells (Vu et al., 2009). All of the major brain drug transporters were found to be expressed in the hCMEC/D3 cell line (Dauchy et al., 2009). hCMEC/D3 have been used to study the mechanisms associated with retroviral-induced BBB disruption, examining permeability to solutes and trans-endothelial migration of lymphocytes (Afonso et al., 2007).

Vascular dementia (VaD)-the vascular hypothesis and link to aberrant vascularisation/vascular damage

Vascular cognitive impairment is a range of deficiencies from subtle deficits to full-blown dementia, these being associated with cerebrovascular dysfunction. It is now recognised that almost all AD and dementia is mixed- with both vascular and neurodegenerative components now being the leading cause of age-related cognitive impairment. Vascular degeneration from blockage or haemorrhage perpetuates inflammation and hypoxic conditions within the brain providing the perfect micro-environment for neurodegenerative processes.

Blood vessels and micro-vessels clearly have a crucial role in maintaining brain health, delivering oxygen and nutrients, and providing the signalling and security of the neurovascular unit preserving neuronal and glial function. Vascular dementia, where cognitive impairment is directly associated to the degree of cerebrovascular pathologies, is responsible for at least 20% of cases of dementia, being second only to AD. Recent experimental findings have shown a previously unrecognized functional and pathogenic synergy between neurons, glia and vascular cells, providing the evidence to explain how alterations in cerebral blood vessels could contribute to the neuronal dysfunction underlying cognitive impairment (Iadecola, 2013).

The vascular hypothesis suggests that AD is initiated by vascular dysfunction that contribute to and significantly instigate and promote the neurodegenerative process. Evidence to support this comes from the fact that AD patients show increased haemorrhagic or ischemic stroke risks and stroke itself is the biggest risk factor for AD. Hence multiple bidirectional connections exist between AD and cerebrovascular disease, and within this, amyloid peptides and filaments as well as the increased hyper-phosphorylation of tau protein are implicated in effects directly on vascular cells (tau aggregation damaging the vessel walls) and blood platelets (capturing the tau protein-levels indicating viral load) (Canobbio et al., 2015).

The molecular understanding of VaD is limited; with most of the available information coming from clinical/stroke imaging studies of cognitive impairment and a correlation of this at the cellular level by histology and ICH, with neuronal death and dysfunction. Pathological changes associated with VaD are seen in both large and small blood vessels by a process of atherosclerosis and lipohyalinosis respectively.

Cerebral vessels, are susceptible to damage based on the same risk factors linked to stroke and heart disease in atherosclerosis e.g. hypertension, diabetes mellitus, and dyslipidemia. The reduction in cerebral blood flow (CBF) starts early during vascular disease resulting in

localised tissue chronic hypoxia. As a result, the brain cellular microenvironment is disturbed, undergoes adaptive changes and these may lead to cellular malfunction, preceding cellular death (Enciu et al., 2011).

A neuro-histo-pathological-histological analysis shows multifocal and/or diffuse lesions, described as lacunes or often silent microinfarcts, including subcortical areas and thalamus/frontobasal and limbic system, or white matter lesions that could represent diffuse post-ischemic lesions. The pathogenesis is multifactorial and damaging effects are associated with neuronal networks involved in cognition, behaviour, execution and memory. Vascular lesions are often seen in the same regions of patients with AD and other pathologies. Minor vascular lesions alone probably don't contribute to cognitive decline in major AD, however, when mild AD pathology and small vessel disease are present together and synergise, the process occurs much more quickly (Smith, 2016).

The lesion pattern in "pure" VaD related to genetic diseases of the microangiopathies differs from mixed dementia (AD + VaD), and is usually associated with large infarcts, suggesting different pathogenesis. Because the disease is so heterogeneous with regard to the cerebrovascular pathology, there is still no clear neuropathological criteria for its measurement and extent/classification of VaD. Where studies have been done, a large variability across laboratories has been found on morphological examination. Further prospective pathologic studies will in the future validate new diagnostic criteria for VaD and at the same time clarify the real impact of vascular lesions on cognitive impairment (Jellinger, 2008).

Indirectly, and perhaps not surprisingly, many of the 'classical' vascular risk factors as mentioned above, including hypertension, diabetes mellitus, and hypercholesterolemia have been shown also to increase the risk of AD. What is clear is that the presence of weak or dysfunctional vessels as seen in vascular pathology creates a lower threshold (i.e. is used

clinically to identify) for the clinical presentation of dementia at any given level of clinically defined AD and potentially directly promotes AD lesions through production of Aβ plaques. *In vitro* and experimental animal models have shown that cerebral ischemia chronically up-regulates expression of the amyloid precursor protein (APP) and the precursor to amyloid β thereby damages the blood–brain barrier (BBB), and in addition, affecting Aβ peptide clearance from the brain (Sadowski et al., 2004).

Cerebral amyloid angiopathy (CAA)

CAA is used to describe the pathology of many disorders associated with dementia and/or cerebral haemorrhage. In AD, CAA and vessel dysfunction is due to the deposition of β-amyloid within the adventitia and media of small/medium sized leptomeningeal and brain parenchymal arteries. Almost all cases of AD show some level of CAA, the distribution of CAA is not uniform and the reason for this is not yet known-in this case, the occipital lobe is the most severely affected region (Allen et al., 2014). The pathological appearance of the abnormal vessels shows that the muscle and elastic elements disappear and are replaced by amyloid fibrils, weakening the overall structure of the vessel. The major end-point is that having severe CAA significantly predisposes towards stroke and cerebral haemorrhage, however, the clinical effects of CAA in AD are masked by the more substantial and greater degree of neuronal dysfunction induced by senile plaques and neurofibrillary degeneration.

Even so, sometimes, serious cerebral infarction occurs resulting in focal neurological deficits in people with AD, and in addition, CAA is a major cause of fatal intracerebral (lobar) haemorrhage. CAA also contributes to white matter lesions with subsequent hypoxia causing myelin loss in AD as well as axon loss. There does not seem to be a direct link between areas

of high plaque load and CAA damage-more the opposite and this has yet to be explained! (Kovari et al., 2015).

The differences may reflect differences in source of the protein since β-amyloid from plaques is from nerve cells and that in CAA has a local vascular origin. There are specific inherited forms of CAA linked to cerebral haemorrhage and these are associated with autosomal dominant mutations in APP and other genes such as cystatin-C, transthyretin, gelsolin etc. However, the majority of CAA/AD does not have a primary genetic origin-apart from the APO E beta-4 allele, which notably increase the severity of CAA in a dose dependent manner, and particularly in the occipital cortex. In the future, with more data and new genomic and epi-genetic studies, these correlations may be helpful in understanding the development of CAA in AD and other disorders (Tian et al., 2004).

Hypothesis and aim

Hypothesis

p17 from HIV is responsible for mediating neurocognitive decline in infected individuals.

Aims

To elucidate the role of p17 in promoting Alzheimer-like neurodegeneration using *in vitro* models and histological analysis of animal model of dementia.

Objectives

- To identify the localization of P17 in HIV infected human brain.

- To Identify the potential effects and histological localization of P17 in a mouse model with Alzheimer disease injected with P17 linked to cognitive function and behavioural changes (analyzed by our collabrators).

- To assess the effects of P17 on brain endothelial cell angiogenesis and associated cell signalling.

- To analyze the potential effects of P17 and the mutants on nueronal function and associated signalling pathways.

Chapter 2
Materials & Methods

Materials

- Chromatography paper (WhamanSchleicher&Scuell international Ltd, England).

- Coverslips (Scientific laboratory supplier Ltd, UK).

- Cryovials (Nunc Corporation, Roskilde, Denmark).

- Eppendorf tube 1.5 ml and 500 μl (Nunc)

- Nitrocellulose membrane (Schleicher&Schuell).

- Pipettes 0.5-10,5-50,50-200,100- 1000 μL (Sicentificlabarotory supplies Ltd (SLS)).

- Sterile bijous (SLS)

- Sterile plates 6-well, 24-well and 48-well (Nunc, Denmark), 96-well Greiner® plates.

- Sterile universal containers (SLS)

- Superfrost plus (76x26) mm (Fisher Scientific, USA)

- Tips

- Tissue culture flasks (T-25 and T-75) (Scientific Laboratory Supplier, UK)

Equipment

- Autoclave (Lab Impex Research, UK)

- Autovortex mixer SA1 (Stuart Scientific Co, UK)

- Axivoert fluorescence microscope (Zeiss, Oberkochen, Germany)

- Axiocam microscope using ZEN lite (Zeiss, Oberkochen, Germany)

- Balancer (Sartorius analytic).

- Centrifuge (Mik20).

- ChemiDoc Touch Imaging System (Bio-Rad, USA)

- CO2 incubator (Lab Impex Research, UK)

- Elecrophoresis unit (ATTO, Japan).

- Freezer -80°C (Juan Quality System, UK).

- G-box (Syngene, UK)

- Ice maker (Borolab Ltd, UK).

- Image J software analyzer (Free online software).

- Laboratory fridge (Scientific laboratory Supplies, UK).

- Laboratory pH/ temperature meter (Model AGB-75, UK).

- Laminar flow hood tissue culture grade (Walker safety cabinet Ltd, UK).

- Liquid nitrogen (BOC CryospeedThermolyne)

- Magent stirrer hot plate (Stuart Scientific CO., UK)

- Microscope (Nikon TMS)

- Nikon camera (Nikon coolpix 4500)

- Power supply PS-251-2 (Sigma-Aldrich)

- Rotating shaker (Grant-bio PS0-300)

- Spectrophotometer (Pharmaxia Biotech).

- TC10™ Automated Cell Counter (Bio-Rad, USA)

- Trans-blot SD semi-dry transfer (Bio-Rad, USA)

- Ultra-low -80 freezer (Nuaire, USA)

- Water-bath (Grant instrument Ltd., UK)

Required buffers

- Blocking buffer: 1% BSA in TBS –Tween. TBS-Tween must be stored in the refrigerator at PH7.4 or 3 % of non-fat dry milk in PBS-Tween.

- Electrode buffer: 12.02 g Tris-base, 4g SDS, 57.68g glycine made up with 2 L of dH2O.

- Milk (required for the secondary antibodies): 5% milk in TBS-Tween with PH adjusted to 7.4. Must be stored in the refrigerator for 7 days.

- Sample buffer (PH 6.8): 1.51 g of Tris-base, 20 ml glycerol mixed with 20 ml of d H2O. Then add 4g of SDS, 3.6 ml of mercaptoethanol and 0.004 g bromophenol blue made up to 100 ml with d H2O.

- Separating buffer (PH 8.8): 36.3 g Tris-base, 0.8 g of SDS dissolved in 250 ml of d H2O.

- Stacking buffer (PH 6.8): 15 g Tris-base, 1g SDS dissolved in 250 dH2O.

- Towbin buffer: 1.51 g Tris-base,7.2 g glycine, 0.167 g SDS, 75 ml methanol. This combination was made up to 500 ml with dH2O.

- Tris buffered saline and tween-20 (TBS-Tween PH 7.4): 2.422 g Tris-base, 16.36 g NaCl and 2 ml of tween 20 mixed up to 2 L with dH2O.

Cell culture medium

Endothelial cell basal medium-2 (EBM-2) supplemented with 2% FBS, hydrocortisone, recombinant human Fibroblast Growth Factor B (rhFGF-B), recombinant human Vascular Endothelial Growth Factor (rhVEGF), Recombinant long Receptor Insulin-like Growth Factor-1(R3 IGF-1), Ascorbic Acid, recombinant human Epidermal Growth Factor (rhEGF), Gentamicin sulphate Amphotericin-B (GA-100).

Experimental procedures

Recombinant Proteins and Antibodies:

Purified endotoxin (lipo-poly-saccharide-LPS)-free recombinant HIV-1 matrix protein p17 (in its monomeric form) was produced as previously described. The absence of endotoxin contamination (< 0.25 endotoxin units/ml) in the protein preparation was assessed by a Limulus amoebocyte assay (Associates of Cape Cod, USA). The p17 mAb MBS-3 was produced in our laboratory.

Ethics statement

Animal tissues:

The mice were bred from the Spanish colony established in the Medical Psychology Unit, Autonomous University of Barcelona, Spain. The study was approved by the local animal experimentation ethics committee "Comité Ètic d'Experimentació Animal" (CEEA) of the UB, under the permit DAAM #6991, issued by the Departament d'Agricultura, Ramaderia, Pesca, Alimentació i Medi Natural of the Generalitat of Catalonia. All procedures were carried out in accordance with the decree 214/1997 of the Generalitat and the Spanish legislation concerning the protection of animals used for experimental and other scientific purposes and the European Commission Council Directive 86/609/EEC on this subject. All experimental protocols were approved by the above authority.

Human tissues:

Regarding the human study, the institutional review board and local ethical committee (CEIC) of the Hospital Universitari Mútua Terrassa provided clearance for the study. All patients signed informed consent. For more information please see Appendix 1.

Animals

24 male 3xTg-AD mice and 24 non-transgenic (NTg) mice were used in this study. The 3xTg-AD mouse model was genetically engineered at the University of California, Irvine to express the familial AD mutations PS1/M146V, APPswe and tauP301L. The NTg mice had the same genetic background hybrid 129 x C57BL6 as 3xTg-AD. Mice were bred from the Spanish colony established in the Medical Psychology Unit, Autonomous University of Barcelona. Genotypes were confirmed by polymerase chain reaction (PCR) analysis of DNA obtained from ear punches. Animals were individually housed in Macrolon cages (Techniplast, Buguggiatta, Italy) with free access to food and water and maintained in a temperature controlled room (22 ± 2 °C) with 12 hours light/12 hours dark cycle. Animal handling, including surgical procedures, behavioural testing and necropsies, was performed at the facilities of the Animal Unit of the University of Barcelona, Spain. The study was approved by the local animal experimentation ethics committee (Ref.: DAAAM, CEEA, UB). All procedures were carried out in accordance with Spanish legislation concerning the protection of animals used for experimental and other scientific purposes and the European Commission Council Directive 86/609/EEC.

Hippocampal injection of p17

The p17 protein was delivered into the mouse hippocampus by stereotactic surgery procedures. Four-month old mice were anesthetized with 10 mg/kg xylacine (Rompun 2%, Bayer, Leverkusen, Germany) i.p. and 80 mg/kg ketamine (Ketolar 50 mg/ml, Pfizer, Alcobendas, Madrid, Spain) i.p. and placed in a stereotactic apparatus (David Kopf Instruments, Tujunga, CA). Bilateral infusions of either p17 solution or artificial CSF (NaCl 148 mmol/l, KCl 3 mmol/l, CaCl2 1 mmol/l, MgCl2 0.8 mmol/l, Na2HPO4 0.8 mmol/l, NaH2PO4 0.2 mmol/l) were performed into the CA1 area of the hippocampus. Solutions of p17 contained 0.5 µg/µL.

Injections were performed at a rate of 1 μl/min at coordinates relative to Bregma of -2.0 mm A/P, ±1.2 mm M/L, -1.5 mm V/D. One microliter of the testing solutions was delivered to the application point with a 25-gauge stainless steel cannula (Small Parts Inc., Miami, FL) connected to a Hamilton syringe through a Teflon tube. The syringe was attached to a micro-infusion pump (Bioanalytical systems Inc., West Lafayette, IN). The cannula was left in position for 5 min after delivery to prevent the solution from surging back. Intracerebral injection into the rodent hippocampus has been widely used by us and other authors and from our experience and published work, no effects on behaviour or cognitive deleterious effects are normally associated with the surgery or in the presence of non-active/control proteins. In behaviour study conducted in Barcelona, four groups of mice were compared:

➢ Non- transgenic mice (normal mice)

➢ Non- transgenic mice injected with p17

➢ Transgenic mice

➢ Transgenic mice injected with p17

Eight mice were injected in each experimental group.

Human brain tissue samples

Samples were obtained from the Brain Bank, Hospital Universitari Mutua Terrassa, Catalonia and ethical approval for the work was granted. The tissue samples were collected within four hours of death from the refrigerated bodies of three HIV-positive patients who died from haemorrhagic stroke (male, age 57 years, A19-92); ischaemic stroke (female age 88 years, A50-96) and aortic aneurysm (male age 72 years, A19-97). The diagnosis of probable Alzheimer's Disease (AD) was confirmed by anatomopathology according to standard protocol and Braak and Braak classification. Prior to death, patients attended an HIV outpatient clinic for at least 2 years. Only patients who had not received any HIV treatment were included (this

was before HAART). On a routine visit patients were screened for neurocognitive impairment. Cognitive impairment was established when the patient scored above 1 standard deviation below the mean of corrected normative data for age, education and other standards recommended in the standardized neuropsychological assessment in at least two neurocognitive areas To decide if neurocognitive impairment was HAND, differential diagnosis was carried out following the internationally accepted recommendations. For more information on behavioural studies please see Appendix 2.

Mouse brain histological analysis

After completion of the behavioural tests, at 1 month after injection, mice were anesthetized and transcardially perfused with 100 mM phosphate buffer (PBS, pH 7.4) containing 0.1 mg/ml heparin (Mayne Pharma, Spain) followed by 4% paraformaldehyde in PBS. Brains were removed and fixed overnight in 4 °C paraformaldehyde, rinsed with cold PBS and then dehydrated in a graded ethanol series, cleared in xylene and embedded in paraffin. IHC was carried out as described below in order to determine expression and localization of a range of markers.

Immunohistochemistry

Double and single immunofluorescence and/or immunohistochemistry were used to assess the distribution in human and mouse brain tissue sections of p17 (mouse monoclonal anti-human p17-specific antibodies) and activated microvessels (CD105 (ab107595) and CD31 (ab28364) as well as the presence of β-amyloid (ab2539) and p-tau (phospho S199) (ab4749), CD68 (ab125047), p-FAK (ab39967) (all antibodies are rabbit polyclonal). Additionally, the following antibodies were used: IRS1 (phospho Y612) (ab66153), p-EGFR (ab40815) (rabbit monoclonal antibodies) (abcam) and p-ERK 1/2, goat polyclonal (Santa Cruz Biotechnology).

Sections were Deparaffinized in Xylene (2x15mins), 100% IMS (2x3 mins), 70% Ethanol (3 mins), Running cold tab water and PBS. After deparaffinization, Antigen Retrieval was carried out in Sodium Citrate Buffer (10mM Sodium Citrate, 0.05% Tween 20, pH 6.0). Sodium citrate buffer was prepared by adding 2.94 g of tri-sodium citrate to 1000 ml of dH2O.

Name of antibodies	Type	Company	Code
Mbs3	Mouse monoclonal	*	*
CD105	Rabbit polyclonal	ab107595	Abcam
CD31	Rabbit polyclonal	ab28364	Abcam
β-amyloid	Rabbit polyclonal	ab2539	Abcam
p-tau (S199)	Rabbit polyclonal	ab4749	Abcam
CD68	Rabbit polyclonal	ab125047	Abcam
p-FAK	Rabbit polyclonal	ab39967	Abcam
p-IRS1(Y612)	Rabbit monoclonal	ab66153	Abcam
p-EGFR(Y1172)	Rabbit monoclonal	ab40815	Abcam
p-ERK 1/2 (N-18)	Goat polyclonal	sc-9479	Santa Cruz Biotechnology

*gift from our collaborators at the university of Brescia, Italy

Table 2. List of primary antibodies used in IHC

pH was adjusted to 6.0 with 1N HCl and then 0.5 ml of Tween 20 was added and mixed well. The buffer was heated in a water bath to about 95°C, and then slides were placed in the buffer for 40 min. After 40 minutes in water bath sections were left to stand for 15 minutes to cool and washed in PBS for 5 mins. Slides were incubated in coplin jar containing 0.3% H_2O_2 in methanol for 30mins (e.g. 1ml of 30% H_2O_2 in 100ml of methanol) and rinsed in 1X PBS for 5mins. Sections were incubated in diluted blocking serum for 30mins with 1% BSA (% 10

horse stock serum), then rinsed in 1X PBS for 5mins. Sections were then incubated in Primary antibody, using the same blocking buffer from previous step, over the night in 4°C.

Slides were washed in 1X PBS (3x 3mins) the next day, then incubated with 1:200 diluted biotinylated secondary antibody (Vector Elite Kit) in block buffer from before as dilutant for 30mins and washed in 1X PBS for 3x 3mins. Sections were incubated for 30min with Vector ABC reagent from kit (1 drop from reagent A to 2.5ml of 1x PBS and then 1 drop from reagent B. The solution was mixed immediately and allowed to stand for 30min and rinsed in 1X PBS (3x 3 mins). Slides were developed with VIP Substrate (Vector VIP SK-4600). 5ml of substrate was mixed by adding 3 drops of reagent 1 (mixed well), 3 drops of reagent 2 (mixed well), 3 drops of reagent 3 (mixed well) and finally 3 drops of hydrogen peroxide solution (mixed well). Sections were then incubated with mixed substrate at room temperature until stain develops (10 mins) and rinsed for 5mins in tap water and 2x3mins in PBS.

After this stage, for double staining and staining for second antigen, the process was repeated from Secondary antibody block, followed by using the second primary, secondary antibody and ABC reaction. Slides were developed with ImmPACT DAB Peroxidase (HRP) Substrate. 1 drop (approximately 30 μl) of ImmPACT™ DAB Chromogen concentrate was added to 1 ml ImmPACT™ DAB Diluent and mixed well. After incubation with a peroxidase (HRP) detection system, slides were rinsed well. Incubated with the substrate working solution at room temperature for 2-10 minutes. Followed by a wash for 5 minutes in tap water.

Nuclear Fast Red (H-3403) was used for counterstaining producing pink appearance. The solution was added directly to the slides, covering the tissue section completely and was incubated for 5 minutes. Slides were washed in tap water for 10 minutes.

Immediately after differentiation sections were dehydrated in 70% ethanol (3 mins), 100% IMS (2x3 mins) and xylene (2x3 mins). Excess Xylene was removed from the slides using tissue

paper and sections were covered with DPX mountant. Glass coverslips were placed on top of the sections, taking care not to produce bubbles under the coverslip, then allowed to dry and set for one hour or more.

Images were captured with Nikon 80i Digital Microscope using Nis Elements 3.21 software with multichannel capture option. Negative control slides were included where the primary antibody was replaced with PBS.

Immunofluorescence

All steps from immunohistochemistry was repeated up to primary antibody block. Then sections were incubated in 1% blocking buffer (serum from the species secondary antibody raised in) for 30mins with 0.1% TweenX20 in 1xPBS. Slides were rinsed with PBS for 5 mins and incubated with diluted primary antibody in blocking buffer and left at 4°C overnight in a dark environment. Slides were washed in PBS for 3 x 3 mins and incubated with 1:300 diluted Alexa Fluor secondary antibody (Goat Anti-Rabbit IgG H&L Alexa Fluor® 647 (ab150079) and Goat Anti-Mouse IgG H&L Alexa Fluor® 488 (ab150113) in blocking buffer for 30 mins and rinsed with PBS for 3 x 3 mins.

One drop of Prolong Gold Anti-fade reagent with DAPI (Thermofisher) was applied to the sample then gently covered with coverslip, taking care not to produce bubbles, then left to cure overnight and edges were sealed with nail varnish.

Fluorescence microscopy

The amyloid binding fluorochrome thioflavine T (ThT) was dissolved in 10 mM PBS, pH 7.4, and added at 3 mM to suspensions of aggregated p17 to a final concentration of 3 µM. After 10 minutes incubation at room temperature, the sample was centrifuged and the pellet washed several times with PBS and applied to gelatin-coated slides. The sample was then examined by fluorescence microscopy (Zeiss) using a filter selective for ThT.

Cell culture and sub-culture

All experiments and procedures were carried out in a sterile environment in a class II biological safety cabinet. Ethanol [70% volume] was used for cleaning all surfaces before commencing work. Only sterile plastics were used and all media were pre-warmed by placing in a 37 °C water bath for 30 minutes before use.

Throughout the study, the cells used in all assay were between passages 15 and 25.

Human Cerebrovascular Microvessel endothelial cell line hCMEC/D3 donated by Prof. Babette Weksler (Division of Haematology and Medical Oncology, Weill Medical College of Cornell University, New York). hCMEC/D3 were grown in EBM-2 medium supplemented with growth factors and hydrocortisone. Cells were seeded into T25 flasks pre-coated Poly-L-lysine solution 0.1 % and maintained in a humidified 5% CO2 atmosphere at 37 °C for 10 minutes. Every three days reaching the adherant, the cells were detached under the enzymatic activity of the trypsin. Briefly, medium was discarded and the cells were washed with approximately 5-10 ml of PBS without Ca++, Mg++. Then, 1 ml of trypsin (2X) was added and incubated for 3 min in order to detach confluent cells from the flasks. Following that, the action of the trypsin was blocked by adding an equal amount of fresh medium. Then, the cells in the suspension were collected in a universal tube and centrifuged at 1300 rpm for 5 minutes. The supernatant was then discarded and the cell pellet was re-suspended with 1ml of fresh complete medium. The cells were seeded into new flasks pre-coated with Poly-L-lysine 0.1%.

Preparation of freezing medium

Freezing medium was prepared with 10% DMSO in FBS, this was achieved by adding 1 ml of DMSO in 9 ml of cold FBS, and it was kept at -20°C until used. Fresh freezing medium was prepared or defrosted shortly before use.

Freezing and thawing of cells

Cells taken from the flask were centrifuged 1300 rpm for 5 minutes, the supernatant was removed and the cells re-suspended in 250 μl of complete medium with the addition of 750 μl of freezing medium. One ml of the medium containing approximately 3.5 x 10^5 of cells was kept in 1.5 cryovials labelled with cell passage, number and date. Cryovials containing cells were kept at -20 °C (30 min). The cryovials were transferred into a -80ºC freezer overnight. After at least 24 hours, cryovials were transferred to liquid nitrogen and their location was recorded. When required, cryovials containing the cells were taken from liquid nitrogen, and wiped with alcohol. The pressure inside the vial was released inside a Laminar flow hood and the frozen cells were defrosted at 37°C water bath. Once defrosted, the cells were transferred immediately to pre-warmed complete medium. The cells suspension was centrifuged at 1300 rpm for 5 min, the supernatant discarded and the cell pellet suspended in 1 ml fresh medium. Cells were washed three times with PBS to remove traces of DMSO and seeded into a T25 or T75 cell culture flask at the required density.

Cell counting

TC10™ automated cell counter was used for counting the cells. From sub-culturing of hCMEC/D3, 20 μl of 1ml cell suspension was added into an eppendorf tube containing 20 μl of trypan blue dye. The sample was then loaded onto a dual-chamber slide. The slide was inserted into the TC10 cell counter and the counting of the cells automatically started. As a final point, total cell count was obtained from the screen.

Angiogenesis assays

Cell migration (Wound Healing)

Cells were seeded at a concentration of 8×10^4 cells/ml in a 500 µl of complete basal medium in each well of a poly-L-lysine pre-coated 24-well plates. After 24 hours incubation at 37 °C in 5% CO2, the medium was replaced with serum poor medium (SPM) containing 2% FBS. Each well of 24-well plates was washed 3 times with PBS and wound was made using a sterile pipette tip. The wells then were washed carefully with PBS to remove any floating cells and 500 µl of SPM containing 2% FBS was added.

Factors pre-incubated with, basic fibroblast growth factor (human recombinant FGF-2, (BD Bioscience, UK) which was used as positive control and added at a final concentration of 25 ng/ml., p17 and S75X (5µg/ml) with or without Epidermal growth factor receptor EGFR inhibitor (Anti-EGFR Antibody, neutralizing, clone LA1. Millipore, USA), was added to the test wells. In all experiments control wells in which no proteins were added were included, Plates were incubated in 5% CO2 incubator at 37 °C for 24 hours. Pilot studies demonstrated that hCMEC wounded under these conditions underwent negligible proliferation up to 24 hours; however, cell movement resulting in wound closure was statistically significant in cells treated with growth factor after 24 hours. 50 µl of 4% paraformaldehyde was added into each well to fix the cells for 5 min. Then, the medium was removed and the wells were washed with PBS. 100 µl of 100% ethanol was added to the cells and left for 5min. Then the ethanol was removed and the wells were left to dry before staining the cells with methylene blue for 5 min. The stain was removed and the wells were washed with distil water. Photomicrograph were taken using phase contrast microscopy (40X) for 10 random areas of each well. Movement of cells into the denuded area was quantified by counting numbers of migrated cells in each field of view. For each well, 10 fields of view (each ~2 mm by 1.45 mm) were examined at random.

To evaluate cell migration, two parameters were taken into account: the number of migrated cells counted under a light microscope (X40) into five random fields of denuded area and the distance of migration from the wound edge obtained by Image J, image analysis software. The number of migrated cells to the denuded area was determined by counting the number of cells in the injured area. Cell migration was examined from the "wound" edge by the aid of a microscope and photographed using a digital camera.

For each experimental condition, cells were treated in triplicate and pictures of five areas of each well were taken.

Tube like-structure formation in Matrigel™.

hCMEC/D3 cells (1.5×10^6 cells/ml) were mixed with equal volume of growth factor-reduced Matrigel™ (10 mg/ml) and different conditions were added, control, FGF-2 (25ng/ml), p17 and S75X (5µg/ml) with or without Epidermal growth factor receptor (**EGFR)** inhibitor, and 35 µl of the mixture (50000 cells/well) was placed in a tear-like drop into the centre of each well in a 48-well plates (Nunc) and left to polymerize for 1 h incubation. Then, 500 µl of complete medium was added into each well. After 24 hours incubation, 4% of PFA was added to fix the endothelial tube-like structures in the gel. Under optical microscope, closed areas surrounded by endothelial tube like-structures were counted in 5 areas from each well.

Volume of the conditions	Volume of cells	Volume of Matrigel
8µl	32µl	40µl

Table 3. Total volume required for a duplicate matrigel assay

Spheroid sprouting assay

Firstly, 6 ml of 1.2% methylcellulose solution was made up with 30 ml of EBM-2 2% FBS. From which 15 ml were added to 250 μl of the initial cell volume (6x10^5 cells/ml suspended in EBM-2 2% FBS).

The cells (150 μl / well) were then added to the 96-well plates and incubated at 37 ºC 5% CO2 for 24 hours. After 24 hours spheroids were collected using a sterile tip, before collecting the spheroids the sterile tip is cut slightly from the tip to avoid damaging them, and added to 15 ml tubes and centrifuged at 1500 rpm for 5 minutes. When clear pellet was distinguished, the supernatant was removed.

In a separate bijou 1.33 ml of collagen gel solution at (2 μg/ml) was added to 920 μl of EBM-2 and kept on ice. Before adding the spheroids in the 48-well plate the collagen solution was neutralised by adding 150 μl 0.1N NaOH. If the 0.1N NaOH was added early the collagen gel solution would have polymerised. The solution turns pink once re-suspended.

200 μl of spheroids was mixed with the 200 μl collagen gel solution, in a separate tube for each condition, with or without FGF-2 (25 ng/ml uses as positive control, p17 and S75X (5μg/ml) with or without Epidermal growth factor receptor (EGFR) inhibitor (Anti-EGFR Antibody, neutralizing, clone LA1 (5μg/ml)).

The spheroids were then added to the 48-well plates at 125 μl/ well and incubated at 37 ºC 5% CO2, after 48 hours, the spheroids were fixed with 4% PFA and pictures were taken. Image J software was used to distinguish sprout length.

Kinexusphospho-protein array analysis

hCMEC/D3 cells (3.8×10^5 cells/ml; 2 ml) were seeded in complete medium in 6- well plate (In a different experiment %80 confluent rat cortical neurones were treated under the condition they arrived from the Thermo fisher scientific). After 48 h incubation, the medium was replaced with SPM for further 24 h incubation then p17 and S75X (5μg/ml) was added to the cells for 8 mins stimulation at 37°C and one well was used for control (untreated cells). Proteins were extracted according to Kinetworks instructions. Briefly, cells were washed twice with cold PBS. Protein was extracted using a buffer (pH 7.2) containing 20 mM 3-(N-morpholino) propanesulfonic acid (MOPS), 2mM EGTA, 5 mM EDTA, 30 mM sodium fluoride, 60 mM β-glycerophosphate, 20 mM sodium pyrophosphate, 1 mM sodium orthovanadate, 1 mMphenylmethylsulfonylfluoride, 3mM benzamidine, 5 μM pepstatin A, 10 μM leupeptin, 1% Triton X-100 and 1 mM dithiothreitol on ice for cell lysis. Cell extracts were then collected and protein concentrations were measured by the Bradford protein assay according to the manufacturer's instructions (Bio-rad, Munchen, Germany). For each sample, protein (100 μg in 50 μl) was transferred to a fresh 1.5 ml Eppendorf screw cap then sent to Kinexus (Bioinformatics Corporation, Vancouver, Canada) to investigate the proteins involved in p17 and S75X signalling pathways.

Statistical analysis

Statistical analysis was made through using Microsoft Excel 2007 program. The results of each experiment determined as the mean ± Standard Deviation. Data shown were analysed for significance using one way ANNOVA and Student t-test. Differences with p values ≤0.05 were considered statistically significant. Each experiment was repeated at least three times.

Proteins extraction for total proteins

hCMEC/D3 cells (3.8×10^5 cells/ml; 2 ml) were seeded in complete medium in 6- well plate. After 48 hours incubation when the cells are confluent, the medium was replaced with SPM containing 1% FBS. Fresh SPM (1% FBS) was added to each well, according to the following experimental conditions:- Control (without any protein added), FGF-2 (25ng/ml), p17 and S75X (5µg/ml) with or without Epidermal growth factor receptor (EGFR) inhibitor, then the cells were incubated for 8 minutes, in a 5% CO_2 incubator at 37^0C. After 8 minutes incubation, the medium was discarded, and each well was rinsed with 500µl of cold PBS. 400µl of ice cold radioimmuno precipitation buffer (RIPA) was added each well and kept on ice. Gently the plate was shaken on ice for a few minutes, cells were scraped using a cell scraper. The total cells lysates were transferred to cold 0.5 ml eppendorfs tubes on ice and stored at -80^0C until used.

Protein estimation for Western blotting:

The protein concentration was determined using the BioRad protein assay. Briefly, BSA was used at 1mg/ml (1 µg/ µl) as a standard protein, 10 µl of protein lysate was added and completed with 90 µl of dH2O in a bijou. After that, 2 ml of BioRad protein assay was added in each bijou. The absorbance of each sample was measured with a spectrophotometer at 595nm. The data outlining the reading of each protein samples and the standard curve required for protein estimation are shown below (table 4):

BSA standard (µg)	BSA volume added (1µg/ µl)	Volume of dH2O (µl)	Volume of diluted Biorad (ml)
0	0	100	2
10	10	90	2
20	20	80	2
40	40	60	2

Table 4. The volume of BSA, dH2O and Bio-Rad required to establish the standard curve
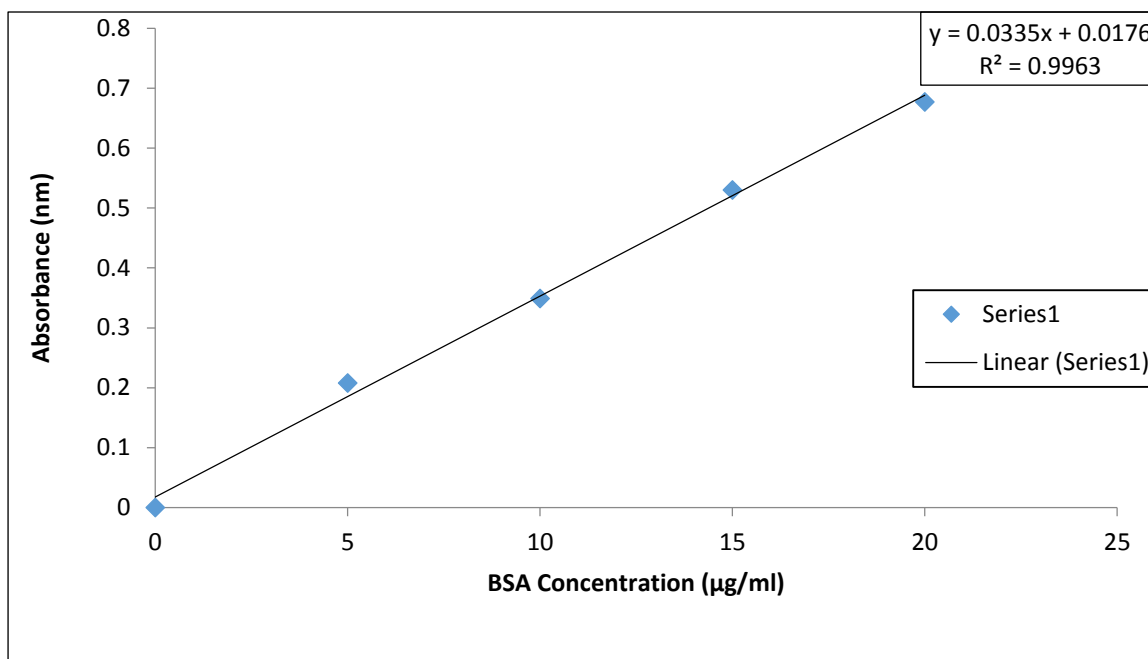
Figure 13. Standard curve for protein estimation in µg

Western blotting

The acrylamide gel was prepared by mixing 3.3 ml of 40% bis-acrylamide with 4.2 ml distilled water and 2.5 ml separating buffer (table 5) in a universal tube. 100 µl of 10% ammonium persulphate (APS) solution was added followed by 10 µl TEMED solutions.

Few drops of isopropanol were added on top of the gel and the gel left to polymerise for 20 minutes. Isopropanol was removed after 15 minutes and rinsed with plenty of dH2O, for one minute. As much as possible, dH2O was removed by filter paper and then the stacking solution was prepared in a second universal tube, by combining 1.45 ml of 40% bis-acrylamide with 6.1 ml dH2O, and 2.5 ml stacking buffer. As before, 100 µl APS was added followed by 10 µl TEMED solution (table 6) and the gel left to polymerise for a minimum of 20 minutes. Slowly the combs, clamps, and gaskets were then removed taking care not to damage the wells and the gel plates inserted into the electrophoresis chamber. The chamber was subsequently filled with

electrode buffer (25 mMtris, 192 mM glycine, 0.1% SDS, pH 8.3). A total of 500 ml electrode buffer was used to fill the tank, in the space between the two sets of glass plates. Take samples, sample buffers and molecular weight marker were taken out of freezer and warm in room temperature. The protein concentration of each sample was determined by Bio-Rad protein assay to insure equal protein loading/well. Equal measures of protein sample and sample buffer were mixed in Eppendorf tube, the tubes were placed in boiling water for 15 minutes. Molecular weight marker 5 µl and the protein samples were gently loaded. Samples containing 15 µg protein (up to 20 µl solution), along with pre-stained molecular weight markers, were separated by SDS- PAGE (12%) for~45 minutes at 60 V (when samples were in stacking gel) and switched to 200 V for separation until the dye, bromophenol blue, reached the bottom of the separation gel.

Material	Volume
dH2O	4.2 ml
40% Acrylamide	3.3 ml
Separating Solution*	2.5 ml
10% APS	100 µl
TEMED	10 µl
	Total volume 10.11ml

Table 5. Preparation of separating gel

Material	Volume
dH2O	6.1 ml
40% Acrylamide	1.4 ml
Stacking Solution*	2.5 ml
10% APS	100 µl
TEMED	10 µl
	Total volume 10.11ml

Table 6. Preparation of stacking gel.

Blotting

Two nitrocellulose membranes (NCM) and 12 pieces of chromatography paper were soaking for 2 minutes in towbin buffer. Stacking gels were removed from the separation gels and discarded. The gels were sandwiched separately. The sandwich was assembled in an electro-blotter for each gel as follows: Three pieces of blotting paper /NCM/gel/3 pieces of blotting paper. Any bubbles within the sandwiches were removed by rolling a clean 5 ml tip over the sandwich. Proteins were transferred to the membrane at 45 mA per gel for one hour.

Blocking

Membranes were blocked with 1% BSA incubation for 1 hour at room temperature on rotating shaker. BSA was discarded and membranes were incubated separately in 10 ml of primary antibody solution at 4°C. Following primary antibodies were used:

Rabbit polyclonal anti- ERK 1/2 (ab196883), mouse monoclonal antibody to pERK1/2 (sc-16982), (beta Tubulin (ab6046) beta Actin antibody (ab8227) – both used as loading Control-, EGFR (phospho Y1172) antibody (ab135560), p-p53 (Ser 37) (sc-135633), p-Akt1/2/3 (sc-7985-R), Rabbit polyclonal antibodies), (Tau (phospho S396) (ab109390) and FAK antibody (ab40794) Rabbit monoclonal antibodies), and PLC γ1 mouse monoclonal antibody (sc-7290).

After overnight incubation on a rotating shaker, primary antibody solutions were transferred into labelled universal tubes and sodium azide was added to a final concentration of 0.02% (w/v) to prevent microbial contamination, the primary antibodies then should be kept at 4°C and can be used for up to a week. The membranes were washed five times in tris buffered saline and tween-20 (TBS-tween) for 10 minutes each at room temperature on rotating shaker.

Membranes were incubated for 1 hour at room temperature in 10 ml of mouse anti- rabbit or rabbit anti-mouse horseradish peroxidase-conjugated secondary antibody diluted in TBS-tween containing 5% (w/v) skim milk (1:1000). After incubation, secondary antibody solutions were discarded and membranes were washed five times in TBS-tween for 10 minutes each at room temperature on a rotating shaker.

Imaging and data analysis

In a dark room, membranes were immersed in enhanced chemiluminescence (ECL) solution. Chemiluminescent is a chemical reaction that generates energy in the form of light and fades over time. To prepare the ECL solution, equal volume of solution-A and solution-B (provided by manufacture) were mixed and put on the membrane in the dark room for one minute, and the excess reagent was then drained off and membranes were quickly wrapped in cellophane films and kept in a box. Then the membranes were taken to the G-Box or The ChemiDoc Touch Imaging System and were detected as a chemiluminescent samples. The intensities of bands on the membranes were quantified by Image-J analysis software. Day to day variations in

luminescence could arise due to protein degradation or experimental errors. Therefore, loading controls are essential for proper interpretation of western blots and can be used to normalize the levels of protein detected by confirming that protein loading is the same across the gel. The expression levels of the loading control should not vary between the different sample lanes. The results were semi-quantitative and compared to the control.

Chapter 3

Immunohistochemical analysis of brain tissue

Immunohistochemical analysis of mouse brain tissue following intra-hippocampal injection of p17 protein.

Introduction:

A critical element of this project was to determine if p17 could affect normal function of the brain tissue. The rationale was to be able to follow the movement and half-life of the protein after injection and to identify cellular localization. Should the p17 protein have biological activity, this could be identified using IHC/IF approaches primarily looking at conventional neurodegenerative changes, as well as possible activation of local microvessels. A triple transgenic animal was used as a positive control-developing strong symptoms of dementia throughout the experimental time period.

Methods:

As part of this internationally collaborative project, co-workers in the CSIC neuroscience building of Barcelona injected p17 protein stereotactically into the hippocampus of mice with additional groups of CSF control, Tg x 3 positive control neurodegenerative (AD) and Tg x 3 plus p17 protein (n=8 per group). The Tg x 3 mutants develop AD within several months and were used primarily as a positive control. Following injection, the 6 month old mice were observed for 6 weeks following which they were euthanized and the brain tissue processed and sent to MMU where tissue sections were cut and an analysis was made of any abnormal effects induced by p17. It is important to note that behavioural and memory studies performed on the mice after injection in Barcelona (and detailed within the materials and methods section of this thesis) revealed a significant loss of motor control function, cognition and certain aspects of memory in mice injected with p17 protein (see paper submitted to eLife; Zeinolabediny et al(2016) for details). Here the aim was to characterise p17 localization within tissue and cells, and to identify regions showing evidence of neurodegeneration or hyper-activity looking at

either conventional AD (tau/Aβ) or other pathology. Note, whilst p17 was also injected into the 3 x Tg mice, their development of AD was so strong that any impact of p17 was not identifiable.

The results are primarily concerned with differences between normal mice and the p17-injected ones and hence the figure panels show mostly p17 injected histology and ICH (normal mice did not express p17 protein as this comes from the HIV virus only). Full panels of negative controls and a panel of 3 x Tg are included (positive controls). The 4th group tested in Barcelona (p17-+3 x Tg) was not analysed in any detail in this thesis since no additional effects were seen caused by the p17 in relation to behaviour or cognition.

At least 10 sections from each block were stained with each antibody and representative staining patterns are shown below.

Results:

3.1.1: Expression of p17 protein in the hippocampus of p17-injected animals: P17 protein was identified within brain sections of animals injected with p17 protein (n=5 analysed; n=3 cut all the way through blocks with serial sections)-showing that the protein was able to remain stable for at least 4 weeks without being degraded within the brain tissue. Normal animals were p17-negative (Fig. 18). Staining pattern showed expression of the protein in quite large quantities within local hippocampal ventrical tracts (Fig. 19), peri-neural expression within hippocampal neurons (Fig. 19), within local cortical microvessels (Fig. 19), in cortical neurons peri nuclear and axonal staining was seen in specific areas it was quite extensive as shown (Fig. 20) and in the form of material with the appearance of 'fibres' or 'fibrils' also within the cerebral cortex (Fig. 21). In some animals and sections, p17 was seen within cells showing the morphology of glia with astrocytic projections becoming positively stained (Fig. 22), and also, p17 co-localised with neurodegenerative plaque-like regions within the cortex (Fig. 22). Expression

patterns varied a little from animal to animal and layer to layer. These data demonstrated that

p17 became stuck after injection within the tissue and ECM for at least 6 weeks and was not

removed or degraded during this time. The question remains as to what effects if any the p17

protein has on each cell type?
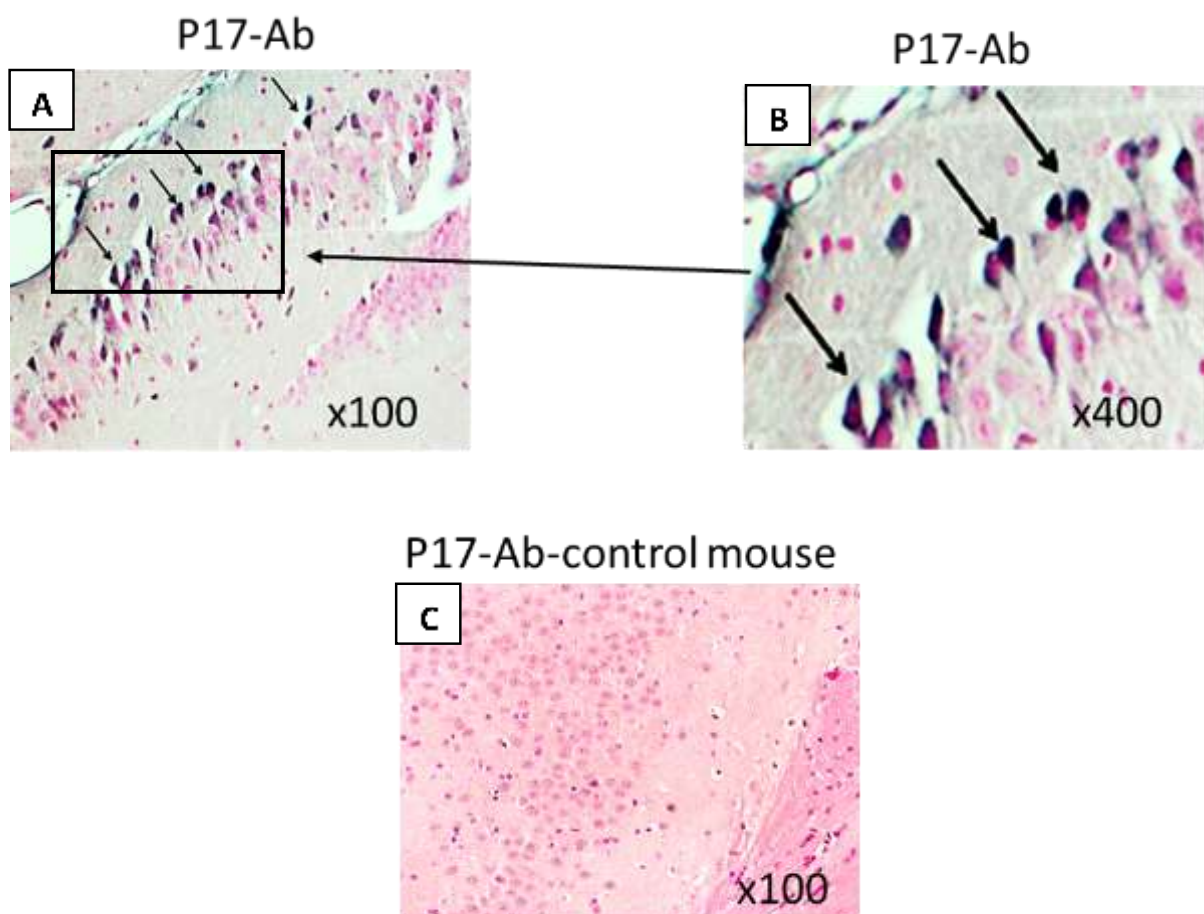
Figure 14. Mouse brain cortical sections from N-tg p17-injected mice, running throughout the

bregma at 6 microns were stained using the antibody to p17 protein (A-B). When the

hippocampus was visible, p17-positively stained nuclear and peri-nuclear neuronal staining

was seen in this region (arrows) whilst staining was negative in normal untreated (-p17) mouse brain sections (C).
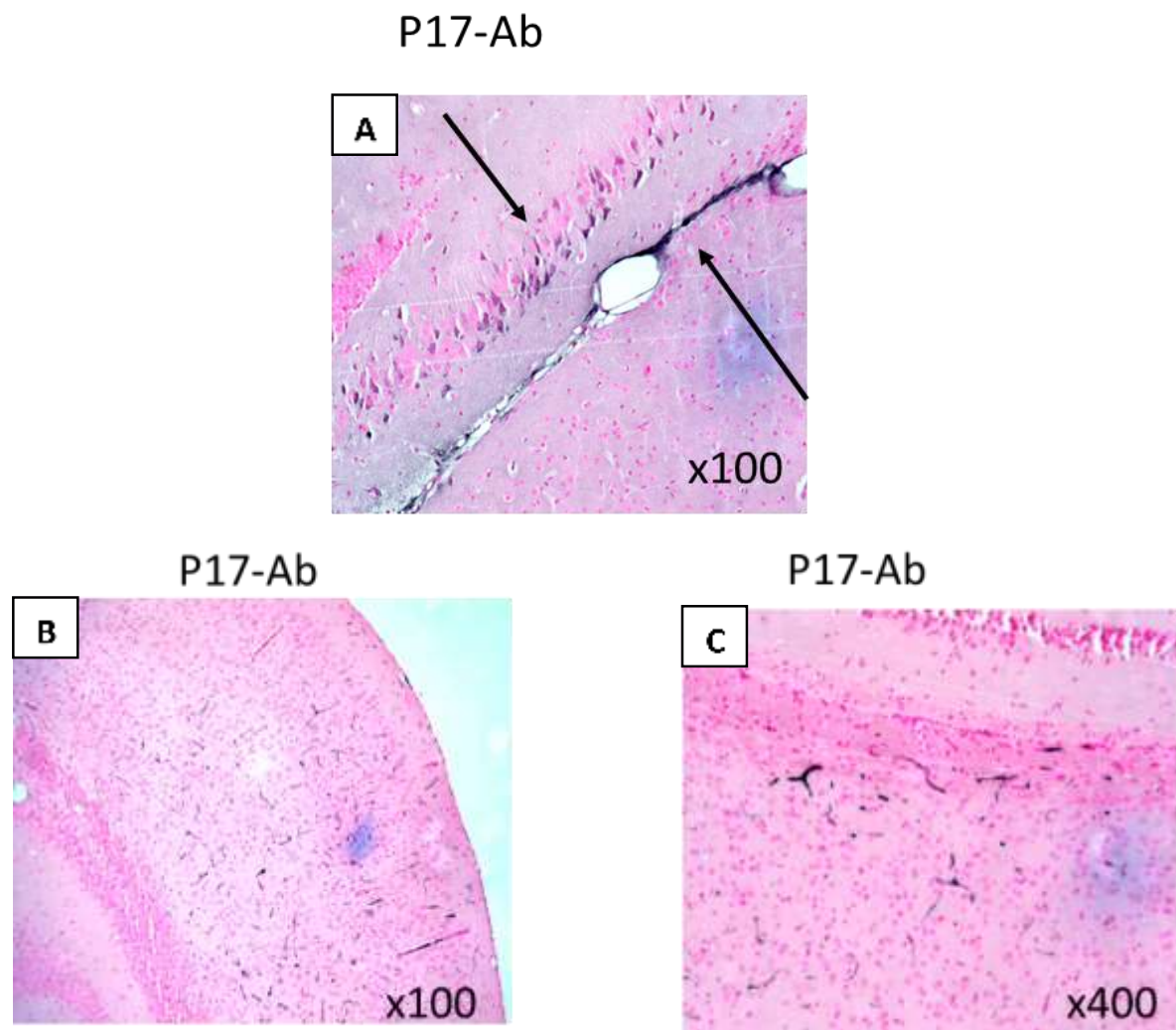
Figure 15. Ntg mice: Top-Cortical ventral tracts (arrows; A) adjacent to the hippocampal injection site and showing positive staining for p17 (lower arrow; A) with local hippocampal neurons also positive in image (top arrow; A). Below-show (B-C) examples of cortical microvessel staining and a ventral tract (larger) from mouse brain sections of mice treated with p17 (hippocampal injection; B x 100 and C x 400).
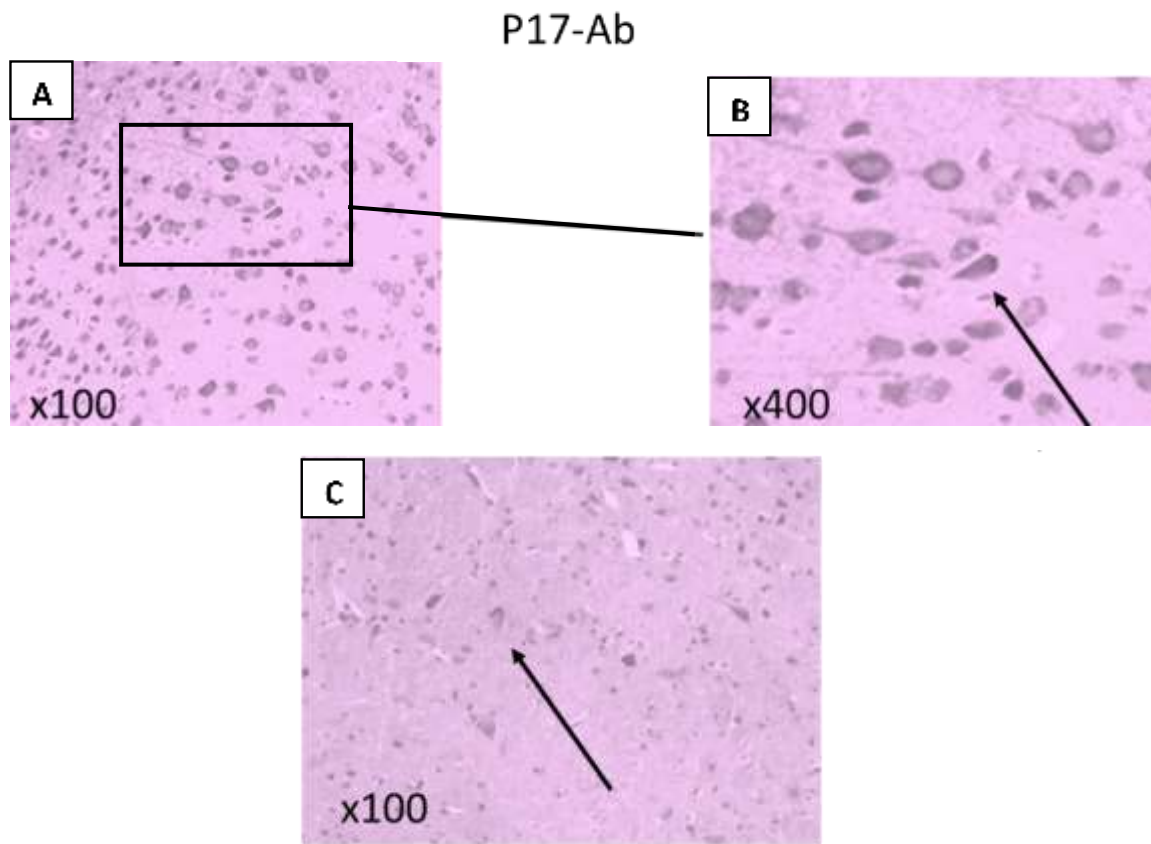
Figure 16. Ntg Images show examples of cortical neuronal staining from mouse brain sections of mice treated with p17 (hippocampal injection). Perinuclear staining with some axonal positivity is seen in (A-B) and also in random scattered cortical neurons in (C; arrows).
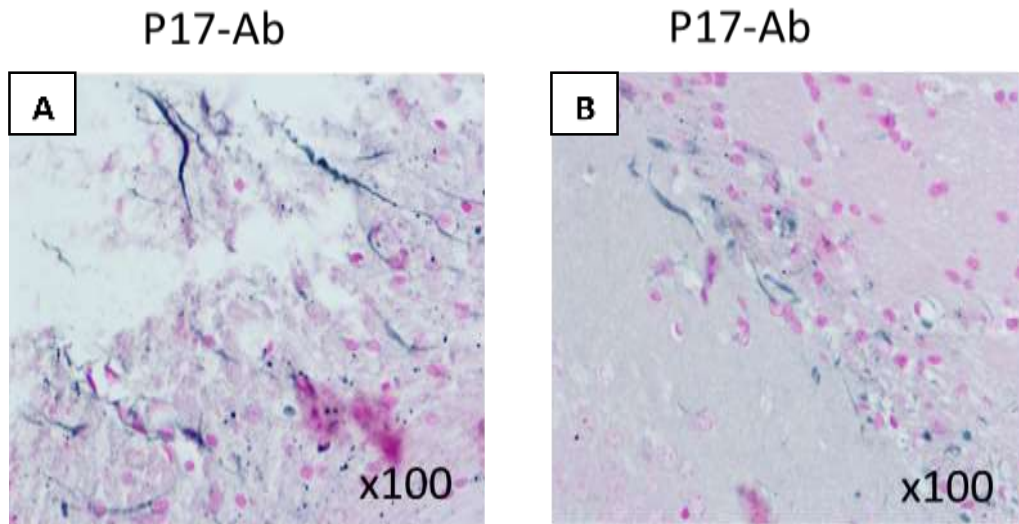
Figure 17. Shows (A-B) cortical fibril-like structures-possibly indicative or similar to a tau-like fibrillary structure development neuropathology stained with the p17 antibody-blue-black staining x 100 magnification

P17-Ab

P17-Ab-TRITC-Ab

P17-Ab

Astrocyte positivity
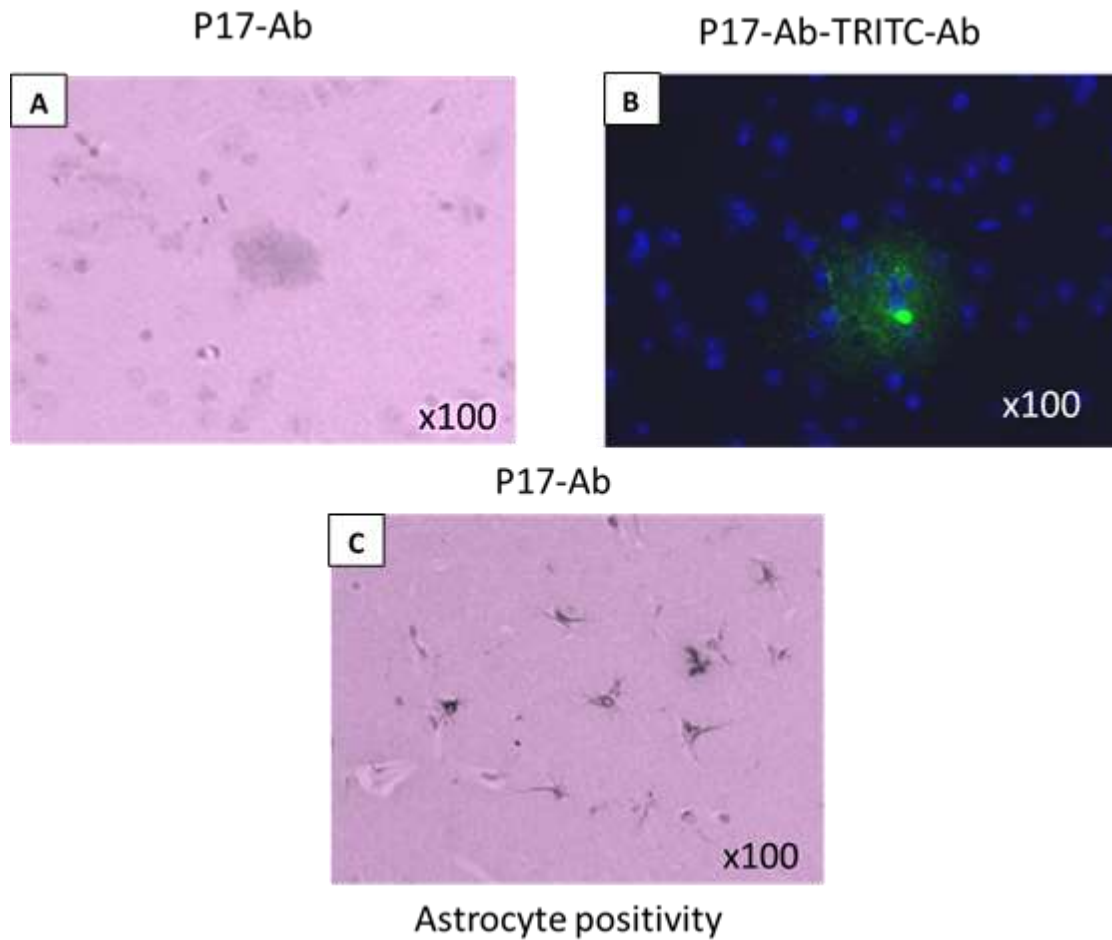
Figure 18. p17-injected mice stained with the antibody to p17 and showing its expression within the cortex in and around unhealthy-pyknotic neurons with the appearance of diffuse plaque-like staining (A; IHC, B; IF-FITC-plaque-like staining). Below (C) -In some mice, injection with p17 resulted in p17 staining in cortical astrocytes adjacent to the hippocampal point of injection. X 100 magnification.

Expression of markers of AD/neurodegeneration in the mouse brain tissue

Neuronal p-Tau expression is a marker of AD neurodegeneration as described in the introduction of this thesis. P17-injected animals showed a large increase in p-Tau-positive hippocampal (Fig. 23) and cortical (Fig. 23) neurons consistent with suggestion of the existence of neurodegenerative effects in the brains of these mice. Similarly, a number of scattered Aβ-plaques were seen in the cortex of these animals, determined using an antibody to the protein-suggesting that p17 can induce neurodegenerative consequences following hippocampal injection, demonstrated by IHC and IF (Fig. 24).
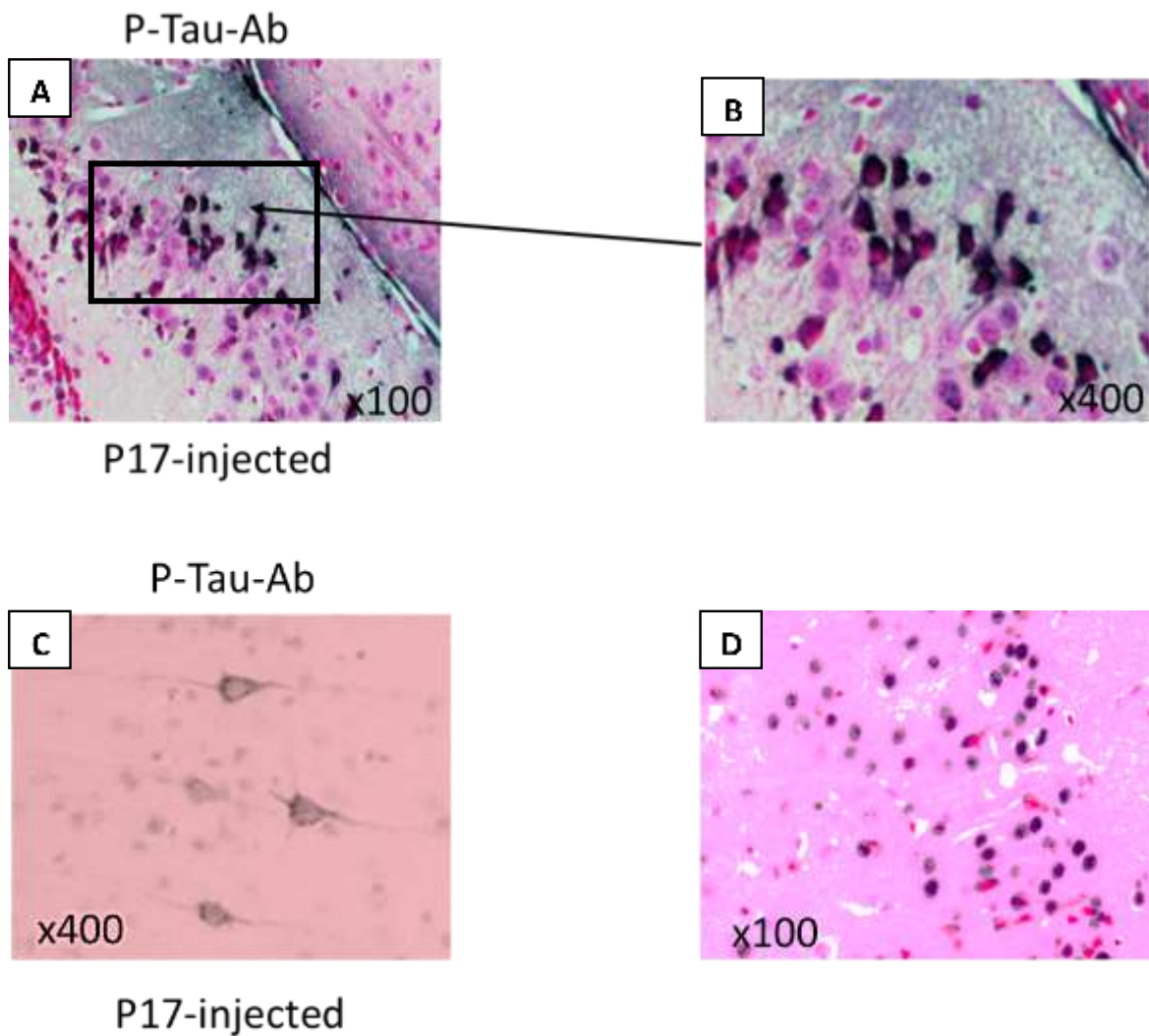
Figure 19. *(A-B)-P17-injected mice showed positive staining for p-Tau-a hall mark of neurodegeneration within hippocampal neurons. (C-D)-P17-injected mice demonstrated scattered p-Tau-positive neurons within the cortex showing peri-nuclear staining.*
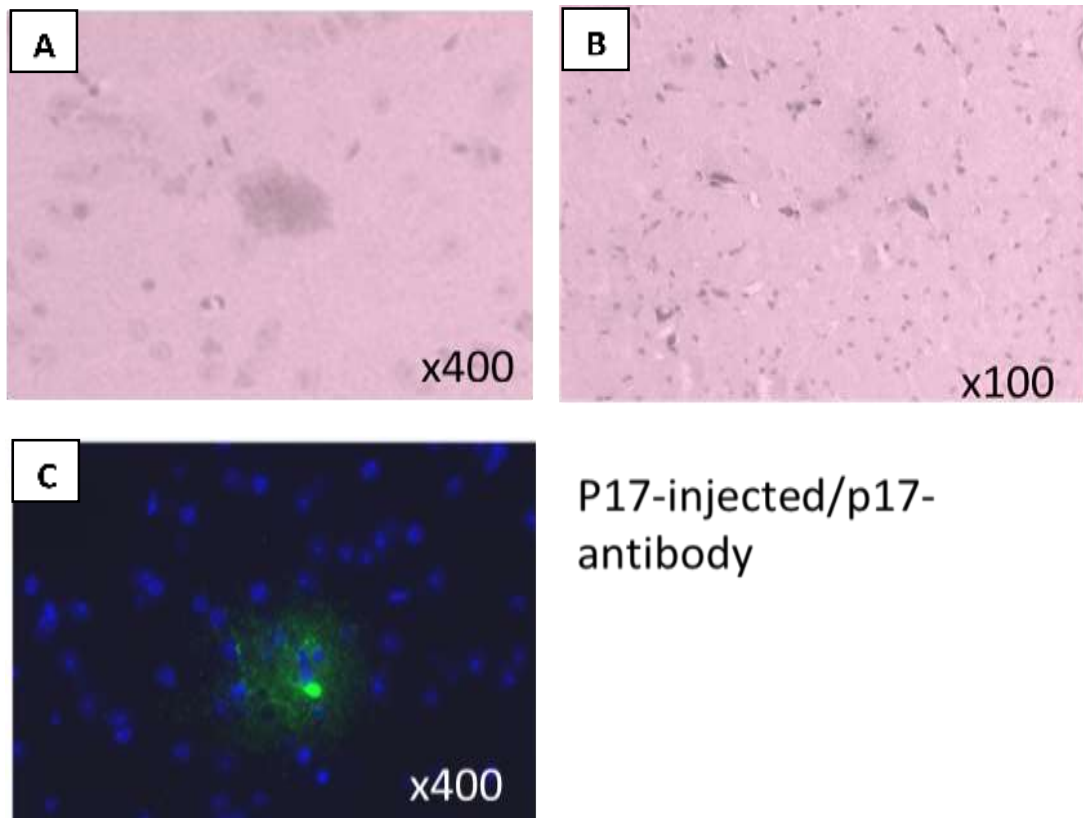
Figure 20. p17-injected mice showed the presence of b-amyloid (anti-amyloid-beta antibodies) cortical plaques by IHC (A) and neuritic cell death associated with diffuse staining (B) and also by IF (C; FITC green) with inclusion of a possible dying neuron (bright green element). Magnification x 100 and x 400.

Co-localization of p17

IF double labelling protocol was used to simultaneously apply two primary antibodies to sections of the rat brain to see if the two proteins (p17 and p-tau) localised in the same areas of tissue and cells. P17 co-localised with p-Tau in hippocampal neurons as shown by double IF (Fig. 25), and also, with CD31 (a marker of normal blood/micro-vessels) and CD105 (a receptor and marker of the endothelial cells from angiogenic-active vessels only) in cortical microvessels within specific localisations suggesting specific transfer to and potential activation of the microvasculature, that could result in neovascularization and immature none-patent vessel formation (Fig. 25). Original single staining channels with single filters are provided as well as combined double fluorescent images.

x400
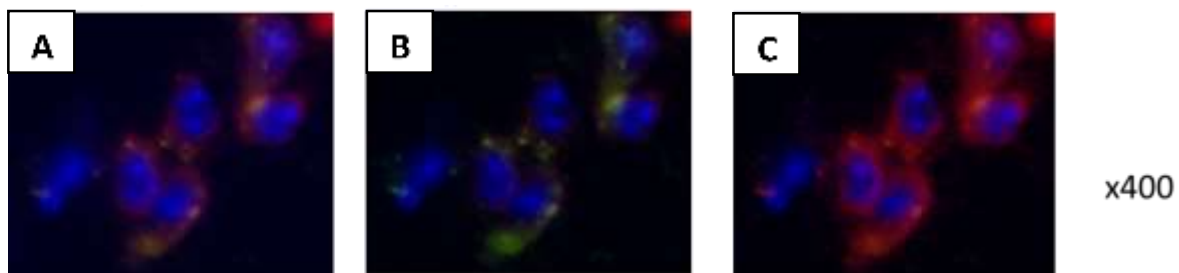
Figure 21. Fluorescent images show hippocampal neurons- stained in the peri-nuclear region- combined FITC and TRITC (A) and single channels green (B-p17 antibody staining) and red (C-p-Tau antibody staining). Tissue sections were stained consecutively with both antibodies and regions of co-localization appear yellow in the combined colour image A.
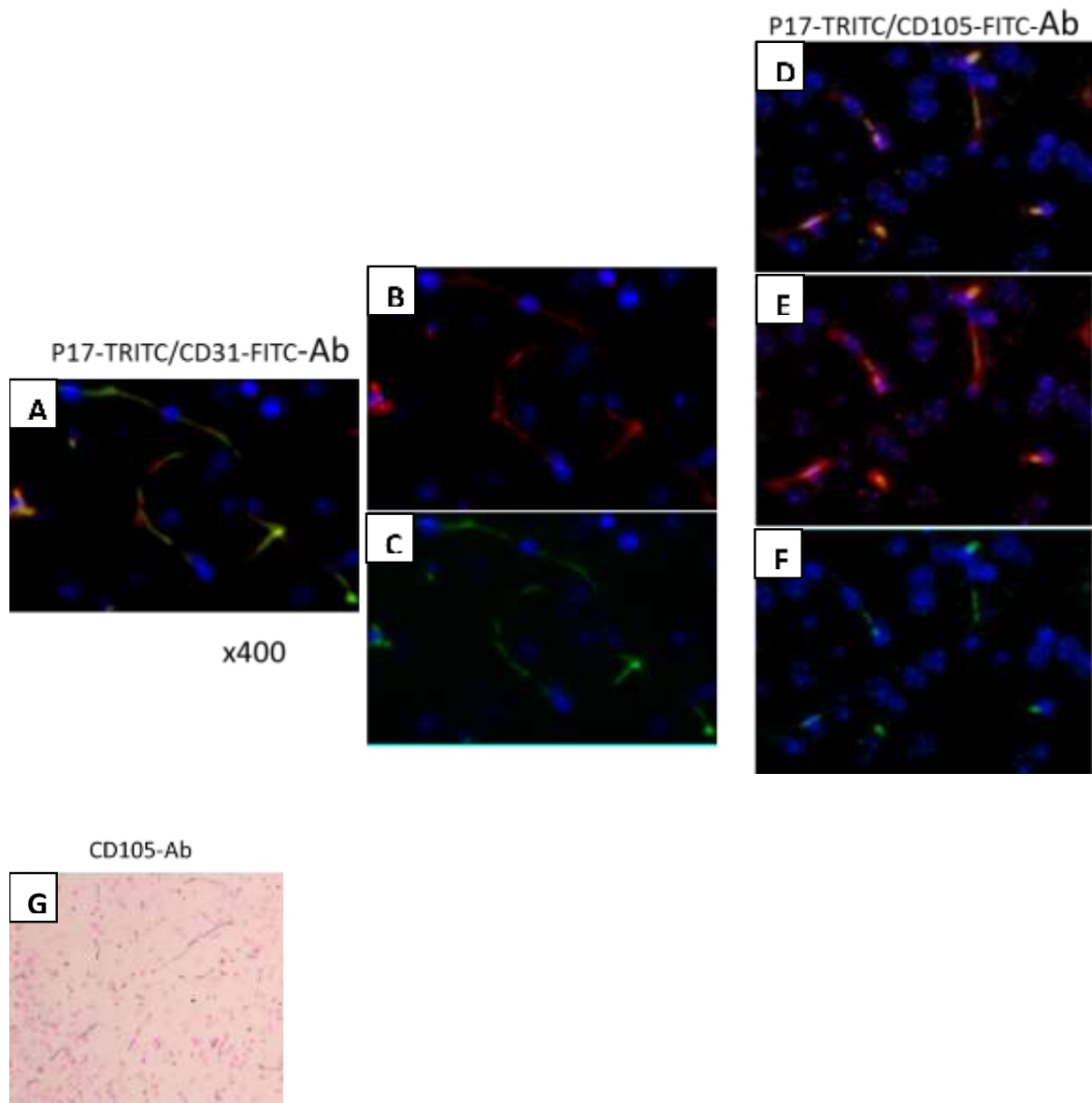
Figure 22. IF pictures show p17 co-localising with CD31 (green) (A-B-C) and (D-E-F)-co-localization with CD105 in the same cortical microvessels. Tissue sections were stained consecutively with both antibodies and regions of co-localization appear yellow in the combined colour image A Lower panel (G) shows IHC of cortical microvessels positive for CD105 in the p17-injected animal.

IHC of Tg x 3 animals with and without p17 stereotactic hippocampal protein injection. Tg x 3 animals containing mutant genes for amyloid, Tau and presenilin represents a valid and well characterised model of Alzheimer's in mice. The positive control Tg x 3 animals showed very strong positive staining for Aβ using the anti Aβ-antibody with many amyloid plaques being visualised throughout the cortex and p-Tau -hallmarks of the AD process-mostly in neurones throughout the cortex (Fig. 27 & 28 respectively; n=3 animals analysed). The amount of staining and volume of affected tissue/cells was greater than that affected in p17-alone injected animals e.g. more plaques and more wide-spread throughout the cortex. This was to be expected as the triple-mutant model causes very dramatic neurodegenerative consequences and death in animals within 6-12 months. When sections from Tg animals injected with p17 were analysed no additional effects were seen i.e. the very strong neurodegenerative consequences seen in the Tg x 3 positive controls was not notably modified in the presence of p17 perhaps as expected (behavioural/cognitive and memory testing of animals studies in Barcelona confirmed this see manuscript published in AIDS 2015-2016 attached). Figure 29 shows sections of cortex from control none-treated animals stained with Aβ and p-Tau antibodies-showing negative staining.
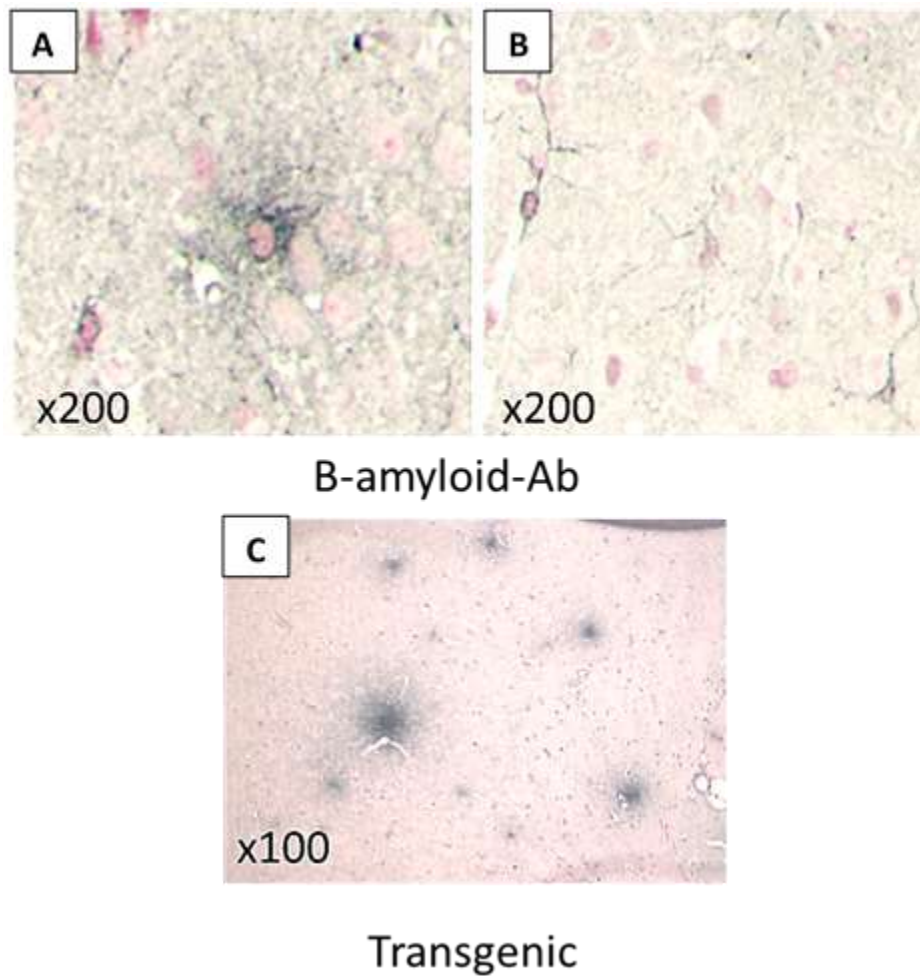
Figure 23. Top left (A) shows Tg x 3 AD mouse section positive for Aβ plaques, top right (B) shows Aβ positive cortical neurons and the lower panel (C) shows numerous Aβ-positive cortical plaques at lower power (x100). There was no evidence of Aβ staining in control animals (not shown).
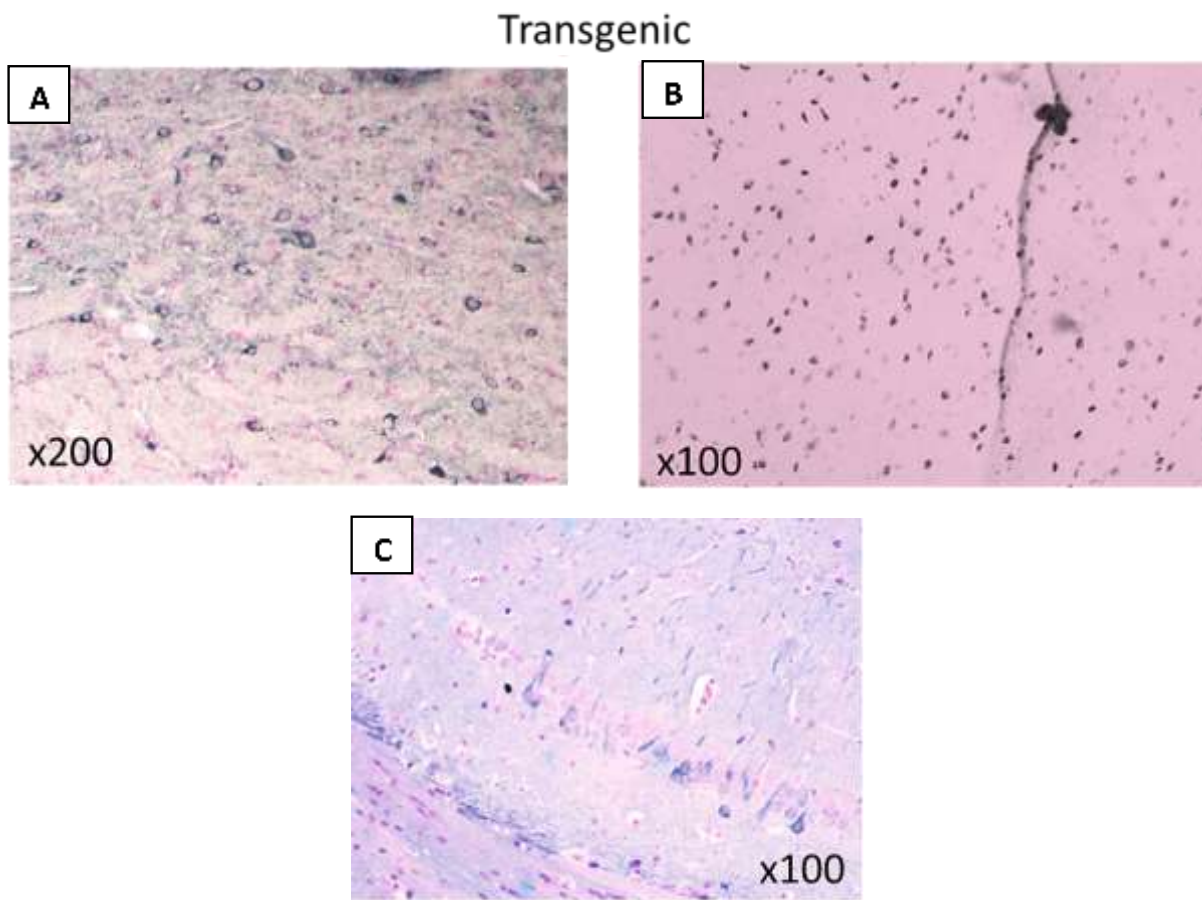
Figure 24. p-Tau 3 x Tg staining of cortical neurons was seen in these sections with a more widespread staining pattern than in p17-injected animals. Top left (A) at x 200 the perinuclear staining of cortical neurons can be seen and right (B)- at x 100 all the blue stained nuclei represent positive staining for p-Tau. Lower panel (C)-hippocampal neurons positive (blue) for p-Tau in the Tg x 3 animals.
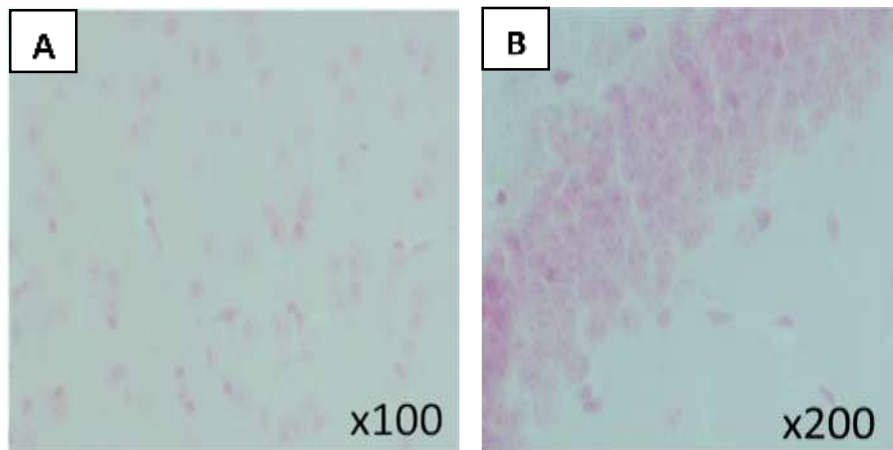
None-treated animals-Aβ (left) and p-Tau Right) negative staining

Figure 25. Ntg none p17 injected animals: Left image (A) shows cortical neurones and other cells negatively stained for Aβ and with no evidence of plaques whilst the image (B) shows hippocampal neurones of a none-treated mouse staining negative for p-Tau antibody.

IHC of novel proteins identified by Kinexus phospho-array analysis and Western blotting within the brain of p17-injected mice. Proteins IRS-1 and EGF-R were identified as phosphorylated by p17 in endothelial cells and/or neurons *in vitro* (see later chapters)-they also may have relevance to abnormal vascularization and neurodegeneration. P-IRS-1 (the phosphorylated/activated form; whose expression is linked to insulin resistance, diabetes and neuroinflammation in dementia) was found in sporadic cortical neurons of mouse sections injected with p17 but not in normal control mouse sections (Fig. 30). In addition, p-EGFR (epidermal growth factor receptor) and p-FAK (focal adhesion kinase) were also observed in cortical neurons of some of the p-17-injected animals (Fig. 30). EGFR is a prime receptor stimulating cell growth in both neurons and endothelial cells, whilst FAK is a cell signalling intermediate again, associated with correct focal adhesion and cell spreading, required for effective co-ordinated cell growth and tissue regeneration during growth phases.
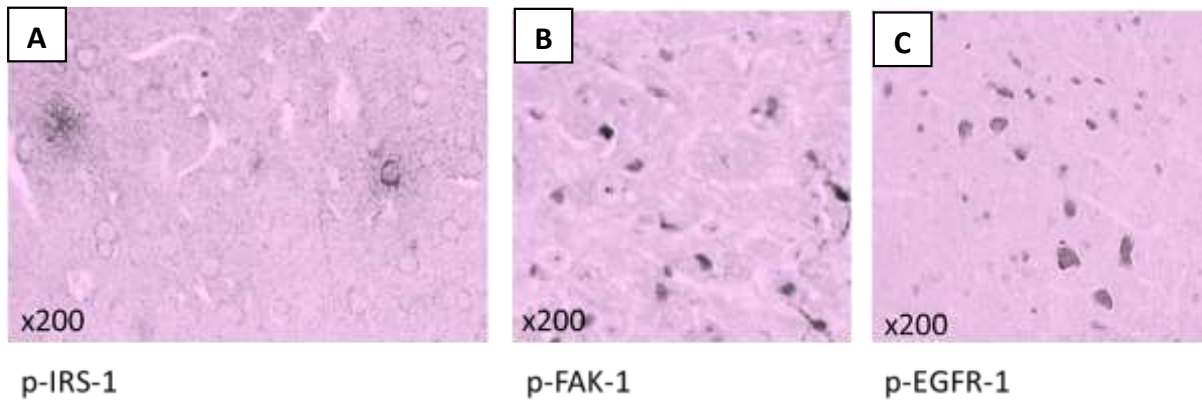
Figure 26. Left image (A) shows p-IRS-1 staining of the cerebral cortex in a p17-injected animal-note positive staining of a plaque-like object and several cortical neurones peri-nuclear. Middle image (B)-p-FAK-1 staining also in the cortex showing positively stained neurones and possibly glia. Right image (C)-p-EGFR-1 staining in a similar section showing strong neuronal positivity in the cortex.
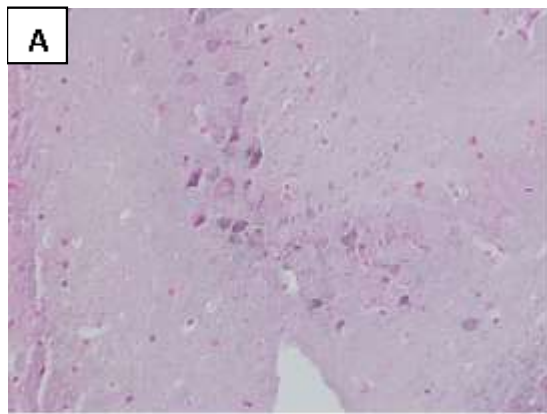
P-EGFR-antibody
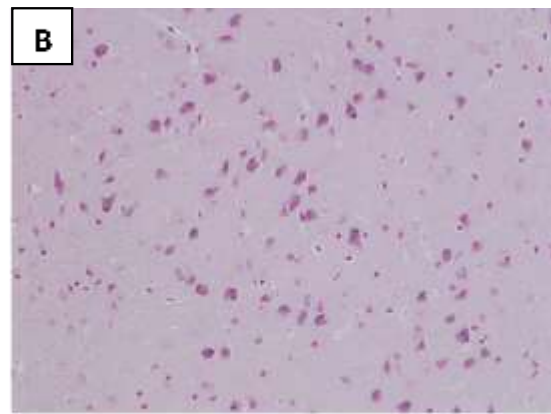
P-FAK-antibody
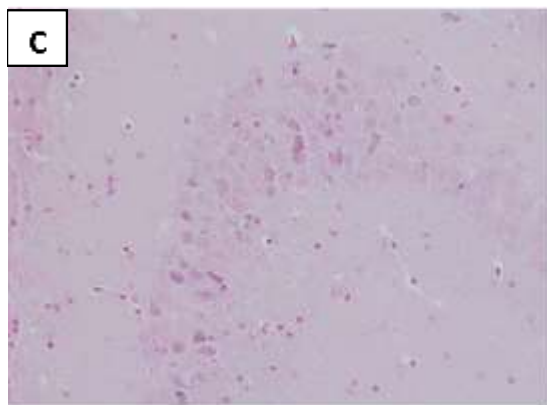
P-ERK-antibody

P17-antibody

Figure 27. Images taken from none-transgenic p17-injected mice showing expression of p-EGFR (A), p-FAK (B), p-ERK1/2 (C) in local neurons. (D shows filaments strongly positive in the cortex for p17 (all magnifications x 200). Ntg none-p17 injected animals showed no staining (data not included).
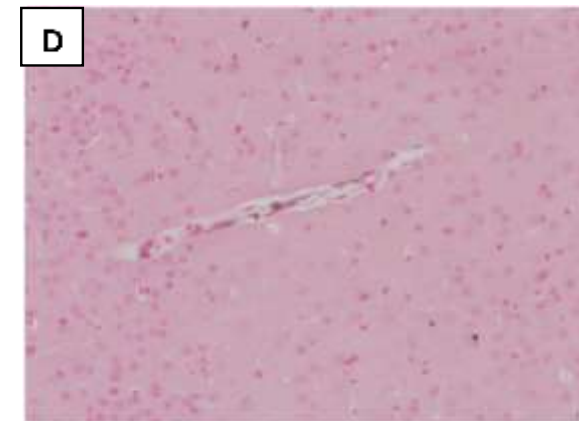
Figure 28. Images taken from none-transgenic p17-injected mice showing expression of p-EGFR in cortical neurones (A), p17 in astrocytes (B), p17 in microvessels in the cortex (C-D) (all magnifications x 200). No staining was seen in none-injected animals (data not shown)

Negative control staining: To ensure that all the staining we observed was specific, none-specific staining was tested for by omission in some sections of the primary antibody

(replacement during incubation with PBS, all other elements of the protocol were the same). There was no apparent none-specific staining found with the antibodies used. Fig. 33 shows examples of anti-rabbit and anti-mouse secondary antibodies without primary antibody.
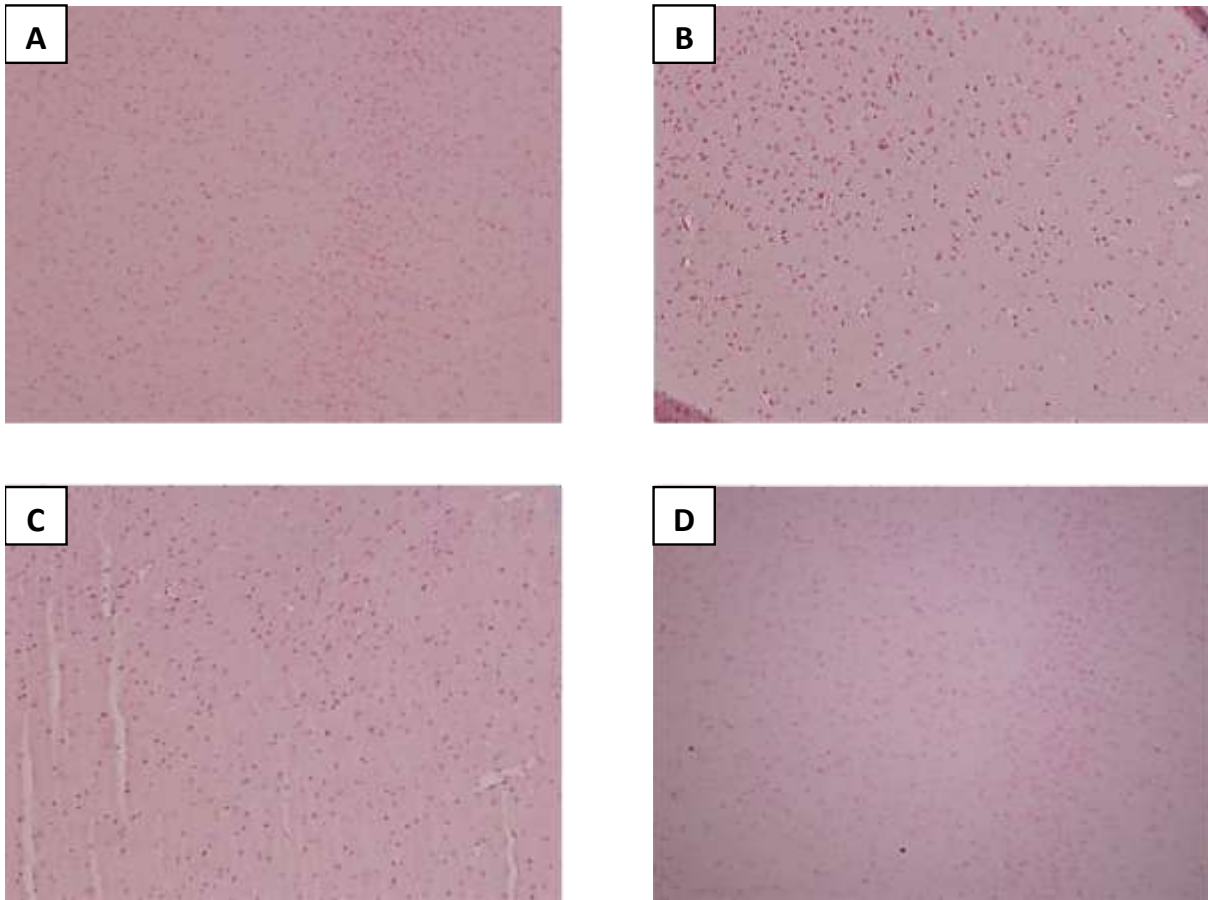
Figure 29. Ntg p17 injected animals: Negative control no primary antibodies top row (A-B) anti-mouse secondary antibodies and bottom row (C-D) anti-rabbit secondary antibodies (x 100).

Human histology

Brief introduction: It has proven almost impossible to request/identify and find samples of brain tissue taken from patients who died from HIV. It seems throughout Europe this is generally not pursued. With the help of the DOS (Jurek Krupinski) who is a consultant Neurologist at Hospital Mutua Terrassa in Barcelona, a trawl through thousands of archived samples revealed 3 brain tissue samples from HIV patients with signs of dementia that we were able to tissue process for histology. Below is the results of IHC examination of these samples for the primary reason to demonstrate the presence of p17 protein within the brain tissue. Sections were cut from blocks from these tissues. The patient details available for the individuals are listed in Appendix 1 at the back of this thesis. At least 10 sections from each block were stained with each antibody and representative examples of images seen are shown below.

Cortical neuronal staining of p17: Expression of p17 as identified using our specific antibody, was found within isolated groups of 'unhealthy' or dying neurons within the cortex (Fig. 34). Sometimes individual, scattered cortical neurons showed weakly positive for p17.

Association of p17 protein with regions of cortical inflammation in a patient with HIV and acute stroke. Top-cells with the appearance of macrophages stained positively (using anti-CD68 antibody-specific marker of macrophages) intracellularly (see magnified insert; Fig. 35), and in cortical areas, a mixture of what appear to be immune cells and glia are positively stained with p17 (by morphology alone).

p17 was also found associated with small and medium sized blood vessels within the cortex (Fig. 38). This could suggest again a role in abnormal activation of the endothelium and vasculature within the brain.

Some diffuse p17 staining of 'footprint' like areas that resembled Aβ-plaques was found in one of the patient samples. In addition, unhealthy neurones with the appearance of neuritic plaques were also p17 positive and several elements visually looking like neurodegenerative plaques were also positive for p17 within the cortex (Fig. 39).

Sections of the human HIV-positive brain from the cerebral cortex stained positive for both Aβ and p-Tau indicating a strong possibility that the patients had some form of cognitive decline and/or dementia (Fig. 40).

None HIV patients did not show any p17 staining as expected. In addition, negative controls without primary antibody showed the absence of none-specific staining (Fig. 41).
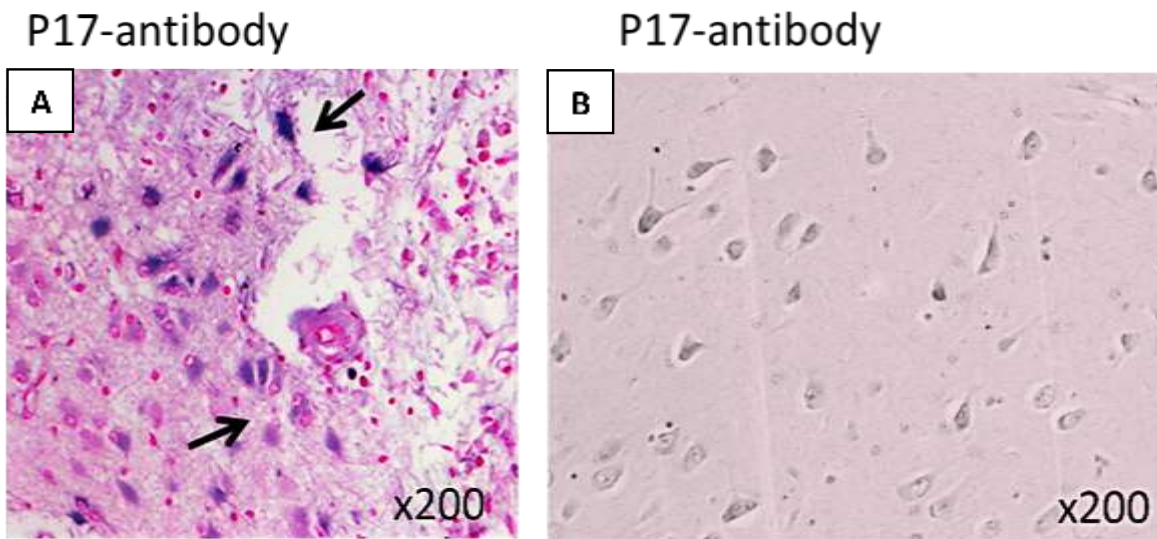
Figure 30. Left image (A) cerebral cortex section from a patient with HIV who died from acute stroke. p17 staining can be seen in groups of neurones within stroke-affected regions (blue). (B)-scattered weakly p17-positive (blue) cortical neurones.
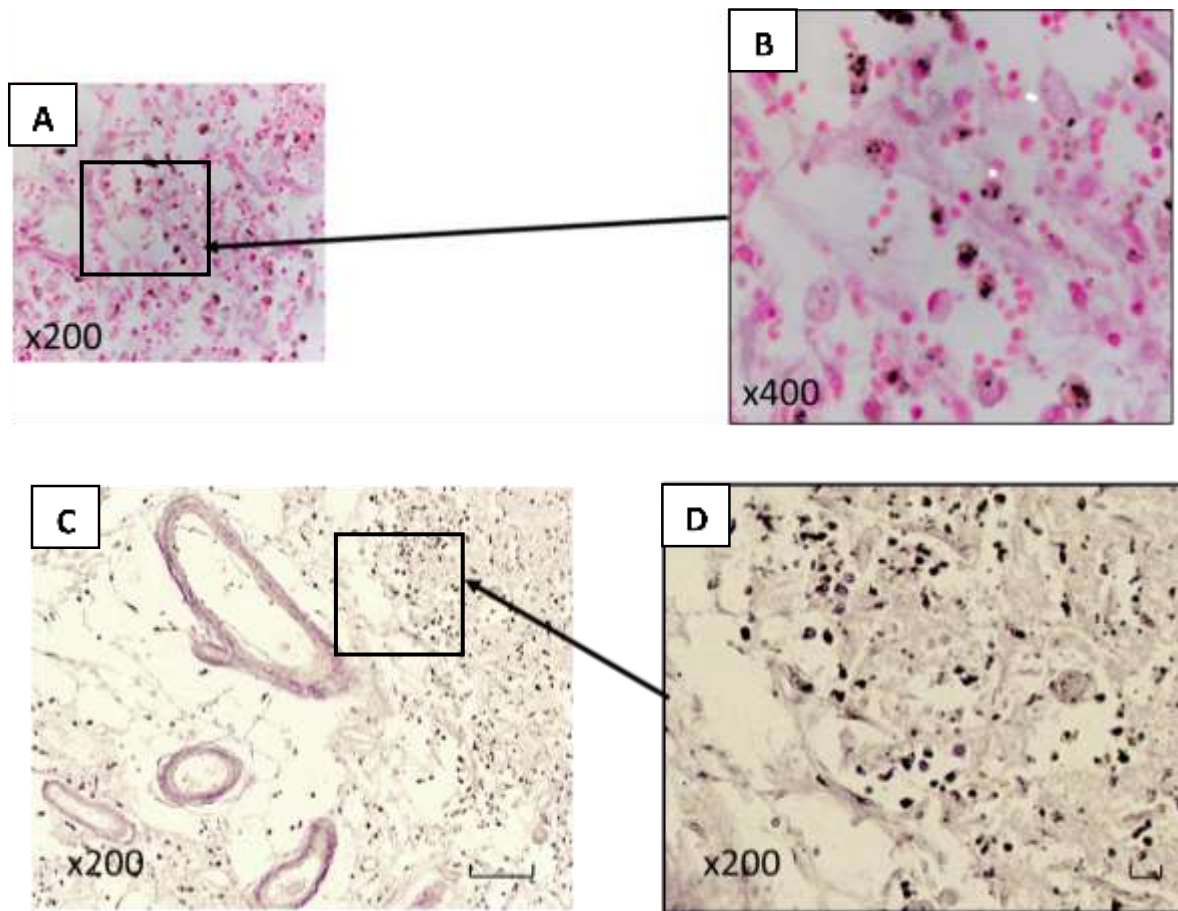
Figure 31. (A-B)-cells with the morphology of macrophages were positively stained using the p17 antibody, they appear to have p17 protein within the cytoplasm. (C-D)- an area of inflammation within the cortex shows many immune-like cells and possibly glia staining positive for p17 (blue/black).
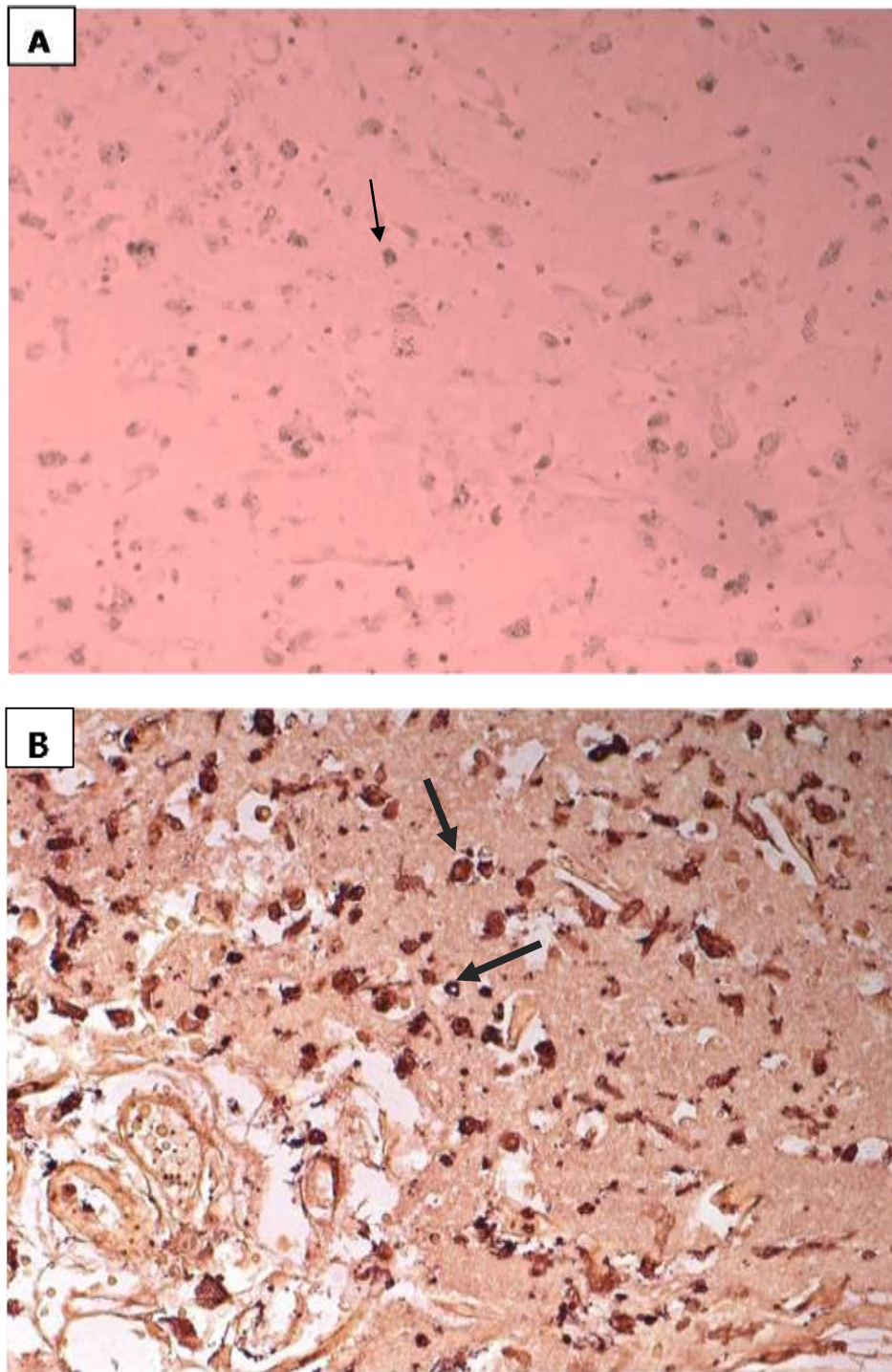
Figure 32. *(A) Immunohistochemical localization of CD68 (blue) and (B) co-localization of*

p17 (purple) and CD68 (brown) in human brain tissue from HIV patients. Sections A and B

are serial sections (approximately equivalent area but not identical tissue regions are shown

in the above images). (C7) (Arrows) thick arrow=CD68, thin arrow=p17. (Magnification x200).
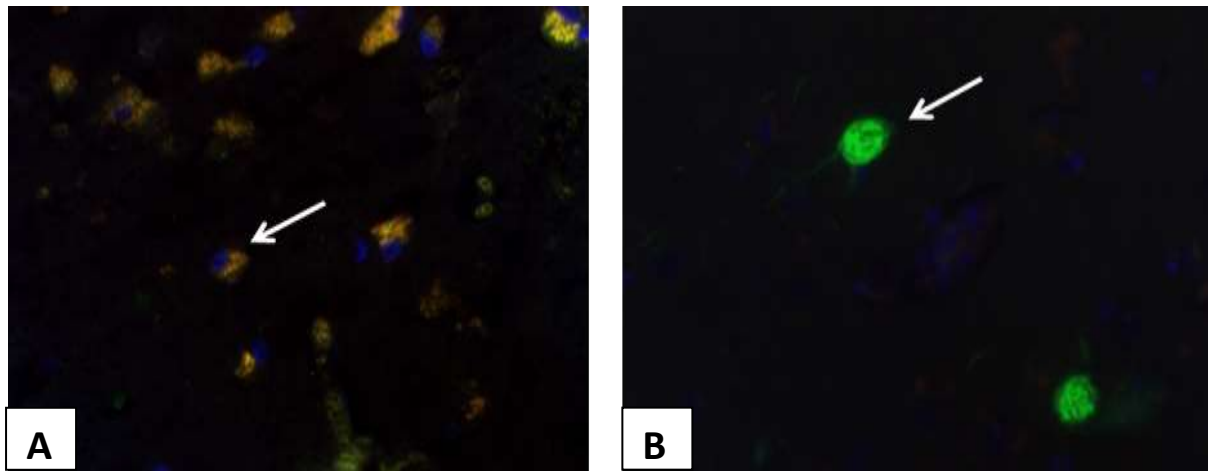
Figure 33. Double IF labelling shows (A)(magnification x200)co-localisation (yellow) of beta-amyloid (green) with p17 (red) in neurones. In (B) (magnification x400) p17 was expressed in neurones' no co-localisation of p-tau (green) with p17 (red)

P17
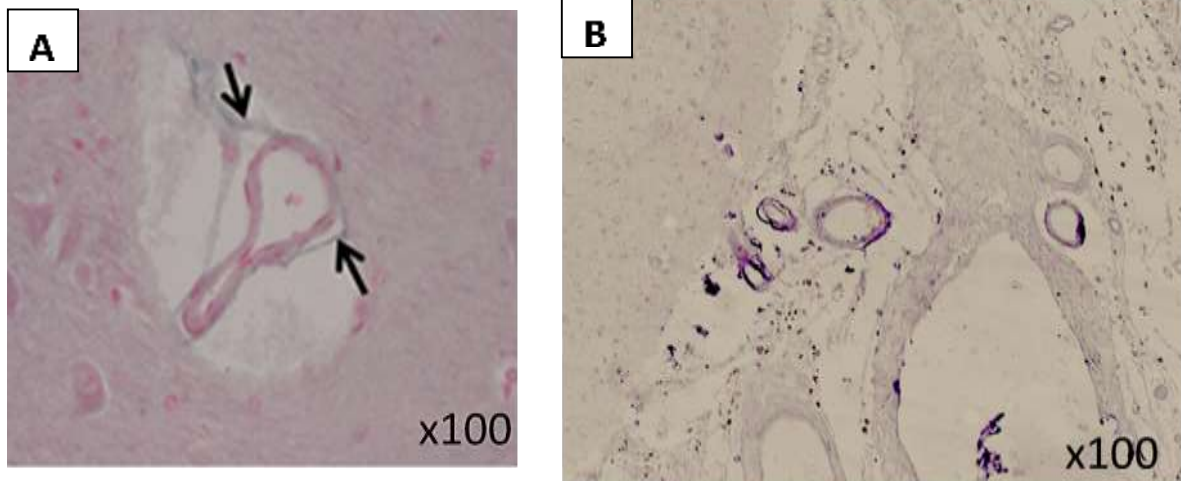
Figure 34. Top image (A)-a medium sized blood vessel within the cortex showing p17-positivity (arrows), the tissue is shrunken explaining the empty space around the vessel. (B)-a number of small-medium sized cortical vessels staining positive for p17 protein (red).
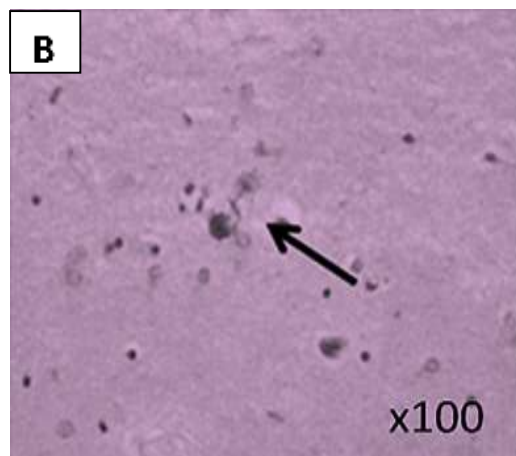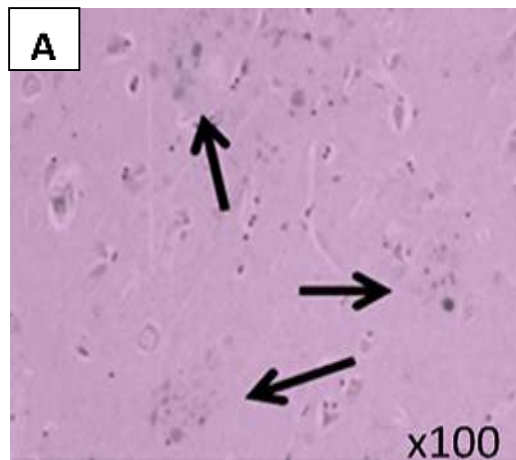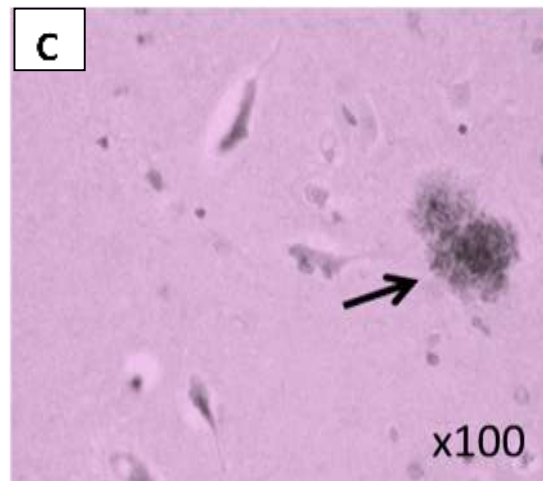
Figure 35. (A)-the arrows point to diffuse p17 staining of 'footprint' like areas of tissue similar in size and shape to Aβ-plaques. (B)-Shows what looks like a neuritic developing plaque also p17 positive and (C)-another plaque-like object within the cortex that stained positive for p17.
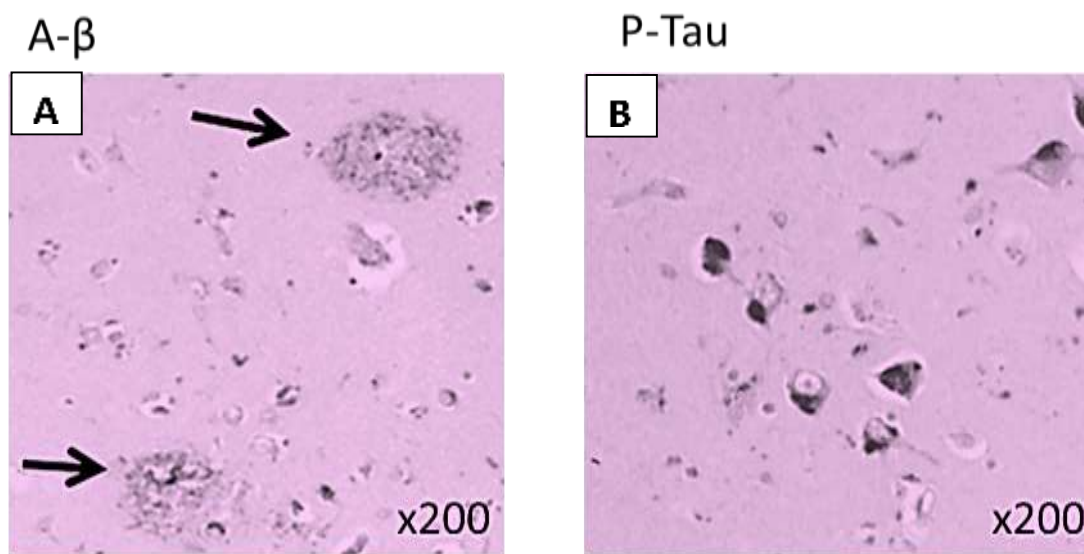
Figure 36. Left image (A)-Aβ positive staining within plaques, in the cortex of a patient with HIV suggesting the presence of dementia (arrows). (B)-neurones within the cortex were sporadically stained positive for p17 (peri-nuclear).
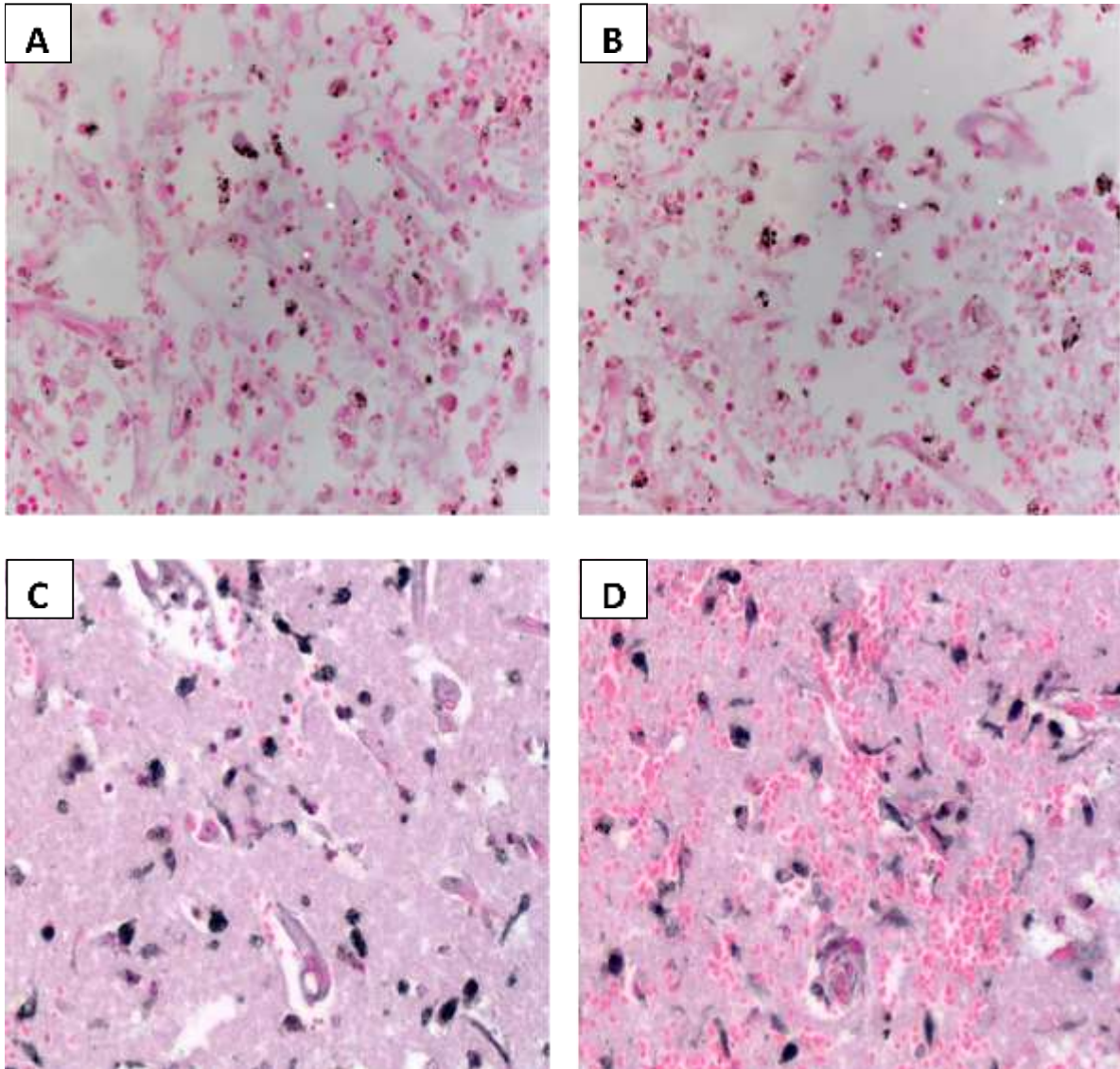
Figure 37. Immunohistochemical localization of p17 and Beta amyloid in human brain tissue from HIV patients. (A-B) p17 staining in immune cells (macrophages) in an inflammatory region of the cortex. (C-D) Beta amyloid staining in macrophages from a serial section (approximately equivalent area but not identical tissue regions are shown in the above images) of the same patient and in the same histological location (cerebral cortex). (Blue/grey staining; C7) (Arrows; magnification x200)

Discussion

Results indicate that p17 injected hippocampally into mice is able to remain within the parenchyma for weeks if not months in an experimental *in vivo* setting-the possibility therefore remains that where it is present it could have a biological action?

Our IHC/IF studies provided strong evidence that in the presence of p17, the brain undergoes what looks like neurodegenerative changes with expression of A-β/plaques and p-Tau, this is backed up with the behavioural studies completed in Barcelona that showed that animals injected with p17 had cognitive and memory deficits similar to that of AD 3 x Tg mice.

We also confirmed here that human patients who died and were HIV positive do express the p17 protein within the brain and localising in regions of inflammation, blood vessels neurons and plaque-like material/fibrils leading to the possibility that it could be a determinant of neurocognitive decline. Images used originate from all 3 of the patient samples of HIV-positive tissue.

For these reasons we subsequently decided to analyse the possible mechanism (s) through which it could be acting by performing *in vitro* experiments on brain vascular endothelial cells (as we found it associated with CD105-positive cortical microvessels) (Chapter 4) and Western blotting-signalling studies using both endothelial cells and neurons (Chapter 5).

Additional IHC images from control, p17-injected, 3 x Tg are supplied here (Fig. 42) with brief descriptions:
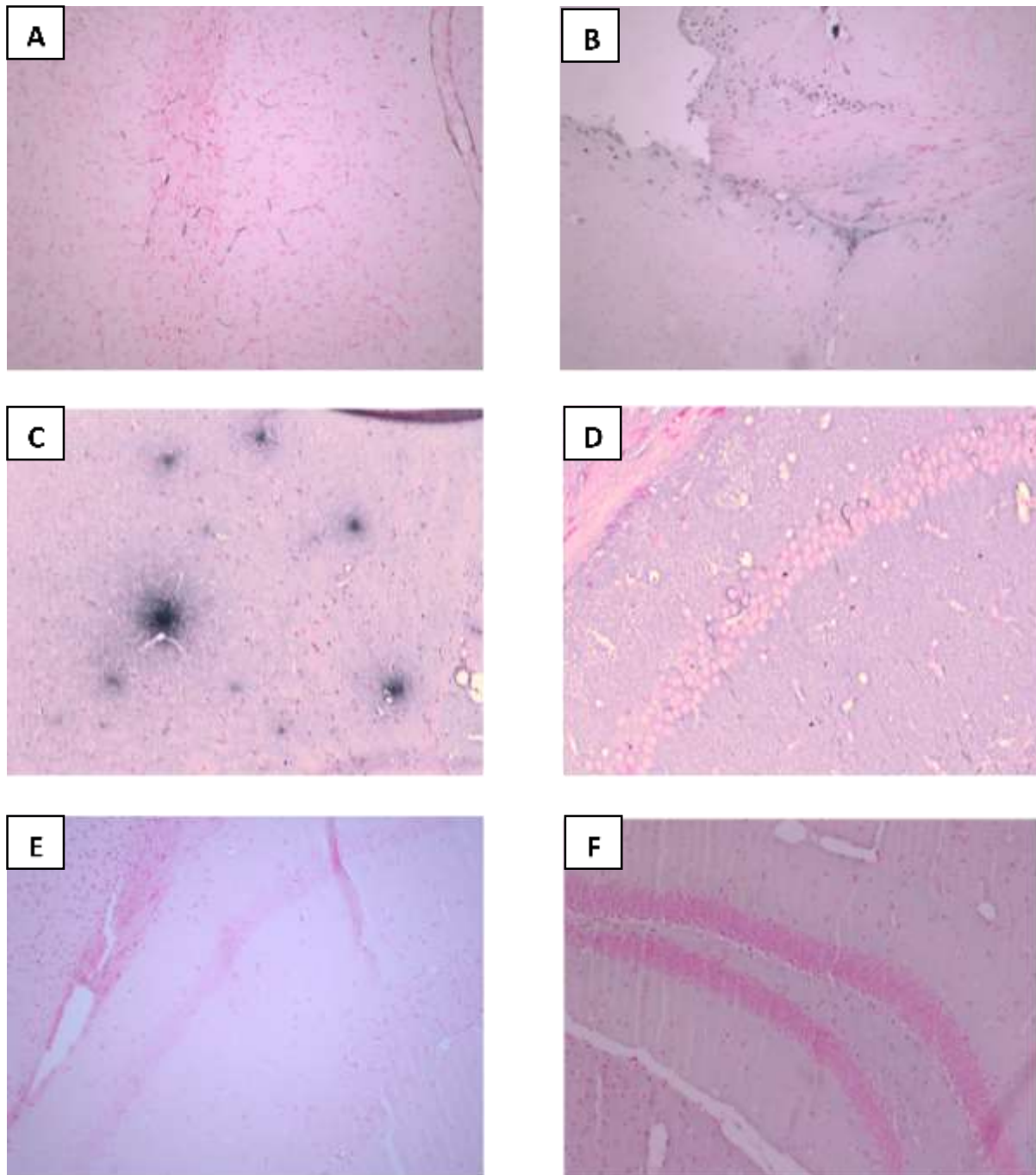
Figure 38. (A)-p17 injected cortical microvessels positive for CD105; (B)-cortical ECM positive and some neurons. (C)-transgenic positive for beta amyloid plaques and (D)-hippocampal positive neurons. (E)-negative control no primary antibody hippocampus (rabbit secondary) and (F)-the same but mouse secondary).

Chapter 4

Analysis of the signalling mechanism and angiogenic effects of p17 in vascular EC and neurons

Investigation of the mechanisms of p17 action in vascular EC and neurons

Introduction

In order to investigate how p17 protein might influence cell behaviour and survival, we firstly carried out a Kinexus phospho-screening exercise to try to identify activated proteins produced following incubation of our brain endothelial cells and rat cortical neurons (RCN). The aim of this chapter was to highlight any protein modifications that could be related to processes linked to neurodegeneration, abnormal angiogenesis (endothelial) and generally cell activation, cell death or apoptosis. Since previous work identified the ability of p17 to activate elements of angiogenesis in HUVEC, here, if we can identify some of the major protagonists defining the mechanisms through which p17 acts, we will have developed a greater understanding of its potential pathology in HIV patients.

Methods:

A Kinexus phospho-microarray screen was conducted using HcMEC and rat cortical neurons (RCN) cells exposed to p17 protein (5µg/ml) for 10 minutes in serum starved medium (our pilot and published data identified these as the ideal concentration and times for peak activation/phosphorylation of proteins *in vitro*). Activation of cells was confirmed by Western blotting of cell lysates and measurement of the phosphorylation of ERK (p-ERK1/2; increased greater than 6 fold compared to control untreated cells). Figure 43 shows the results for HcMEC and RCN compared with control untreated cells-and β-tubulin is used as a house-keeping/loading control. Angiogenesis assays were used to understand the importance of EGFR signalling and p17 in HcMEC with a specific inhibitor (anti-EGFR antibody; Millipore, USA).

Results:

Table 7 shows Kinexus profile summary and changes observed in expression of phospho-proteins between control and p17-treated HcMEC (8 minutes, 5µg/ml). Increased phosphorylation patterns are seen with EGFR, c-Jun, MEK and PLC-ɣ and others. Table 8 shows a Kinexus summary profile of changes in phospho-protein patterns between RCN control and p17-treated as above. Increases in phosphorylation included JNK, Tau and Akt.

A
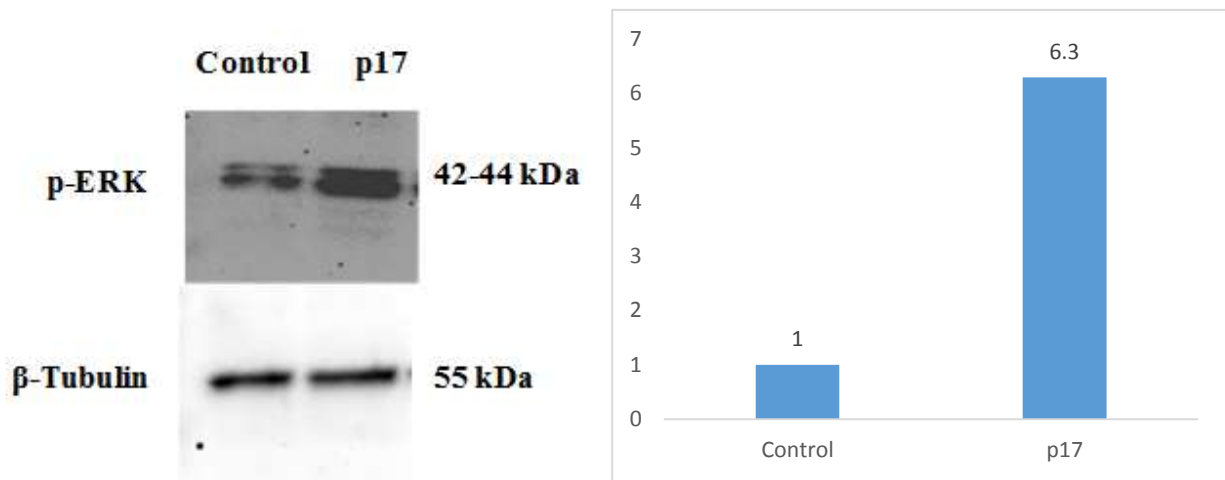
B
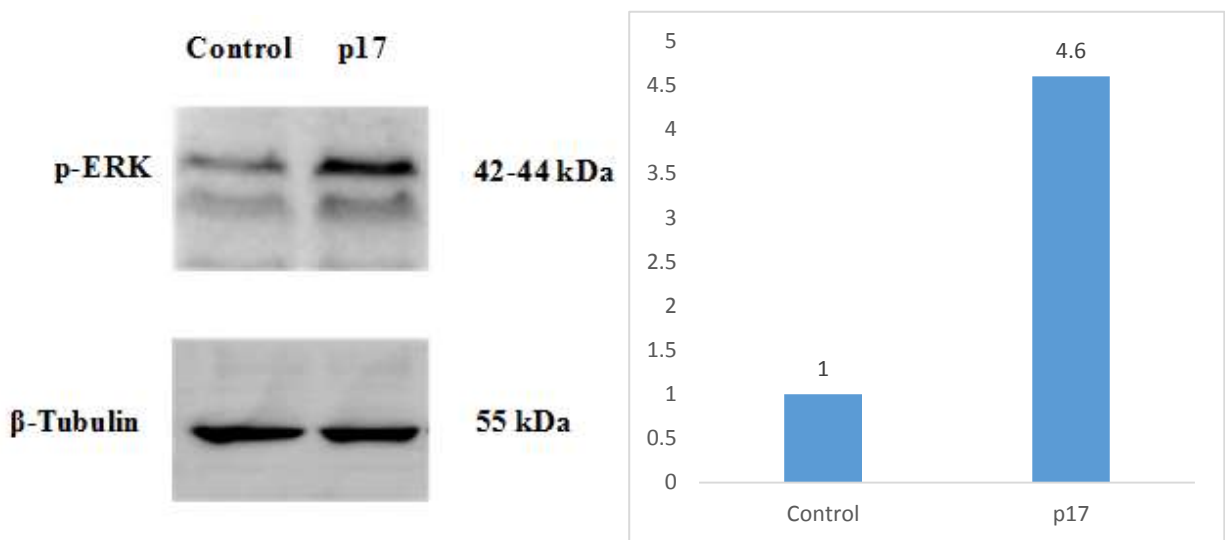
Figure 39. Top (A) shows Western blot of p-ERK1/2 control HcMEC cells (left) and p17-treated for 8 minutes (right) demonstrating a significant-approximate 6.3 fold increase (±2.5 for 3 experiments) in expression of the phospho-protein. Below shows identical results using RCN and showing a fold difference of approximately- 4.6 fold. (±2.8 for 3 experiments).

Target Protein Name	Phospho Site (Human)	Full Target Protein Name	Z-ratio (P17 (1), Control)	Z-score Difference (P17 (2)-Control)	Z-ratio (P17 (2), Control)	Z-score Difference (SO75X-Control)	Z-ratio (SO75X, Control)
CDK6	Y13	Cyclin-dependent protein-serine kinase 6	1.09	0.08	0.33	0.40	1.45
Chk1	S280	Checkpoint protein-serine kinase 1	1.09	0.54	2.21	0.43	1.56
MEK1 (MAP2K1)	T292	MAPK/ERK protein-serine kinase 1 (MKK1)	1.02	-0.12	-0.50	0.26	0.95
S6K	S411	p70 ribosomal protein-serine S6 kinase	0.99	0.34	1.38	0.30	1.07
PLCg1	Y771	1-phosphatidylinositol-4,5-bisphosphate phosphodiesterase gamma-1	0.71	0.23	0.92	0.35	1.28
p53	S37	Tumor suppressor protein p53 (antigenNY-CO-13)	0.60	0.13	0.53	0.54	1.94
PLC R(PLCg2)	Y753	1-phosphatidylinositol-4,5-bisphosphate phosphodiesterase gamma-2	0.44	0.10	0.39	0.31	1.10
EGFR	Y1172	Epidermal growth factor receptor-tyrosine kinase	0.34	-0.15	-0.61	0.30	1.07
Paxillin 1	Y31	Paxillin 1	0.34	0.31	1.26	0.15	0.53
FAK	S722	Focal adhesion protein-tyrosine kinase	-0.20	-0.06	-0.26	-0.34	-1.24
EGFR	Y1172	Epidermal growth factor receptor-tyrosine kinase	-0.38	-0.12	-0.51	0.28	1.02
pThr(RpAb)	pThr	pThr(RpAb)	-0.44	-0.16	-0.67	-0.39	-1.40
Rb	T826	Retinoblastoma-associated protein 1	-0.45	0.26	1.06	0.15	0.54
JAK2	Y1007+Y1008	Janus protein-tyrosine kinase 2	-0.62	-0.32	-1.32	-0.17	-0.62
PKCb2	T642	Protein-serine kinase C beta 2	-0.63	-0.29	-1.18	-0.12	-0.44
PKCm (PKD)	S910	Protein-serine kinase C mu (Protein kinase D)	-0.86	-0.34	-1.39	0.18	0.66
IRS1	Y612	Insulin receptor substrate 1	-1.23	-0.32	-1.32	-0.28	-1.01
Paxillin 1	Y118	Paxillin 1	-1.46	-0.27	-1.10	-0.27	-0.98

Table 7. Kinexus summary profile results for changes in phospho-protein expressions in HcMEC treated with p17 for 8 minutes. p17-phospho- increase c-Jun/PAK-1/PKC-Theta/PLC-gamma-1/p-EGFR/Jun and MEK/p53 and p-AKT. (Pink= increase- yellow= decrease)

Serial No.	Antibody Codes	Target Protein Name	Phospho Site (Human)		
181	PN027	Dok2	Y139		1.63
413	PK149	Lck	Y394		1.59
237	PK017-1	FAK	Y397		1.54
154	PN024	CREB1	S133		1.17
286	PN036	Histone H2A.X	S140		1.14
384	PK035-1	JNK1/2/3	T183+Y185		1.08
741	PK156	S6K	S424		1.02
285	PN035	Histone H1	phospho CDK1 sites		1.01
807	PN085	Tau	S516		-1.00
714	PN071	Rb	T826		-1.01
735	PK101-2	RSK1/2	S380/S386		-1.06
229	PK016	Erk5 (MAPK7)	T218+Y220		-1.10
585	PK072-5	PKBa (Akt1)	S473		-1.13
172	PN026	Dab1	Y198		-1.17
788	PN082-1	STAT3	Y705		-1.30
230	PK016-3	Erk5 (MAPK7)	T218+Y220		-1.47
746	PK145	S6Kb1	T252		-1.59
811	PN091	Tau	S717		-1.68
812	PN092	Tau	S721		-1.68
682	PP003	PTEN	S380+T382+S385		-1.90
848	CN003	pThr(MmAb)	pThr		-2.20

Significant increases beyond control included p-FAK, CREB1, JNK1/2/3/, Tau, and AKT-1

Table 8. Kinexus summary profile results for changes in phospho-protein expressions in RCM treated with p17 for 8 minutes.

The microarray data-produced by the company shows increases and decreases compared with control untreated samples (=1.0) as a function of fold differences. Above 1.0 in duplicate shows a significant increase according to the tabulation and less than -1.0 a decrease. The greater the difference the higher the fold increase. We chose proteins that showed increased phosphorylation linked to endothelial and neuronal signalling cascades.

Western blot confirmation of key Kinexus results (HcMEC): To confirm the array results, Western blotting using protein- specific antibodies was used and proteins associated with key

signalling pathways relevant to the study e.g. angiogenesis, neurodegeneration and apoptosis were examined. For HcMEC, p17 (8 minutes exposure at 5µg/ml) increased phosphorylation of the receptor EGFR by approximately 2.5 fold compared with the untreated control (Fig. 44). Figure 45 shows that inhibition of the EGFR using a specific peptide, was sufficient to block receptor activation and down-stream signalling via ERK1/2. Figure 46 shows the results of additional Western blotting experiments.
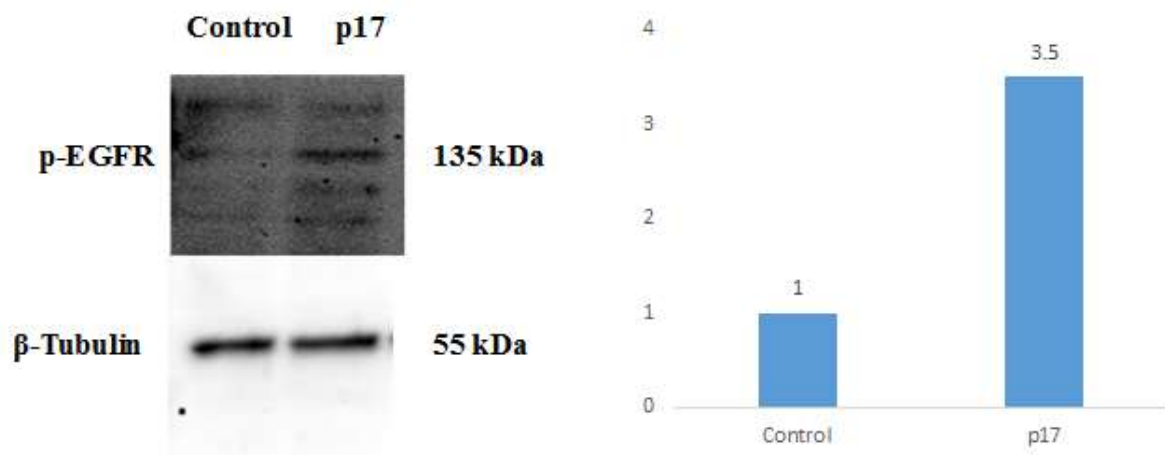
Figure 40. Western blotting result showing approximately a 3.5 fold increase(±1.7 for 3 experiments) in p-EGFR after exposure to p17 (8 minutes; 5µg/ml). Experiments were performed at least twice with a representative example shown here.
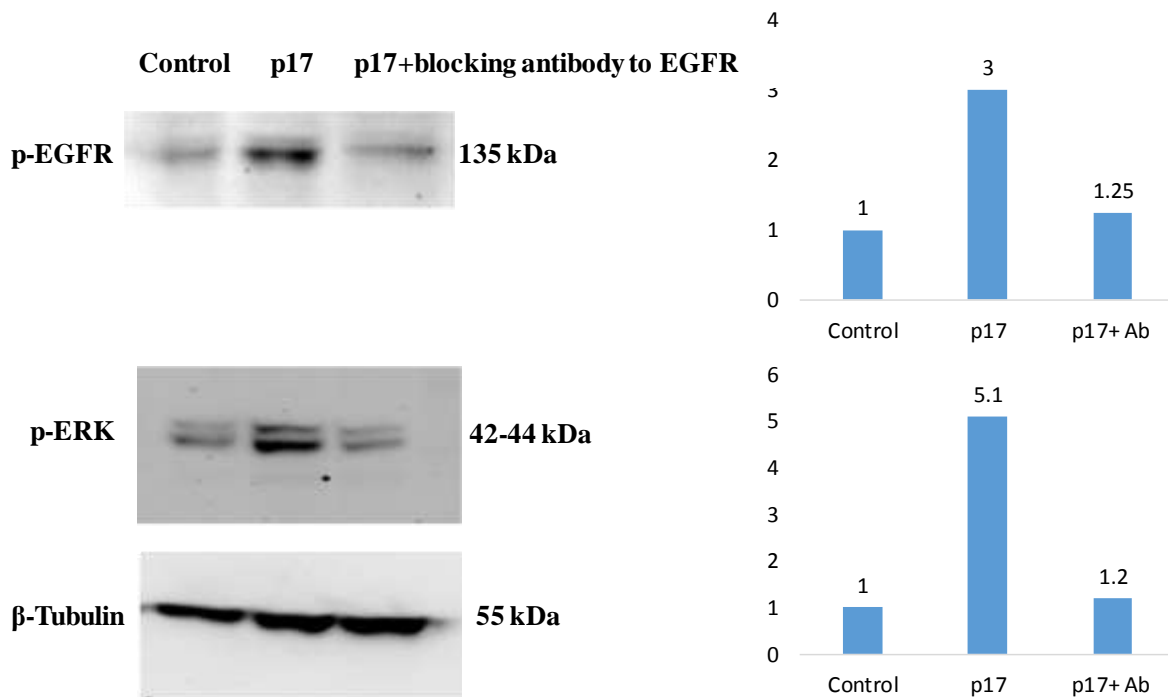
Figure 41. Here, HcMEC were exposed to p17 (8 minutes; 5µg/ml) and increases in expression of both p-ERK1/2 and p-EGFR can be seen by Western blotting compared with the control (lane 1=control, lane 2=+p17). In addition, following 4h incubation with an EGFR receptor blocking peptide, both p-EGFR and down-stream p-ERK1/2 were notably inhibited (lane 3) (±1.5 EGFR and ±3.2 ERK1/2 for 3 experiments).

A

	Control	FGF-2	p17	S75X	
p-Tau					79 kDa
p-PLCγ1					155 kDa
p-Akt					60 kDa
β- actin					42 kDa

B

	Control	p17	
p-p53			53 kDa
β- actin			42 kDa
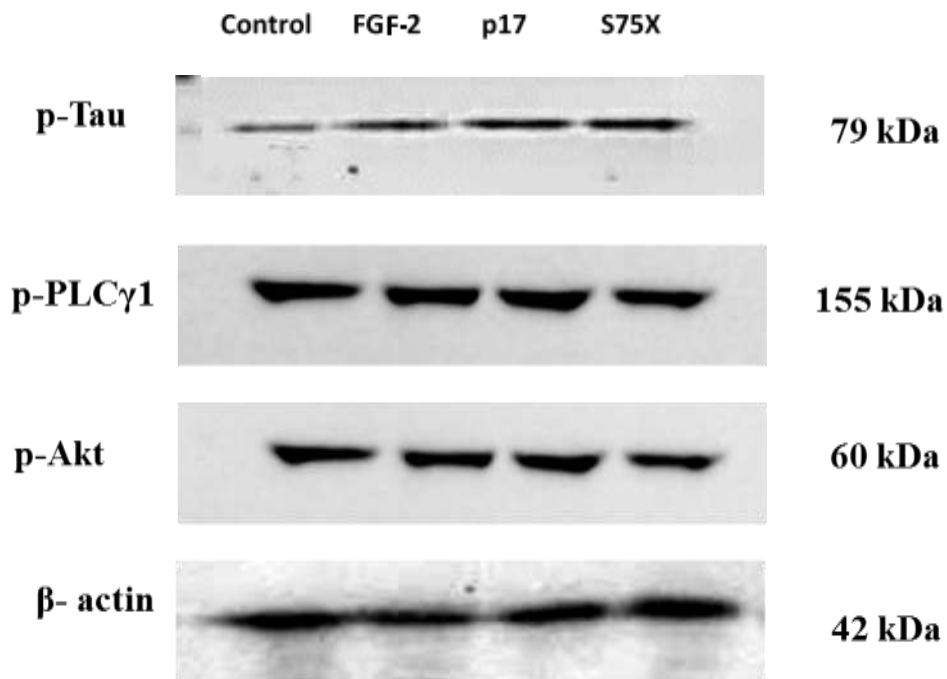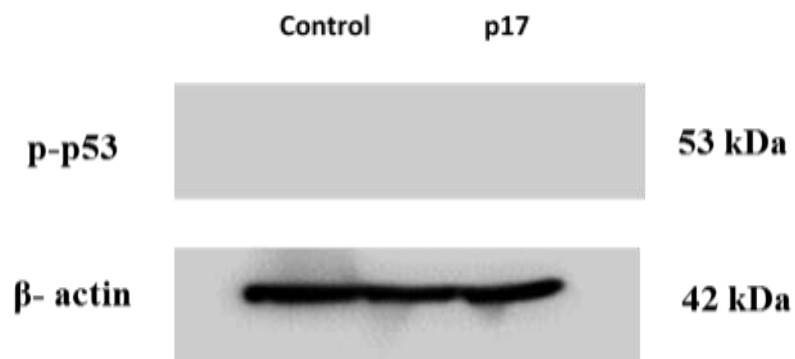
Figure 42. Additional western blots showing HcMEC expression of various phosphorylated proteins after p17 incubation (8 minutes). All experiments were repeated and above is a representative example. Bar charts are not included as no clear differences were found between control and treated samples in these cases. Here, there was a small increase in phosphorylation of Tau but this was not considered significant.

Western blotting results for RCN: as above, RCN were treated with p17 for 8 minutes and Western blotting demonstrated a notable increase in expression of p-ERK1/2 (5.5. fold) and p-IRS-1 (2.5. fold) compared to control untreated cells (Fig. 47). Figure 48 shows a similar although weaker increase in expression of EGFR (2.0 fold), whilst in Figure 49 p17 is shown to phosphorylate FAK by approximately 2.5 fold compared with control untreated cells. FAK is known to regulate cell spreading and movement and hence p17 and variants might impact upon these processes through a signalling pathway involving FAK (see Discussion section for more detail). All experiments were carried out at least twice and representative examples are shown. Figure 50 shows results of additional Western blotting experiments.

The additional Western blotting results showing none-affected proteins/phosphorylation in p17 treated samples. PLC-gamma, AKT and p-53 did not show increased activation after exposure to p17 and hence they were not investigated further within the confines of this project. p-P53 was not identified in our experiments, we are considering the validity of the antibody.
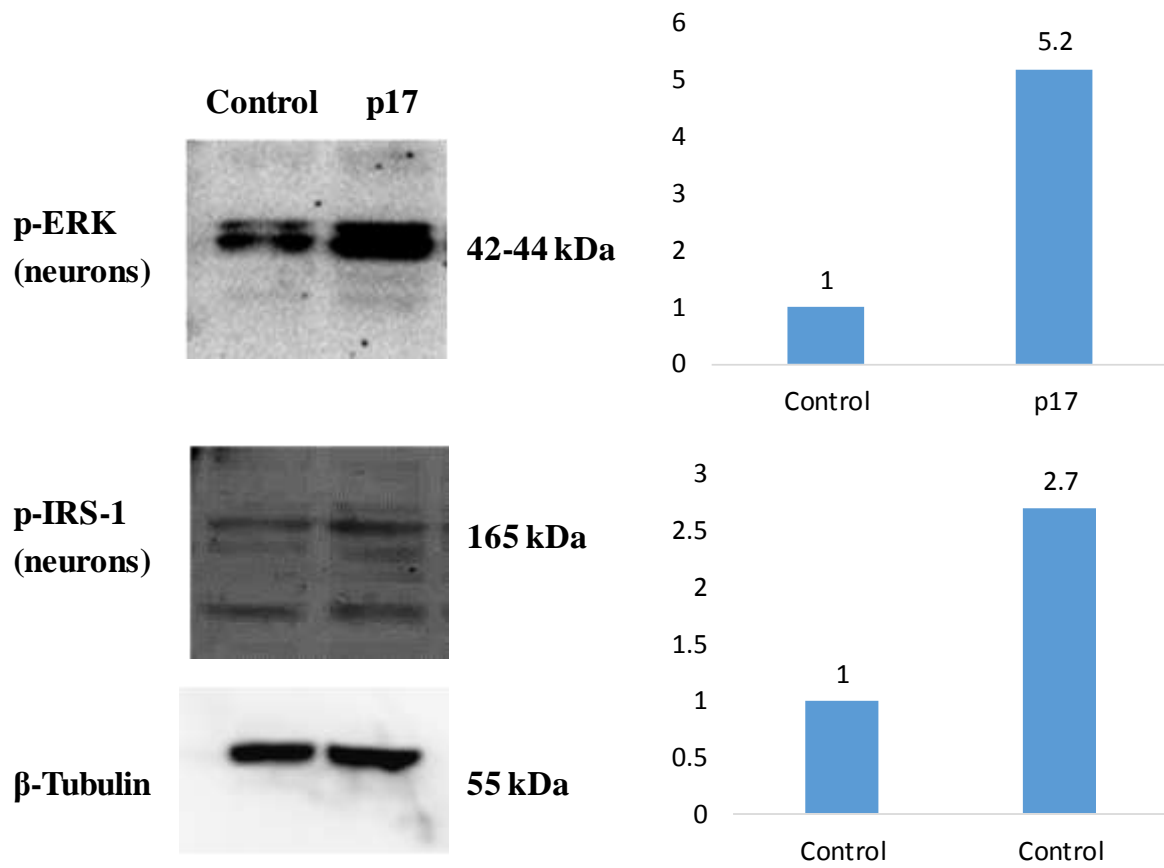
Figure 43. RCN were exposed to p17 in culture for 8 minutes (5µg/ml) and Western blotting carried out. Results showed that both ERK1/2 (5.2. fold ±2.8 for 3 experiments)) and IRS-1 (2.7. fold ±2.3 for 3 experiments)) were increased compared with the control cells. Representative experiment of two shown above.
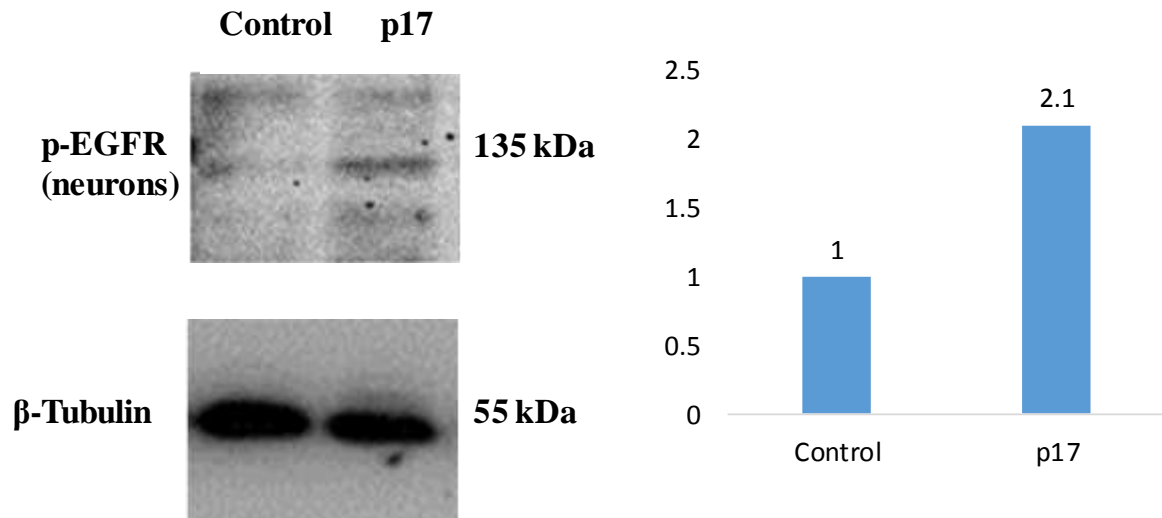
Figure 44. Western blotting showed that 8 minutes exposure to p17 increased phosphorylation of EGFR although only weakly in RCN (2.1 fold ±1.5 for 3 experiments) compared with control untreated cells). Above is a representative example of two experiments.

Figure 45. Western blotting showed that 8 minutes exposure to p17 increased phosphorylation of FAK in RCN (3.5 fold ±2.8 for 3 experiments) compared with control untreated cells). Above is a representative example of two experiments.
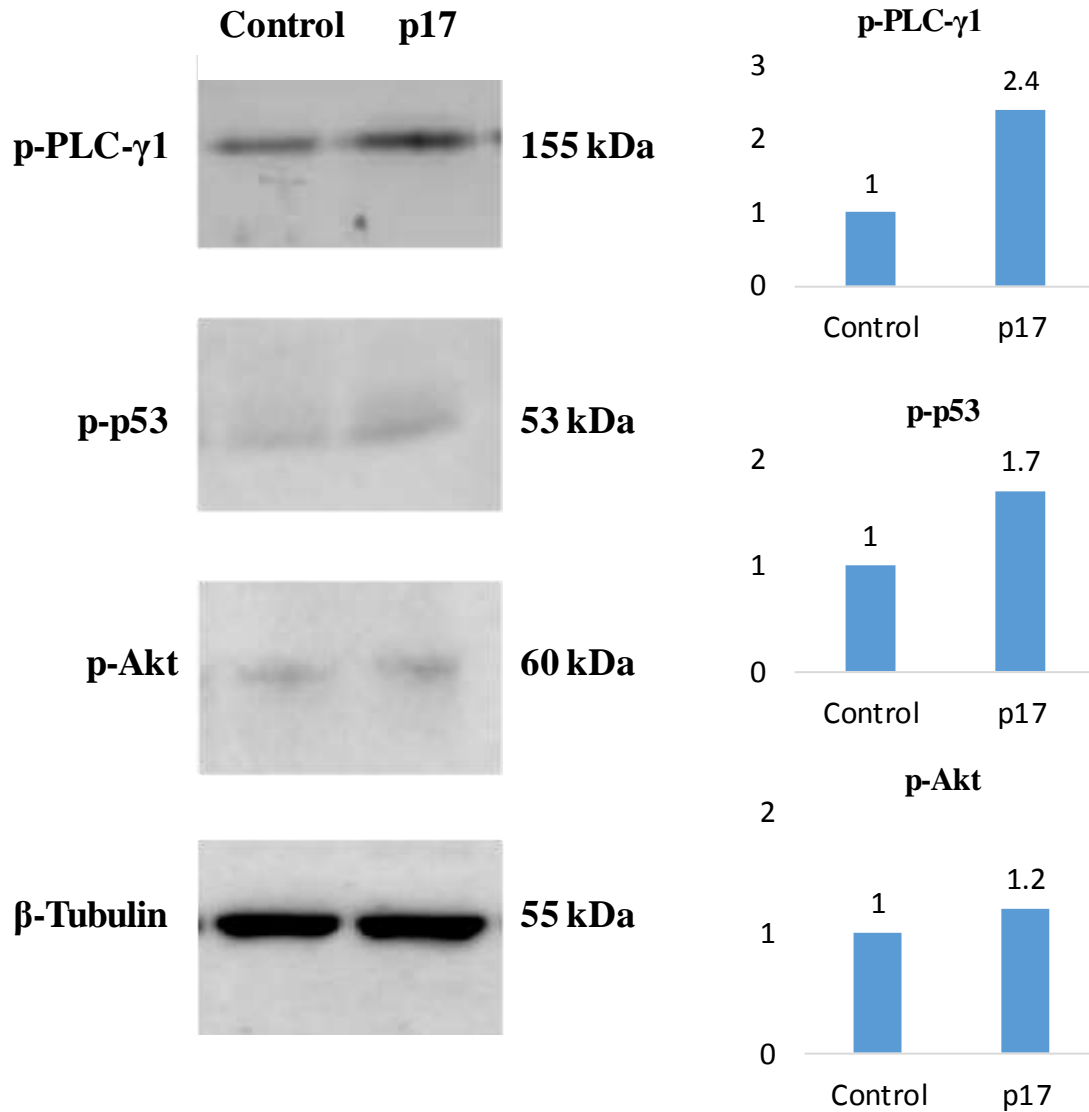
Figure 46. Additional western blots showing neuronal expression of various phosphorylated proteins after p17 incubation (8 minutes). All experiments were repeated and above is a representative example. Bar charts are not included as no clear differences were found between control and treated samples in these cases with the exception of PLC-ɣ1(±1.9 for 3 experiments) 2.4 fold .

Angiogenesis assays:

Basic angiogenesis assays were used to identify the effects of p17 on endothelial cell activity and here we compared one of the mutants supplied by our collaborators S75X as they showed differing activity of this variant in their previous experiments with B-cells.

Migration: p17 and a mutant peptide S75X: p17 significantly increased the number of cells migrating and the distance migrated in the razor wound assay after 24h compared with control cells (Fig. 51). S075X produced similar results but the cells became more polarised (i.e. directional), had larger gaps between them and therefore migrated further. The figure represents an example and all experiments were performed twice.

Angiogenesis assays
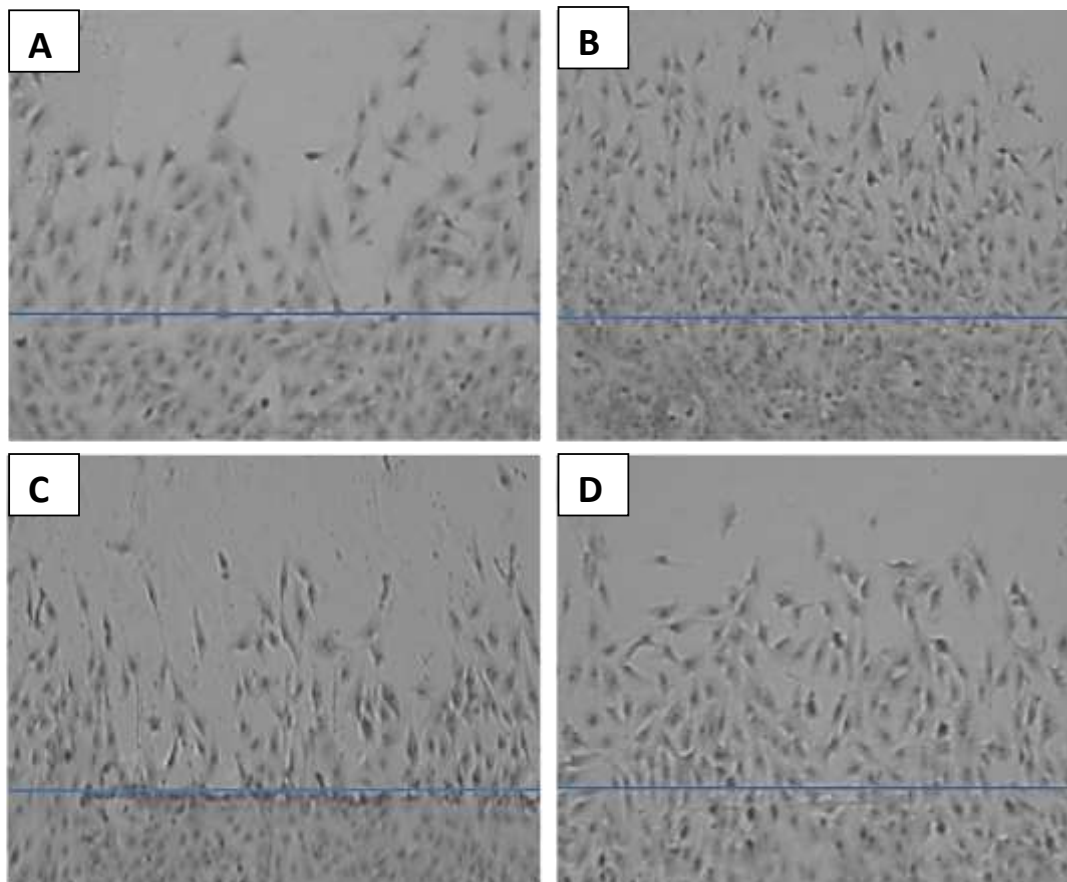
Cell migration distance
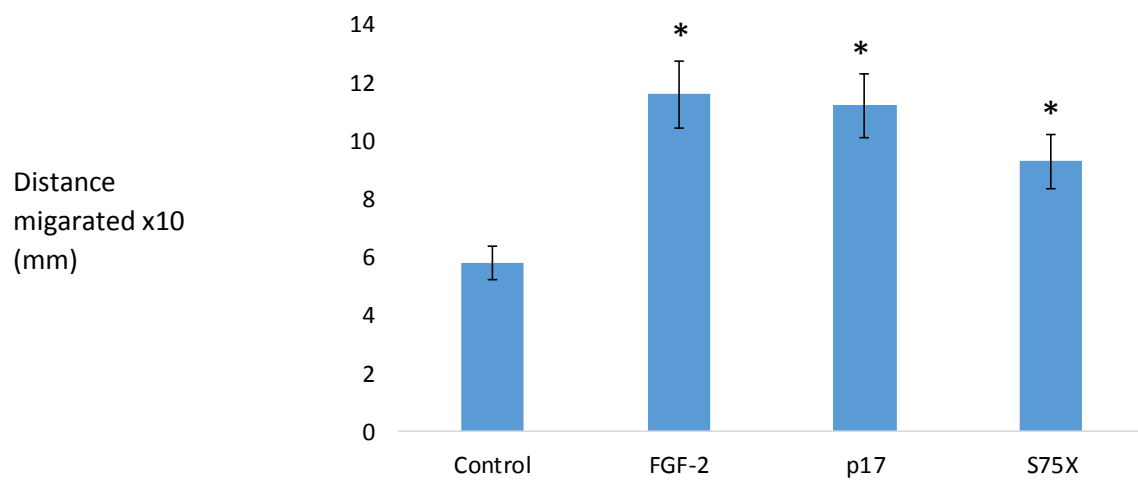
Number of cells migrated
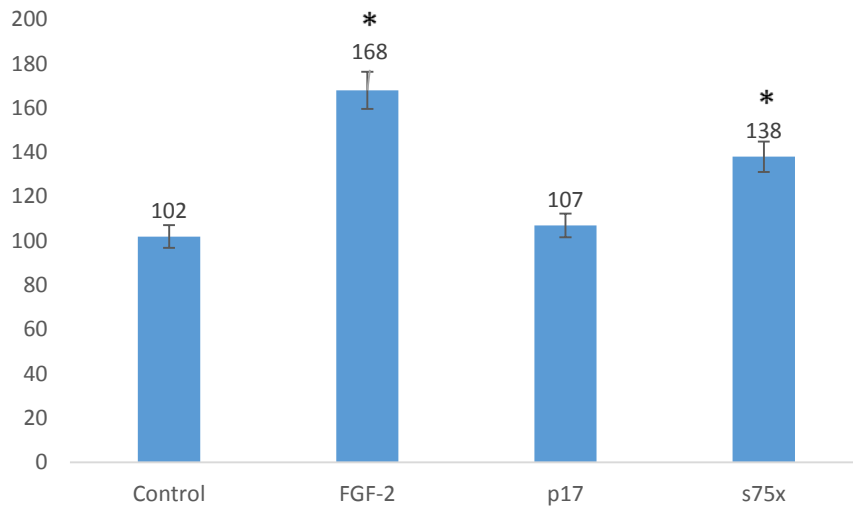
Figure 47. Photomicrograph showing the pro-angiogenic effects of (B) FGF-2, (C) S75X and (D) p17 on razor-blade-wound healing in hCMEC. (A) is a control. The numbers of migrated cells in the denuded area were counted. Experiments were performed in triplicate wells and repeated three times. A representative example is shown. The bar graph shows the stimulatory effects of FGF-2 (25ng /ml), p17 and its mutant S75X (5µg /ml) on wound healing in hCMEC. The bar graph shows the mean ± S.D. (*) (**) signify a statistically significant difference (p < 0.05 and p < 0.01) compared with the control. The bar-garph (top) shows the distance (cm) the cells migrated from the wound scratch. The second (bottom) bar-graph shows the number of cell migrated from the wound scratch.
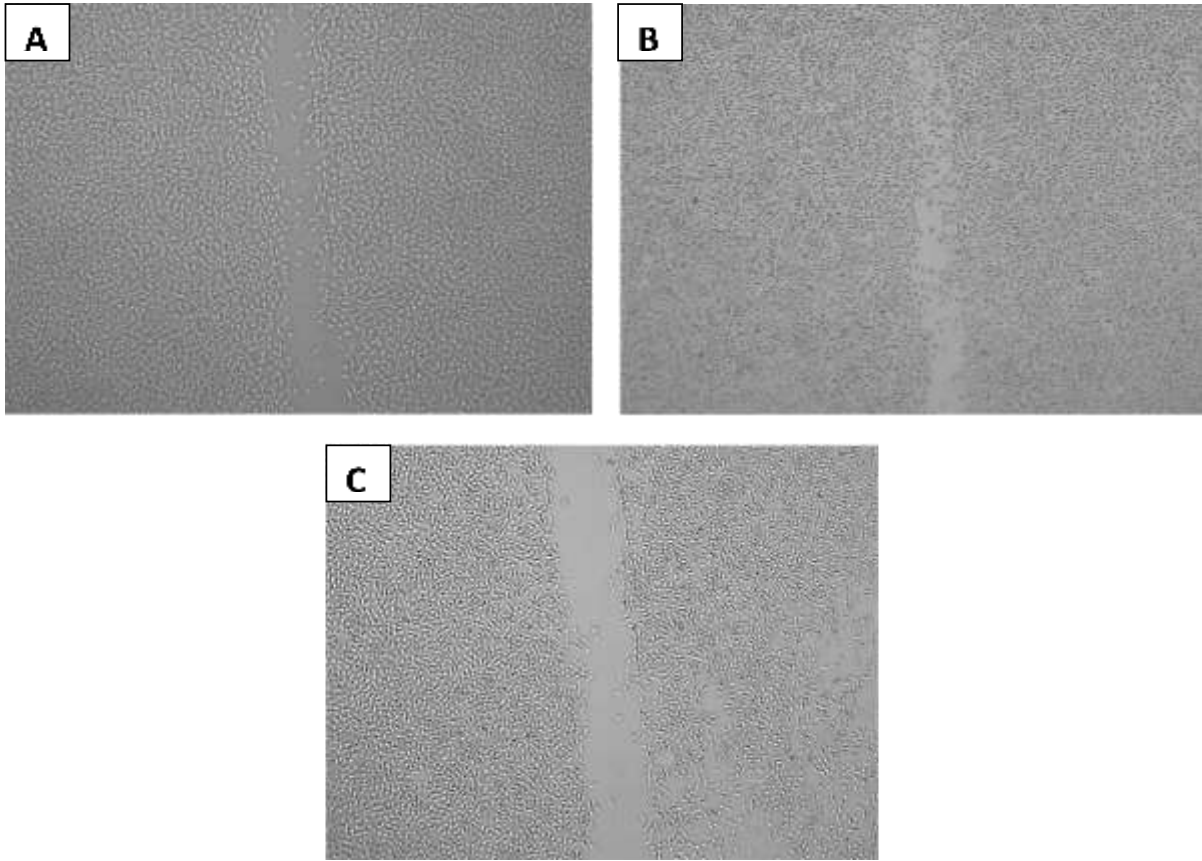
The degree of wound closure (percentage)
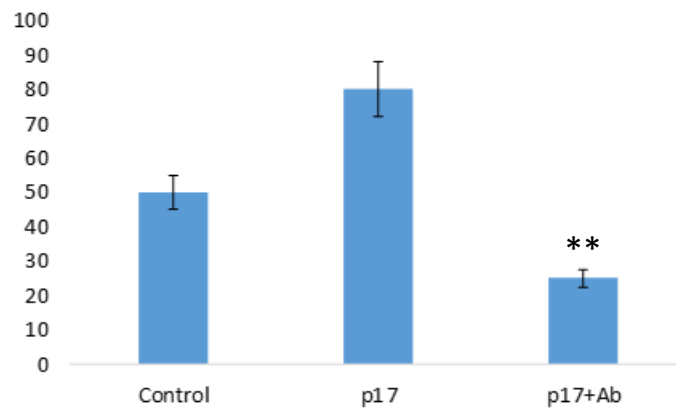
Figure 48. Above, Top left (A) control none-treated scratch-wound after 24h showing some wound closure (approximately 50%), top right (B)-treatment with p17 (5µg/ml) showing enhanced wound closure (75-100%) and bottom image (C)-pre-treated cells with EGFR

inhibitory peptide (24h) then cells incubated with p17 showing that the inhibitor inhibited cell migration. Experiments were repeated in triplicate and a representative example is shown. The bar graph shows the mean ± S.D. (*) (**) signify a statistically significant difference (p < 0.05 and p < 0.01) compared with the control. The bar-graph shows the percentage of wound closure of control and treated cells.

Angiogenesis assays (spheroid formation and sprouting) and the effects of p17 and a mutant peptide S75X: Figure 53 shows single 3-dimensional spheroids sprouting after 24h in serum poor medium with and without p17, S075X or FGF-2. Sprouting can be seen in all three treated samples. Figure 54 shows examples of 2 spheroids in close proximity where we are examining the chemotactic responses during sprouting. S075X appears to produce the strongest chemotactic response (sprout to sprout). Also shown in this figure are close up images of some sprouts demonstrating that S075X again, produces longer thinner sprouts than the native protein p17.
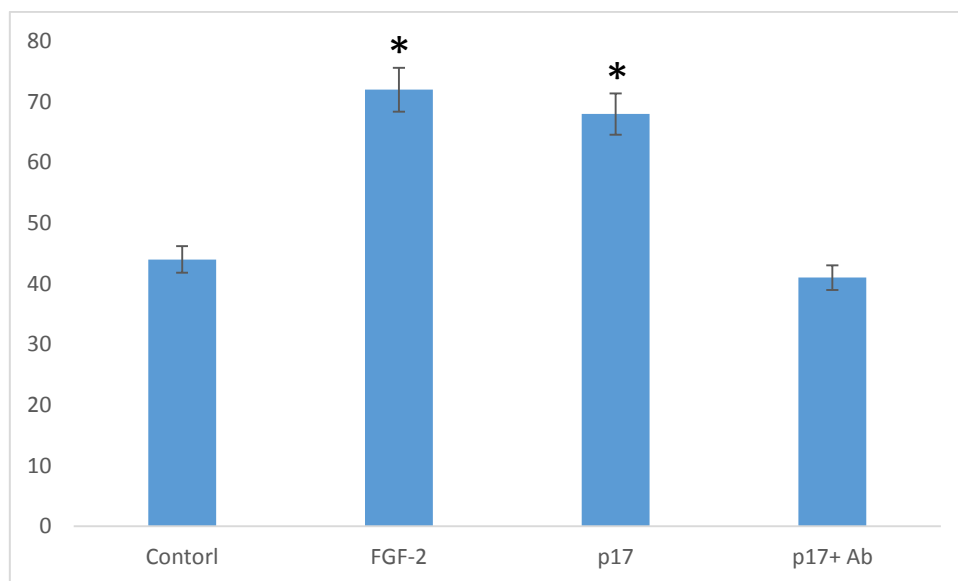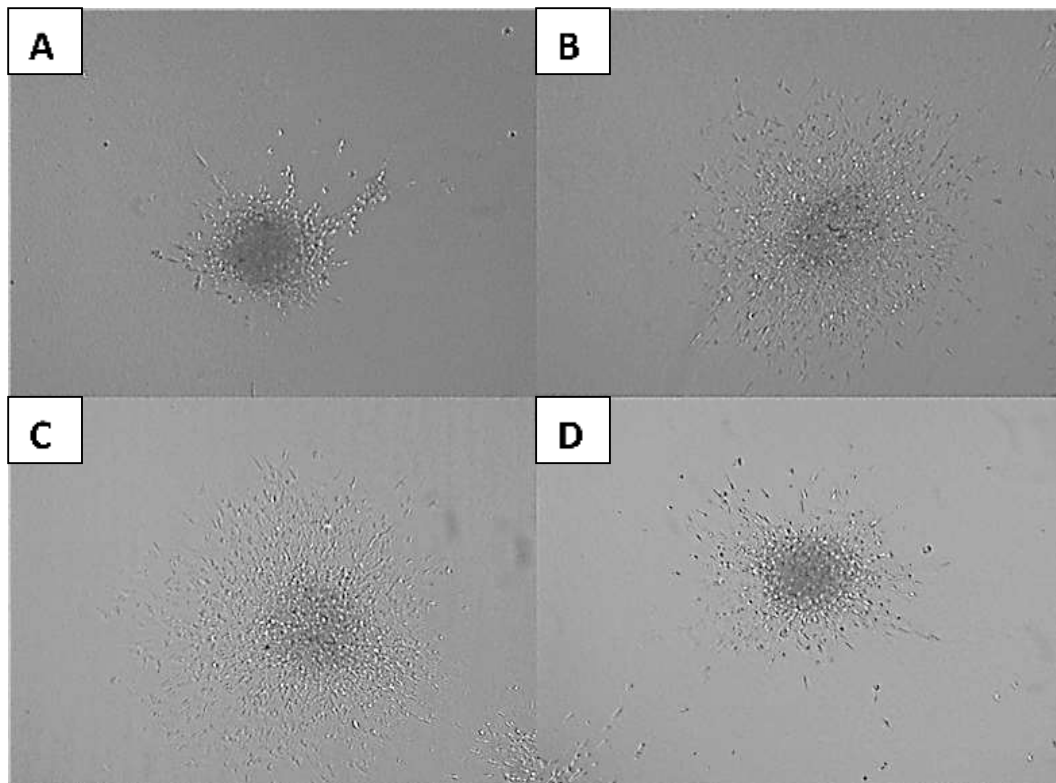
Figure 49. Photomicrograph showing the effects of (B) FGF-2, (C) p17 and (D) p17 plus EGFR inhibitor on 3D-spheroid sprout formation. (A) Is a control. Experiments were performed three times and a representative example is shown. The bar graph shows Pro-angiogenic effects of p17 and a specific inhibition when combined with EGFR inhibitor on spheroid formation. Mean distance sprouted from edge of spheroid (pixels).
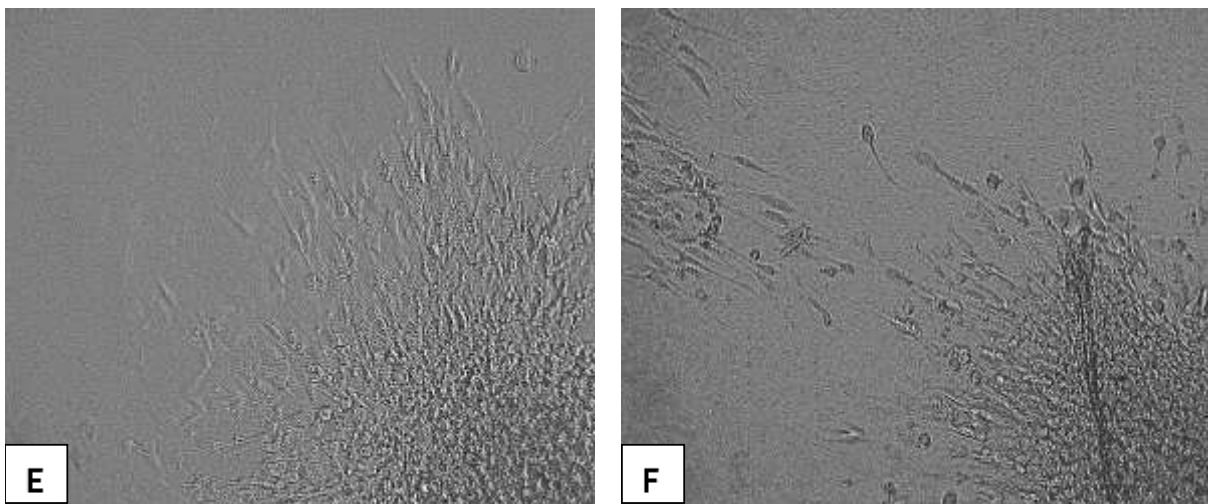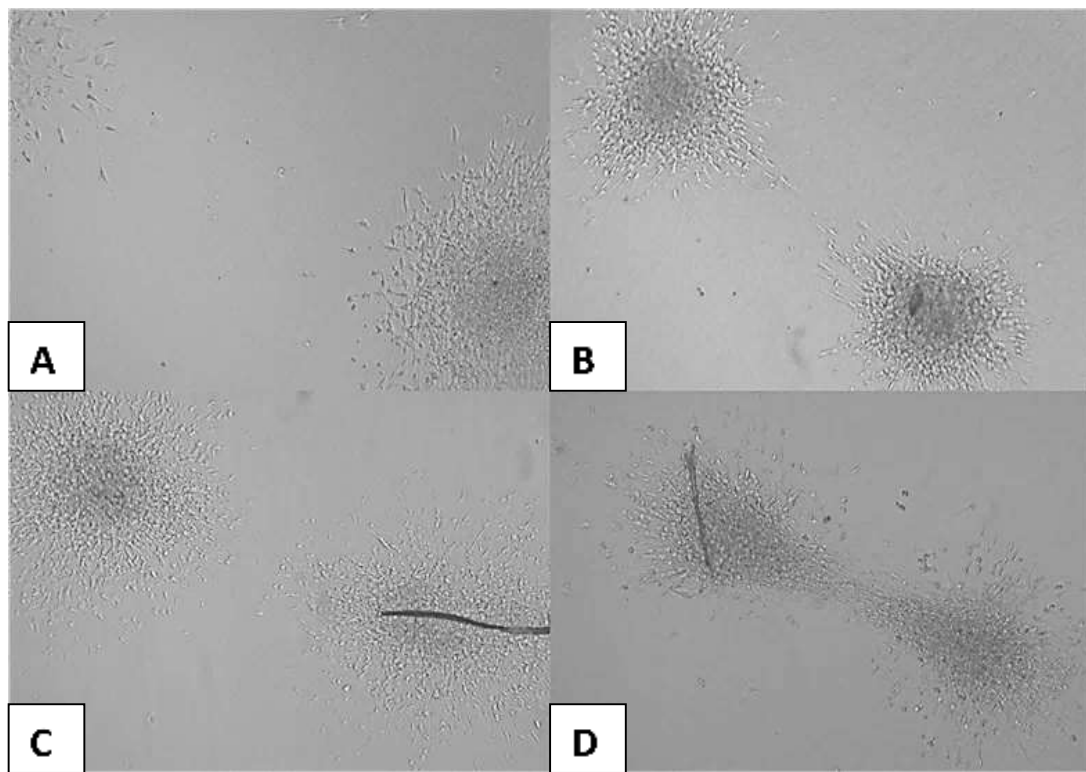
Figure 50. Photomicrograph showing the effects of the (B) FGF-2, (C) p17 and (D) S75X on two adjacent 3D-spheroid sprout formation. (A) is a control. (lower panels) shows magnified version of p17 (E) and S75X (F).

Angiogenesis assays (spheroid formation and sprouting) and the effects of p17 and other mutants. Figure 55 shows EGFR antagonist inhibition of p17 and S075X-induced chemotactic directed sprouting between two proximal spheroids.
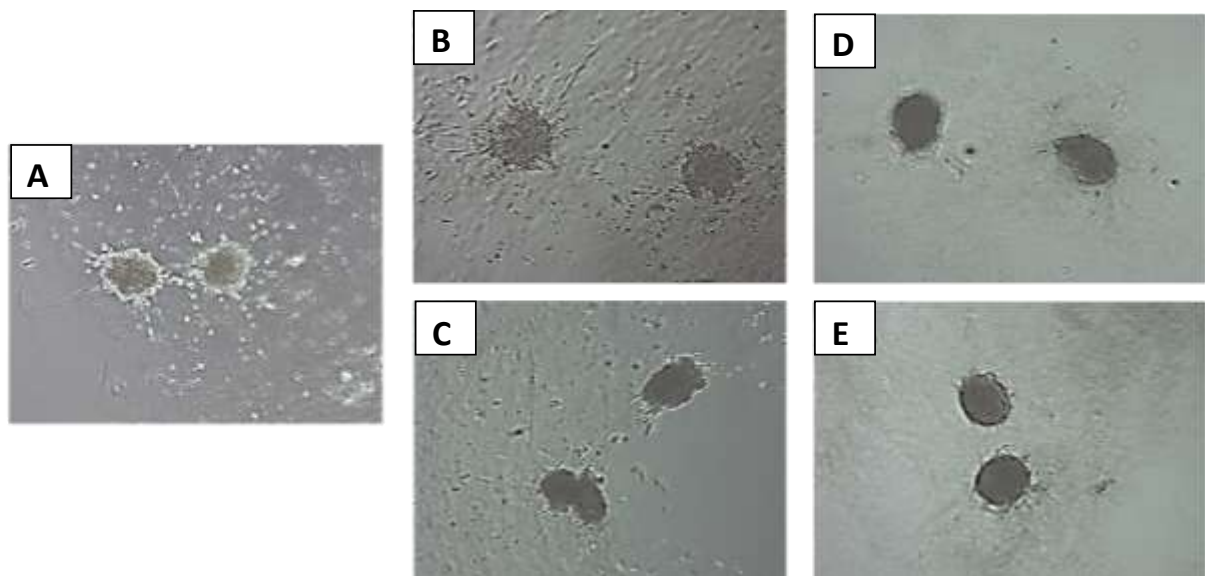
Figure 51. Left image (A)-control spheroids showing sprouting directed towards each other; middle panel, (B)-p17-treated spheroids and (D)-with EGFR inhibitor blocking the sprouting and chemotactic response. Lower middle panel (C)-S075x treated and right panel (E) with EGFR inhibitor showing the same effect. Experiments were repeated twice with similar results.

Spheroids from other mutants:
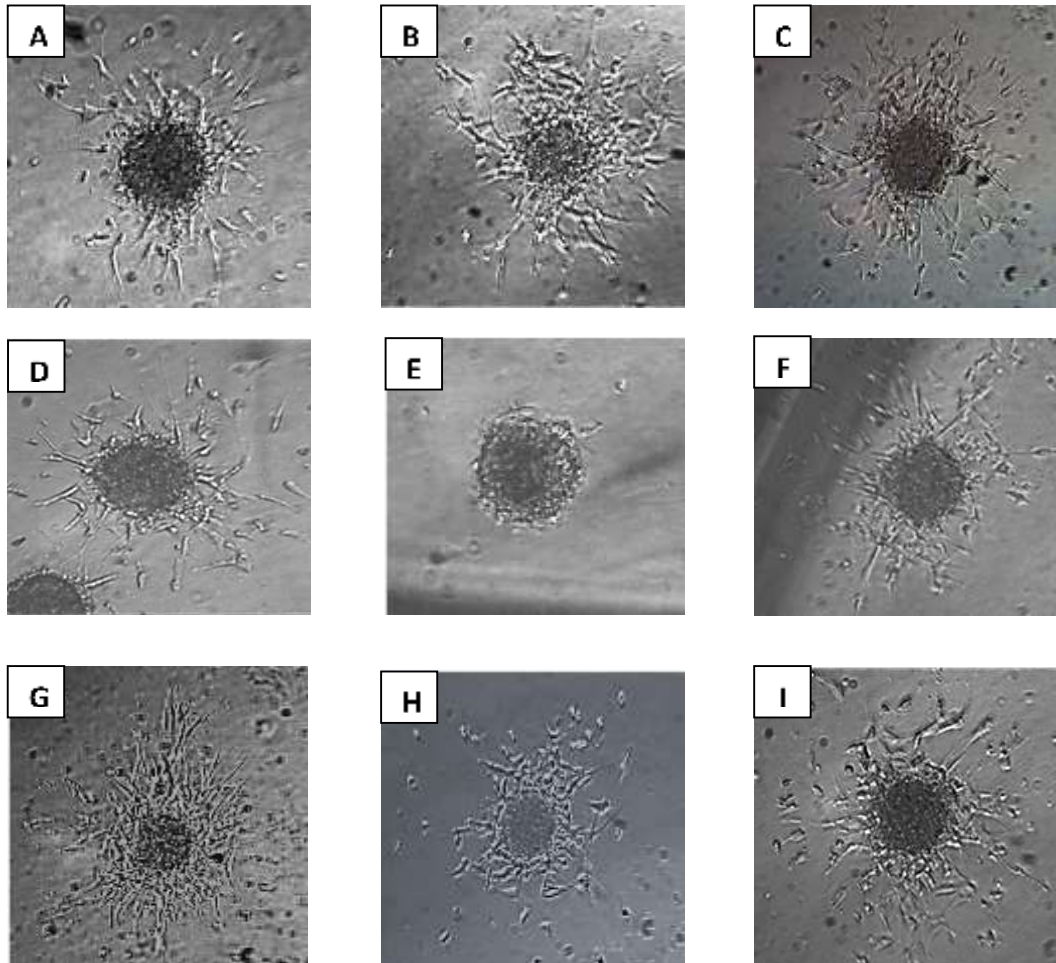
Figure 52. Above are representative images of spheroid sprouting using a variety of mutant proteins obtained from our collaborators In Brescia, Italy and all used at 5µg/ml. SO92X and ELD are none-active mutants synthesised in Brecia. No further studies have been performed on these proteins as yet but the study shows differing levels of activity between them. Pictures represents:

(A)-control, (B)-p17, (C)-RLR, (D)-FGF-2, (E)-S092X, (F)-AAA, (G)-S85X, (H)-ELD and (I) S92X.

Angiogenesis assays (tube-like-structure formation) and the effects of p17 and a mutant peptide S75X. Both p17 and S75X stimulated tube-like structure formation in matrigel with notably S75X producing thinner tubes than the native protein p17 (Fig.57).

This data demonstrates that pre-incubation with the EGFR inhibitor peptide (24h; 10.0μg/ml) inhibited p17-induced angiogenesis but did not affect FGF-2-induced tube formation showing specificity for the p17 and EGFR (Fig.59 & 60).
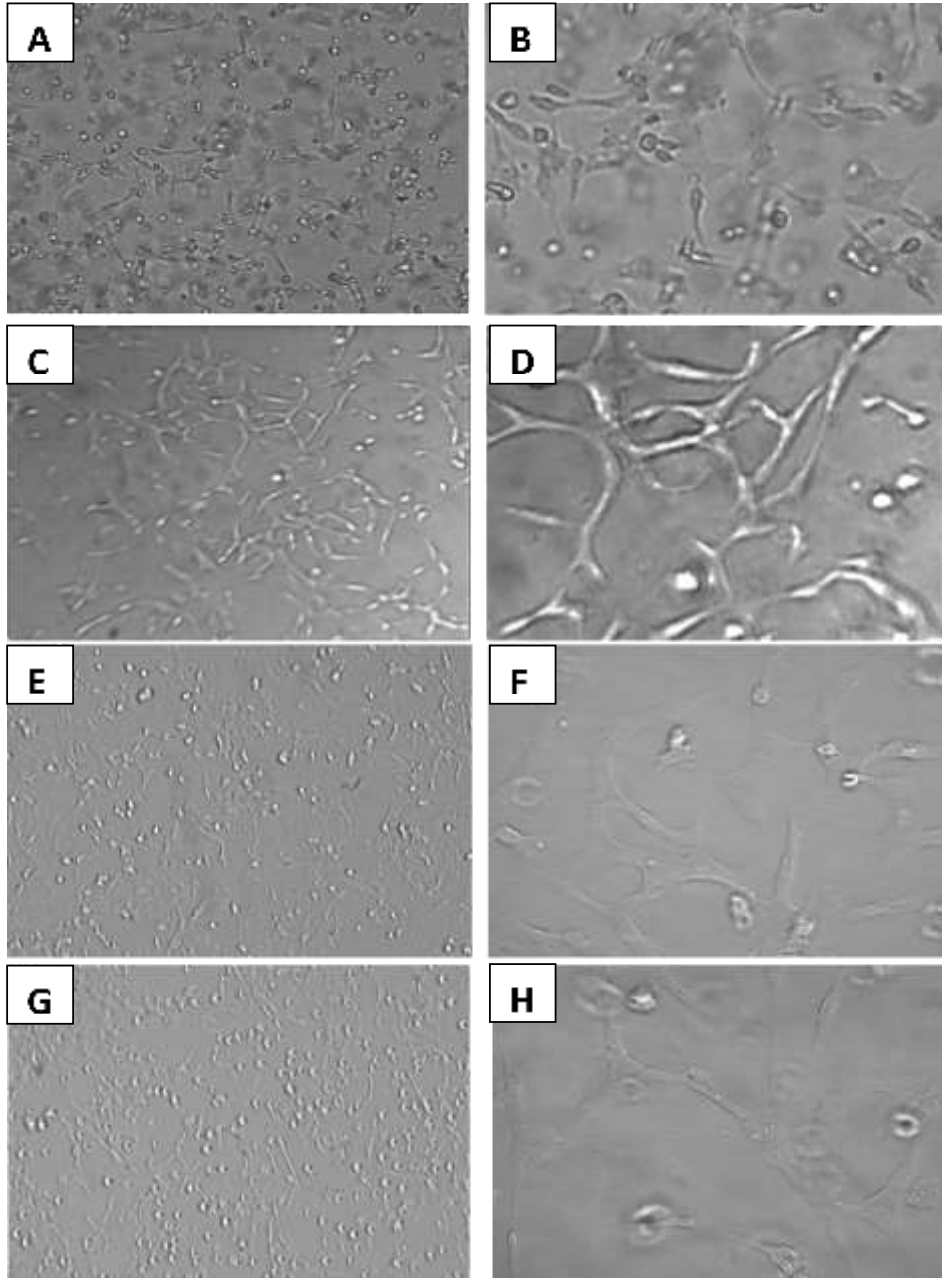
Figure 53. Photomicrograph showing the pro-angiogenic effects of p17 and S75X on hCMEC tube formation. (A-B) Control, (C-D) FGF-2, (E-F) p17 and (G-H) S75X. (B-D-F and H) show a closed area of a matrigel tube, which was used to quantify the results (original magnification X100; number of closed areas counted). Experiments were performed in triplicate wells and repeated three times. A representative example is shown.
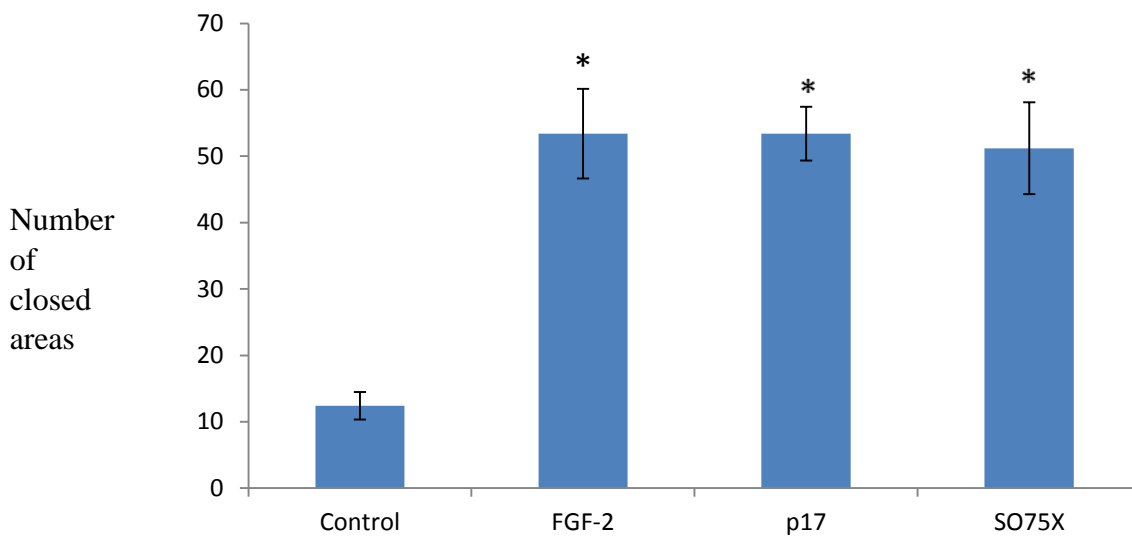
Figure 54. The bar graph shows the stimulatory effects of p17 and its mutant S75X (5µg /ml), FGF-2 (25ng /ml) hCMEC tube formation after 24 hours. The number of closed areas was counted. The bar graph shows the mean ± S.D. (**) signify a statistically significant difference (p < 0.01) compared with the control.
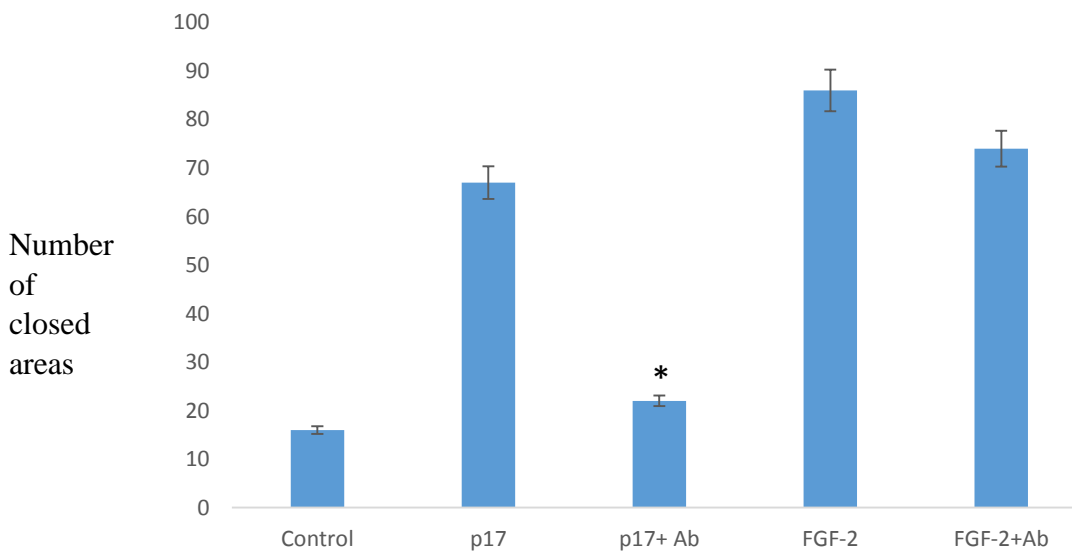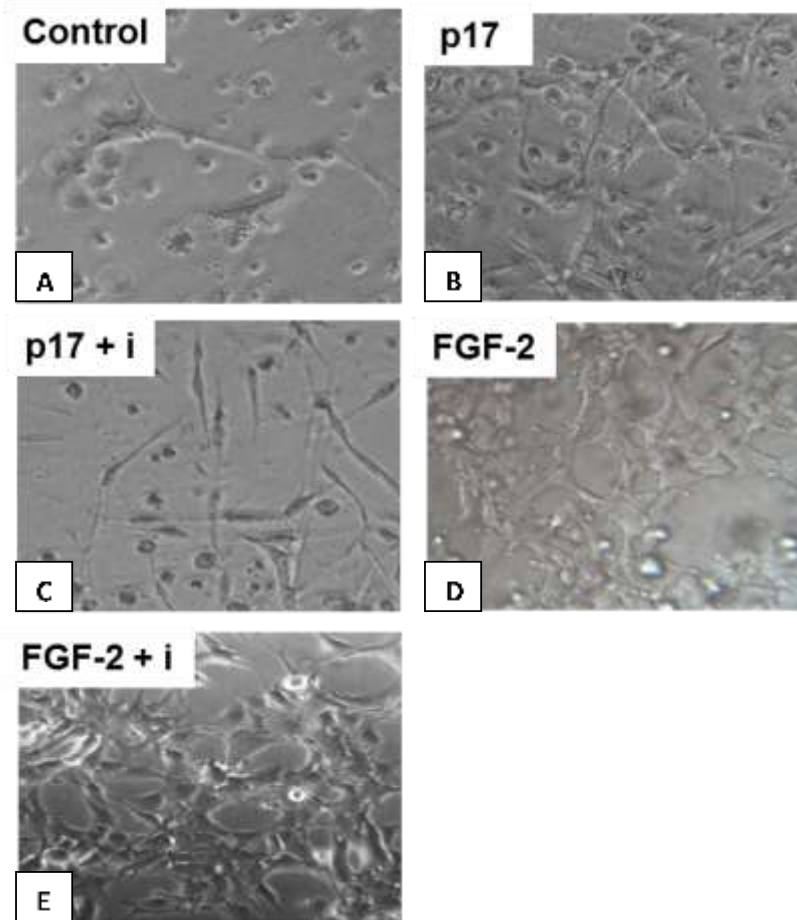
Figure 55. P17-induced tube-like structure formation was significantly inhibited in the presence

of the EGFR inhibitor (C) however FGF-2 was not affected (E). Hence this angiogenesis

response of p17 required the EGFR activation and was specific for EGFR not affecting FGF-2.
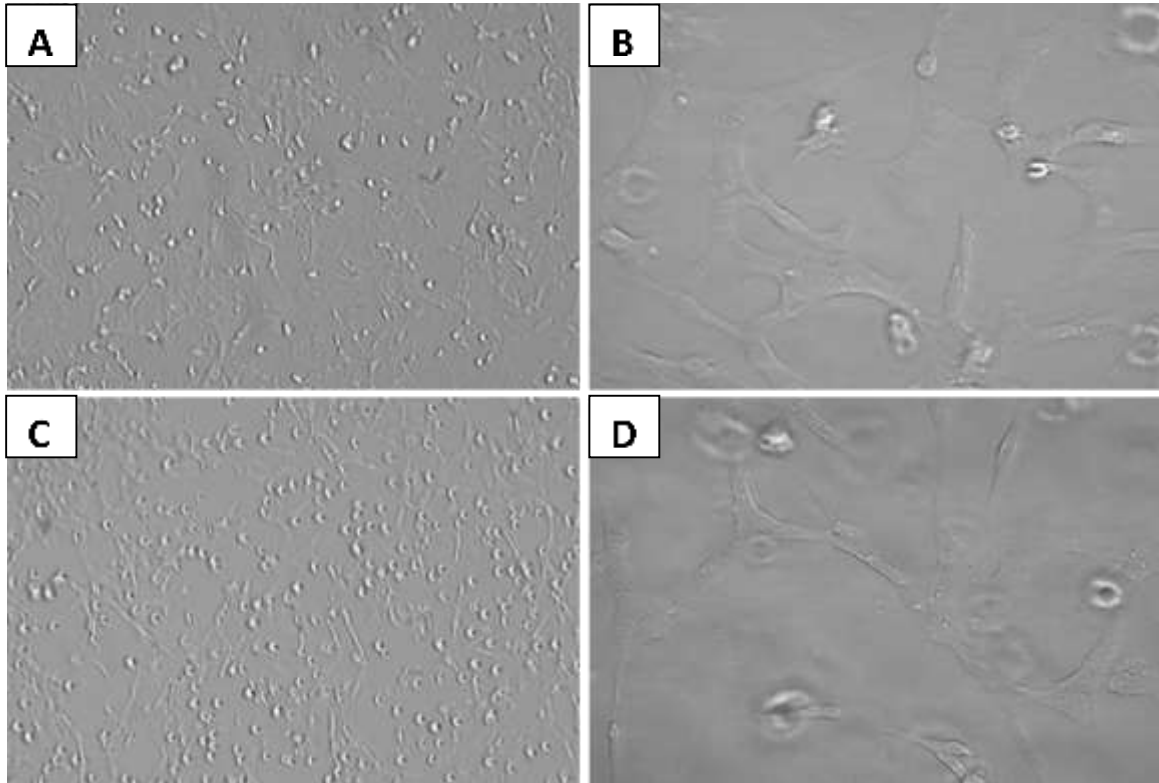
Figure 56. Top images show low (x 20; (A)) and high (x 100; (B)) images of p17-induced tubes. Lower panels (C-D) show the same but S75S induced. Note overall, the thickness of the tubes appeared notably reduced in S075X mutants compared with p17 native protein.

Discussion:

Western blotting experiments using HcMEC demonstrated that p17 was able to induce phosphorylation of cell signalling proteins associated with angiogenesis, in particular the novel finding of activation of the EGFR which requires further investigation as part of a future study.

In regard to neurons, p17 also stimulated cell signalling including phosphorylation of IRS-1, a protein associated with insulin signalling that might be linked to brain neurodegenerative signalling in neurons if chronically over-activated.

Angiogenesis assays showed that p17 stimulated blood vessel growth *in vitro* and that mutants of p17 may have different (sometimes higher activity) and that could have impact and consequence in relation to patient prognosis. If the production of new vessels occurs within the brain where not required, and/or if they do not function effectively in areas of hypoxia, then this will perpetuate the neurodegenerative consequence in the microenvironment of the neurovascular units.

These assays also showed that blocking the EGFR signalling pathway was sufficient to block angiogenesis suggesting a key role in the process and highly novel finding with potentially important consequences as EGFR signalling corresponds to transduction of pathways associated with growth, apoptosis, cell movement and cytoskeletal function.

Different mutants of p17 also showed different physiological tube-like-structure formation that could impact on the patency of new blood vessels *in vivo*. This suggests a further study to examine in detail differences in pro-angiogenic nature of variants of p17 that could contribute to differing patient outcomes of the major diseases.

Chapter 5

Discussion

In this thesis, I have conducted a series of experiments to try to assess the likely involvement of the HIV protein p17 in the process of HIV-associated neurocognitive decline (HAND). The studies have ranged from IHC analysis in human infected individuals and mice injected directly into the hippocampus with p17, through to *in vitro* experimentation and analysis of the potential signalling impact on EC and neurones *in vitro*, and a detailed analysis of the angiogenic effects of both p17 and one of its variants S75X. In summary, I have shown that p17 from HIV is a highly active protein possessing strong pro-angiogenic properties directly inducing polarised-directed vascularization of human brain endothelial cells *in vitro* and concomitantly activating cell signalling pathways associated with cell growth such as ERK1/2 EGFR and PLC. In addition, p17 also stimulated signal transduction of rat brain neurons, causing phosphorylation of proteins including Tau, IRS-1 and FAK. Some experimentation with a variant of p17-S75X showed it had slightly different and even higher activity-therefore, individuals with mutant p17 may suffer differently from diseases such as HAND. *In vivo*

, I showed histologically that following p17 injection into the hippocampus of mice, a couple of months later the p17 remained within the brain ECM and there was strong evidence of a neurodegenerative process (plaques, activated microvessels and phosphorylated tau) whilst the animals suffered cognitive and memory deficits. Brain sections from human patients who died with HIV also showed evidence of p17 associated with amyloid plaques and abnormal looking neurons. Overall the work provides strong evidence that p17 has a major role in initiating/perpetuating cognitive decline and dementia in HIV patients.

The following discussion attempts to relate these findings to the available literature and consider if analysis and determination of p17 could be a potential therapeutic and/or prognostic marker in HIV patients.

Our collaborators previously demonstrated that p17 from HIV can be found within tissues of HIV-infected patients with dementia (Giagulli et al., 2012), and in addition, there is considerable evidence supporting potent biological properties, stimulating lymphangiogenesis and B-cell activation *in vitro* (Caccuri et al., 2014).

The results here from the IHC analysis of 3 patients, demonstrate for the first time characterization of the expression of p17 within the brain of patients with HIV and evidence of dementia.

Immunohistochemistry results demonstrated co-staining of amyloid-β and p17 in human HIV patient neurons, particularly dead or dying neurones, and plaques which are associated with the progression of and are a major hallmark of Alzheimer's disease (Bloom, 2014). p17 was expressed in medium and small sized blood vessels in both grey and white matter, mainly in the cerebral cortex. Since previously published studies showed that p17 can promote angiogenesis *in vitro*, an effect on vascular alteration cannot be ruled out (Basta et al., 2015).

Further studies showed the co-localization of CD68 and p17 in macrophages. Macrophages are the principal immune cells in the central nervous system (CNS) associated with inflammatory brain disease and play a significant role in the host defence against invading microorganisms. In an earlier study, p17 was found to induce a functional program in monocytes related to activation and inflammation (Basta et al., 2015).

Here it seems that macrophages may be attempting to 'mop up' the p17 but failed.

In addition, it was demonstrated that CXCR1 is the receptor molecule responsible for p17 chemokine–like activity on monocytes. After CXCR1 binding, p17 triggered rapid adhesion

and chemotaxis of monocytes through a pathway that involved Rho/ROCK. In addition, p17 mimicked IL-8, the natural high-affinity ligand of CXCR1 (Giagulli et al., 2012), therefore p17 may induce or contribute to inflammation within the brains of HIV patients and this could be a reason for the increase in the incidence of cognitive decline.

In HIV patients, a combination of immune system activation, macrophages, and astrocyte activation leads to an increase in the production of neurotoxins (a chronic neuroinflammatory environment-known to make the brain susceptible to neurodegenerative proceses). These effects alter the neuronal structure and function during pathogenesis of HIV-1-associated dementia (HAD) and Alzheimer's disease (AD). Human Immunodeficiency Virus (HIV)-1-infected macrophages are involved in the pathogenesis of HAD and produce toxic molecules including cytokines, chemokines, and nitric oxide (NO) (Minagar et al., 2002). Therefore, p17 activation of macrophages could have a detrimental effect on neuronal health in HIV patients.

Using an animal (murine) model of dementia (experiments conducted in the University of Barcelona), it was shown that, hippocampal injection of p17 into murine brain induced behavioural and cognitive decline similar to that seen in a characterised dementia model- Tg x 3 animals.

Tg x 3 animals containing mutant genes for amyloid, Tau and presenilin represents a valid and well characterised model of Alzheimer's in mice. The positive control Tg x 3 animals showed very strong positive staining for Aβ with many amyloid plaques being visualised throughout the cortex and p-Tau -hallmarks of the AD process-mostly in neurones throughout the cortex (n=3 animals analysed sections all the way through the brain) (Garcia-Mesa et al., 2011).

The amount of staining and volume of affected tissue/cells was greater than that affected in p17-injected Ntg animals e.g. more plaques and more wide-spread throughout the cortex. This

was to be expected as the triple-mutant model causes very dramatic neurodegenerative consequences and death in animals within 6-12 months.

The results of our collaborators (submitted for publication) showed that, Intra- hippocampal (CA1; since this is the region linked to memory and cognition) stereotactic injection of p17 (n = 8 per group) distinctly deteriorated several aspects of general behaviour and cognitive function in wild-type (NTg) mice as compared with controls injected with a control Cerebrospinal fluid (CSF)-derived protein mixture. At the same time, 3xTg-AD (Tg) mice (described earlier) injected with p17 showed affected behaviour and a reduced capacity for learning and memory, as expected in this mouse strain, but the effects induced by p17 were less evident than in NTg mice probably because the p17 was administered locally and as a one off hippocampal injection. In patients, theoretically, widespread distribution of p17 could initiate neurodegenerative consequences similar to that found in the Tg mice or human AD/dementia.

Reflex responses or coarse motor coordination on a rod were not affected by p17 treatment, neither was grip strength when clung on a wire, in either mouse strain. However, p17 reduced the fine coordination for sideways movement on the wire during the wire hang test in NTg mice. No significant changes of overall general behaviour were observed in the open field but significant effects induced by p17 were detected in some of the other specific tests performed. Namely, p17 induced neophobia in the NTg mice although it did not increase further, that of Tg mice.

Treatment with p17 reduced the exploratory behaviour of NTg mice in the Boissier's hole board test down to the levels of the Tg mice. Furthermore, p17 induced in NTg mice a behaviour of anxiety in the dark and light box test similar to that of Tg mice, but it did not

induce depression-like behaviour as determined in the tail suspension test nor increase that of Tg mice.
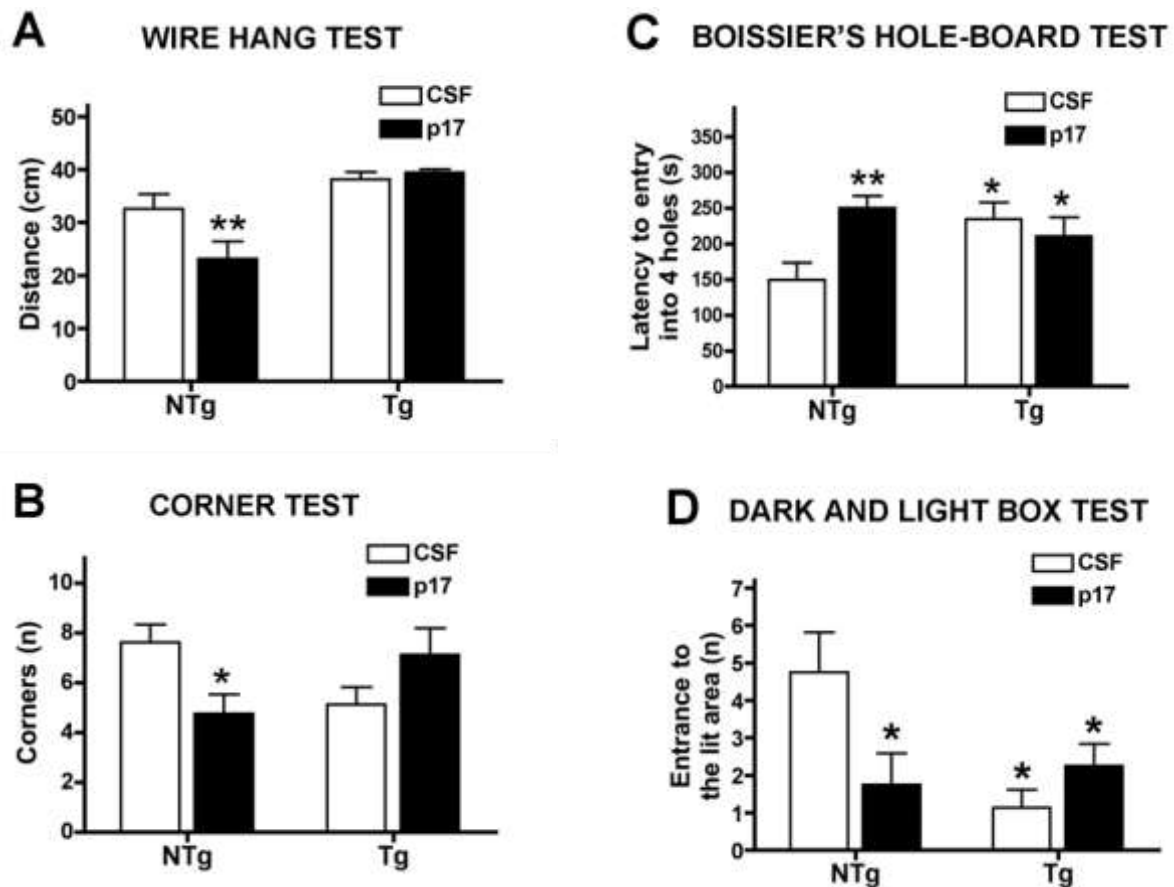
Figure 57. Collaborators results: Shows the effects of p17 injection on behaviour in mice (left-white bars normal mice and black bars with p17 injection. Right the same but transgenic mice. A- p17 reduced distance moved in the wire hang test; note the anomaly of the Tg-longer wire hanging? B-more time was taken by p17-injected mice to explore new holes; C-exploration of corners was much lower and D-entrance to lit areas in a light box reduced in number.

Differences in the transgenic mice between groups were generally none-significant (Unpublished data from Zeinolabediny et al).

The intrahippocampal injection of p17 induced cognitive loss in NTg mice, but cognition-related effects could not be detected in Tg mice because of their own low capacity for learning and memory. NTg mice treated with CSF showed higher attention time to a novel object, whereas p17 treated NTg mice and all Tg mice − treated or not with p17 − showed a lack of visual discrimination of a new object versus a previously explored one, as detected in the novel object recognition test. Reduced acquisition of spatial learning and lack of retention of memory induced by p17 were demonstrated in the MWM test.

In this test, only the control group of NTg mice showed a distinct reduction of the distance covered along the 6 days of place task acquisition. This NTg group of mice demonstrated a longer search time in the correct quadrant during the final probe of retention without the platform, but not all the other groups. Swimming traces confirmed the random swimming of NTg mice treated with p17 and of Tg mice, either treated or not with p17.
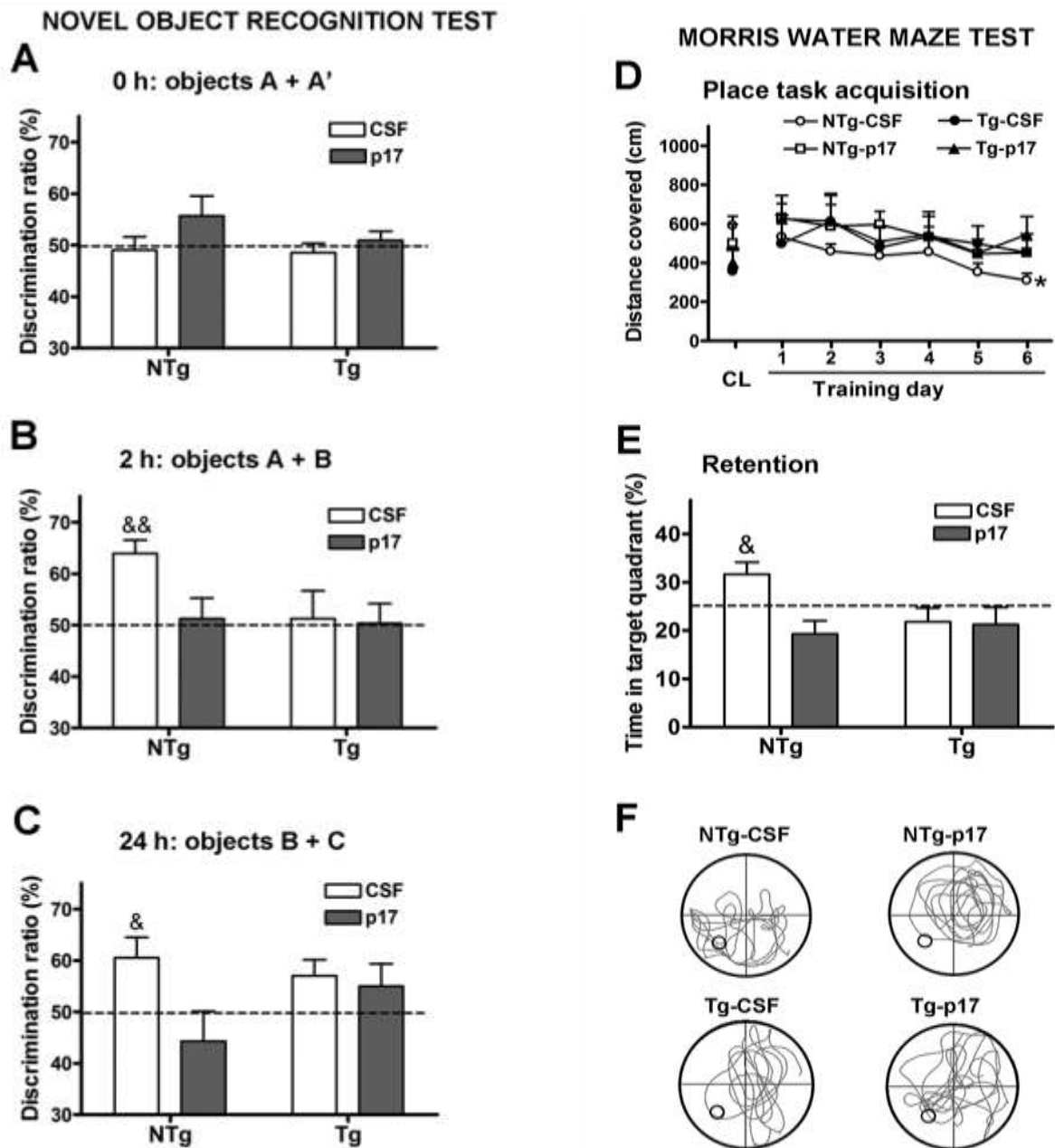
Figure 58. Collaborators data: Shows the effects of p17 injection on memory in mice (left-white bars normal mice and black bars with p17 injection. Right the same but transgenic mice. A-C p17 reduced the ability of the mice to recognize new objects (not A +A-same which acts as the control first step); D-F-more time was taken by p17-injected mice to find the underwater platform in the water maze and less time was spent by them in the correct quadrant. Differences

in the transgenic mice between groups were generally none-significant (Unpublished data from Zeinolabediny et al).

Allied directly to this study, detailed analysis of the brain tissue specimen from the same mice provided by our collaborators showed an interesting profile of p17 within the brain, and concomitant up-regulation of proteins β-amyloid and phosphorylated tau-associated with neurodegenerative cell signalling.

Expression patterns varied a little from animal to animal and layer to layer. This data demonstrated that p17 became stuck after injection within the tissue and ECM for at least 5 weeks and was not removed or degraded during this time, allowing it time to initiate and potentiate any neurodegenerative effect. P17 may be able to enter the brain via the circulation within activated macrophages or directly within the virus through a disrupted BBB.

The staining pattern showed expression of the protein in quite large quantities within local hippocampal ventrical tracts, peri-neural expression within hippocampal neurons. In addition it was seen within local cortical microvessels, in cortical neurons and peri-nuclear and axonal staining was seen in specific areas. Staining was quite extensive and in the form of material with the appearance of 'fibres' or 'fibrils' also within the cerebral cortex. The protein seemed able, therefore to be carried some distance by the local micro-circulation.

Alterations in the blood brain barrier and brain vasculature may be involved in neurodegeneration and neuro-inflammation. Desai et al. showed that vascular density was associated with Aβ load in the hippocampus (perhaps indicating a hypoxic aberrant angiogenic response) and αvβ3 reactivity was associated with neurofibrillary tangles in the mid-frontal cortex and in the substantia nigra (Desai et al., 2009). The results of this study showed that there is an active angiogenic process in the brain regions affected by AD pathology and could

be linked to tissue injury and a vascular dementia phenotype where damaged or none-functional intra-cortical vessels provide a hypoxic environment suitable for perpetuation of neurodegeneration (Desai et al., 2009).

P17 was also present in hippocampal neurons as demonstrated by co-staining with p-Tau. P17-injected animals showed a large increase in p-Tau-positive hippocampal and cortical neurons consistent with suggestion of the existence of neurodegenerative effects in the brains of these mice. Previous studies have indicated that soluble forms of Aβ and tau act synergistically, in addition to their build up within plaques and tangles, to push normal neurons toward cell death (Bloom, 2014).

A number of scattered Aβ-plaques were seen in the cortex of these animals, determined using an antibody to the protein-suggesting that p17 can induce clear and potent neurodegenerative consequences including generation of amyloid fibrillation and linkage to neuronal toxicity following hippocampal injection, demonstrated by IHC and IF.

Injection of p17 apart from indirectly contributing to induce this pathological process was seen directly co-localised with neurodegenerative plaque-like regions within the cortex. Note, normal none-injected animals did not express plaques.

p17 localised to cortical microvessels, revealed by co-staining with CD105 which is a well stablished marker for active endothelial cells from microvessels, suggesting that p17 is able to activate vascularization and potentially promote new vessel growth (Legan et al., 2005), similarly, with CD31 (a marker of normal blood/micro-vessels) and CD105 (a SMAD receptor and marker of the endothelial cells from angiogenic-active vessels only) in cortical microvessels within specific localisations suggesting specific transfer to and potential activation of the microvasculature, that could result in neovascularization and immature none-

patent vessel formation. Original single staining channels with single filters are provided as well as combined double fluorescent images.

A remarkable observation associated to the presence of p17 in human and mice brain was the presence of fibrillary-like structures as determined by immunohistochemistry. The HIV-1 matrix protein is known to possess self-interaction properties since it forms trimers and hexamers. However, the ability of p17 to form amyloid fibrils has never been considered up to date. Our collaborators investigated potential p17 fibrillogenesis by atomic force microscopy (AFM).
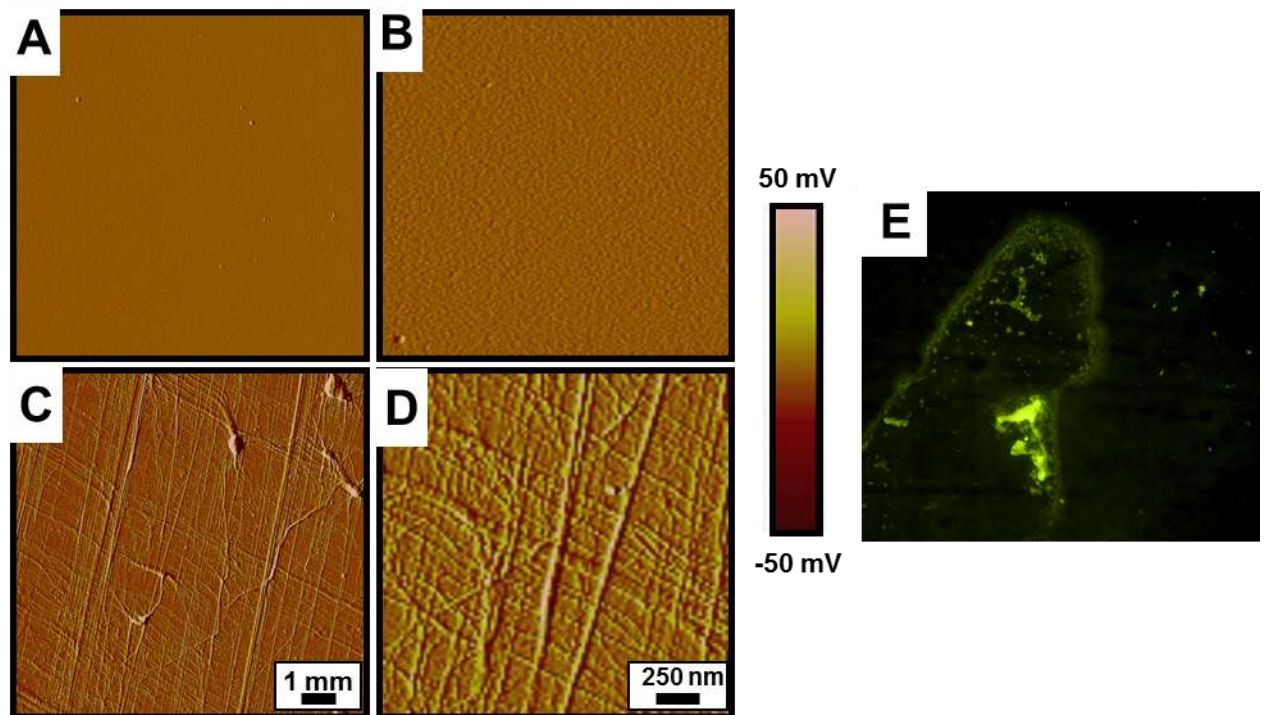
Figure 59. Collaborators results: Atomic force microscopy (AFM) identified fibril and proto-fibril formation of p17 in-vitro and interaction of p17 with Aβ1-42WT. (A-B) no fibrils were seen (C-D) Unbranched fibrils of ~ 15 – 20 nm in diameter and several μm in length, whilst at time zero. (E) Fluorescence microscopy of these p17 aggregates incubated with ThT showed a strong green fluorescence indicating the presence of fibrillary structures.

A feature of Alzheimer's disease is amyloid fibrils. Amyloid refers to the abnormal fibrous, extracellular, proteinaceous deposits found in organs and tissues, which is insoluble and is structurally dominated by β-sheet structure. These fibrils are usually associated with pathology seen in a range of diseases known as the amyloidosis including AD (Rambaran and Serpell, 2008).

In addition, many peptides and proteins self-assemble into amyloid-like fibrils. Examples include mammalian and fungal prion proteins, polypeptides associated with human amyloid diseases, and proteins that may have biologically functional amyloid states. One example is prion proteins (Tycko and Wickner, 2013).

Closer examination of the pathophysiological processes involved in prion disease further indicates a neurodegenerative, rather than infectious disease. Indeed, the age requirement, the numerous point mutations in an amyloidogenic protein, the copper binding properties, the evidence of free radical damage, the presence of polymorphisms that influence disease susceptibility, the formation of amyloid plaques, and in some cases the presence of neurofibrillary pathology, are features common to both prion disease and AD. p17 may therefore entertain some or all of the features of other fibrillary proteins such as the prion proteins and contribute directly in this way to neurodegeneration (Castellani et al., 2004).

The cross-sectional analysis on the top of a fibril segment showed a helicoidal profile along the longitudinal direction of the fibrils with a single filament of ~ 15 – 20 nm of diameter and ~ 2 nm in height. Furthermore, samples of p17 after incubation showed an extremely large heterogeneity as far as their morphology and height distribution are concerned, accounting for the presence of a variety of sub-filament constituents. In summary, the p17 self-fibrilised and

produced parallel dimers similar to A-beta sheets. Therefore, the presence of p17 in these fibrils within the brain could suggest strong association with a pathological process perpetuating neurodegeneration.

In some animals and sections, p17 was seen within cells showing the morphology of glia with astrocytic projections becoming positively stained. A growing figure of evidence proposes that glial cells, namely astrocytes and microglia, could play a vital role in the pathogenesis of AD. Astrocytes and microglia are important for the development and outcome of AD either because they function as effector cells releasing cytokines that play a role in neuroprotection, or because they fail to achieve their homeostatic functions, ultimately leaving neurons to face excitotoxicity and oxidative stress (Dzamba et al., 2016).

The effects of p17 on 'glia' is not known, however the disruption of normal function of glia could result in amplification of neurodegenerative effect as described above.

Recently it was shown that in B cells S75X (a variant of p17) derived from a Ugandan HIV-1 strain A1, differing from the prototype clade B isolate BH10 p17, triggered an activation of the phosphorylation status of ERK1/2 and Akt signaling pathway, opposite to the effects of native p17 protein. The patient with this variant died quickly and dramatically from complications of HIV! Therefore these two proteins were compared, looking for differences in angiogenesis and angiogenic signaling (C. Giagulli et al., 2011).

```
       1                                                                          40
p17    M G A R A S V L S G   G E L D R W E K I R   L R P G G K K K Y K   L K H I V W A S R E

S75X   . . . . . . . . . .   . K . . M . . . T .   . . . . . R . . . R   . . . L . . . . . .

       41                                                                         80
p17    L E R F A V N P G L   L E T S E G C R Q I   L G Q L Q P S L Q T   G S E E L R S L Y N

S75X   . . . . . L . . S .   . . . T . . . Q . .   M N . . . . A . G .   . T . . . G . . F .

       81                              96                                         120
p17    T V A T L Y C V H Q   R I E I K D T K E A   L D K I E E E Q N K   S K K K A Q Q A A A

S75X   . . . V . . . I . .   . . D V . . . . . .   . . . . . . . I . .   . . Q . T . . . . .

       121                   132
p17    D T G H S S Q V S Q N Y

S75X   . . . S . . K . . . . .
```

Figure 60. Alignment and comparison among p17, p17D36 and S75X aa sequences. Sequences are represented by the single-letter aa code. Each aa residue of Ugandan variant S75X not differing from p17 sequence is represented by a dot (C. Giagulli et al., 2011).

In order to identify possible signalling pathways associated with angiogenesis in EC, a Kinexus phospho-protein-array analysis (KAM^{TM} 1.2-500), was carried out using HBMEC exposed to p17 or S75X for 8 minutes and this identified increased phosphorylation of ERK1/2, EGFR1 (Y1172), IRS-1 (Y1179), focal adhesion kinase (FAK-Y397) and Tau (S214), confirmed by Western blotting.

Focal adhesion kinase (FAK) is a cytoplasmic tyrosine kinase that plays critical roles in integrin-mediated signal transductions and also participates in signalling by other cell surface receptors. The activated FAK forms a complex with Src family kinases, which initiates multiple downstream signaling pathways through phosphorylation of other proteins to regulate different cellular functions. Multiple downstream signaling pathways are identified to mediate FAK regulation of migration of various normal and cancer cells. Hence p17/ S75Xmight enhance EC adhesion, spreading and migration through a pathway involving FAK (Zhao and Guan, 2011).

Western blot demonstrated that both p17 and S75X also induced phosphorylation of ERK, AKT and EGFR which are known to be involved in angiogenesis. EGFR is a very well stablished promoter of angiogenesis and the activation of the receptor should significantly regulate angiogenesis both directly and indirectly (De Luka et al., 2008). The EGFR becomes activated by receptor overexpression-however the mechanism through which p17 might interact with EGFR is of course not yet known. Since increased receptor phosphorylation was observed within 5 minutes of exposure to p17, a direct action on the receptor is presumed. The details of the precise intracellular signalling subsequent to this is the subject of further research.

There are numerous ligands that bind to the EGFR, such as EGF itself and transforming growth factor-α. Ligand binding to the receptor induces a conformational change of the receptor and the receptor protein becomes activated. P17 and its mutant S75X may act as a ligand which binds to the receptor, and in addition may stimulate increased production of other ligands that then subsequently bind to the receptor. Further studies will be carried out by blocking the receptor and examining p17 and S75X signalling-beyond the ERK1/2 and angiogenesis assays performed within this body of work.
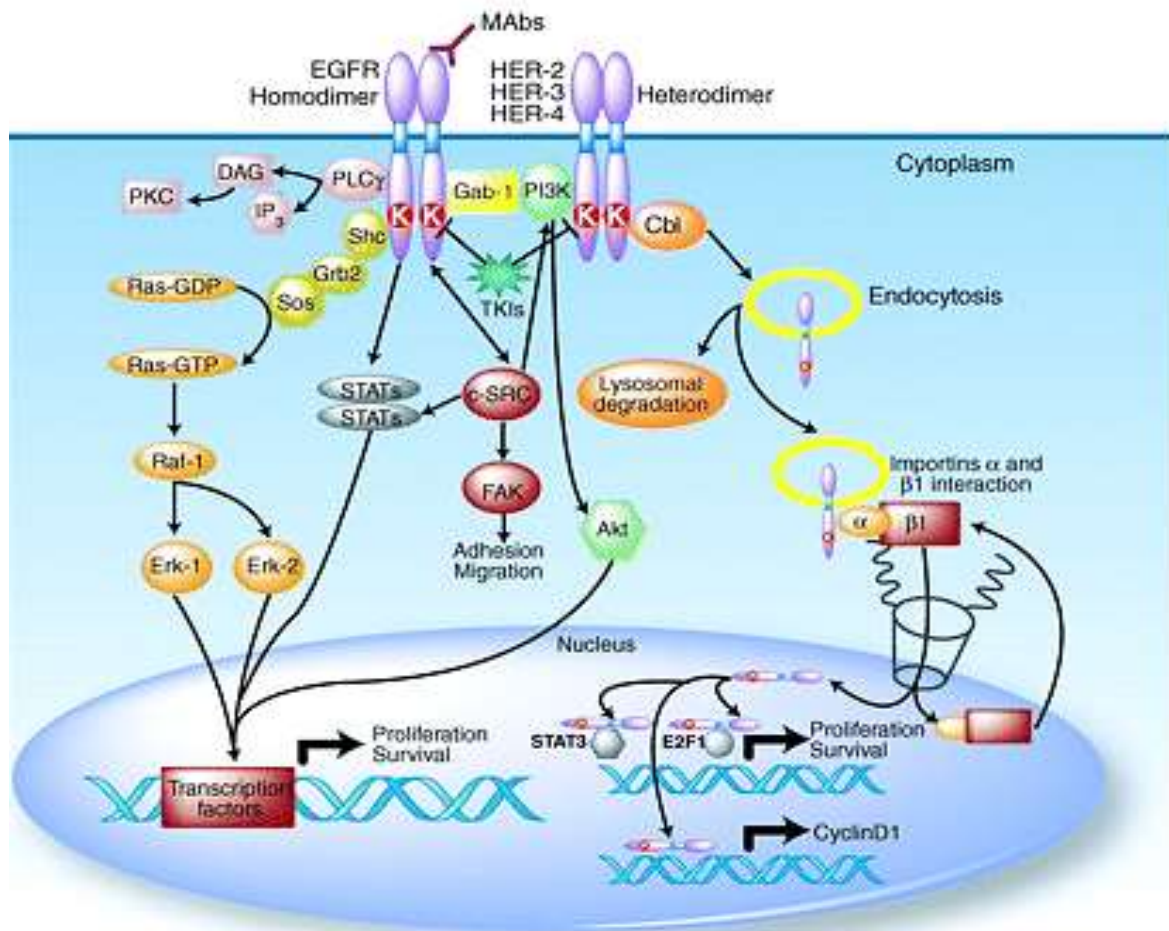
Figure 61. Signalling pathways and inhibitors of EGFR. Figure shows the activation of EGFR and subsequent phosphorylation of specific tyrosine residues, Complex and multiple signalling pathways that overlap are then activating including intermediates such as Phospholipase Cγ and STAT transcription factors Ras/Raf/MAPK and PI3K pathway. Once in the nucleus, EGFR acts as a transcription factor and/or co-regulates other gene trans-activators. Both pathways result in nuclear activation of genes related with cell proliferation, survival, invasion, and metastasis. DAG, 1,2-diacylglycerol; IP₃, inositol 1,3,5-triphosphate; PLCγ, phospholipase Cγ; Erk-1, extracellular signal-regulated kinase-1; Erk-2, extracellular signal-regulated kinase-2; FAK, focal adhesion kinase; PKC, protein kinase C (Scaltriti and Baselga, 2006).The effects of the interaction of p17 with the EGFR and down-stream signalling need to be investigated further.

Whilst angiogenesis is normally a positive element of tissue remodelling, abnormal vascularization in otherwise normal tissue may lead to an increase in inflammation by increasing vascular permeability e.g. via VEGF and have a negative effect on neuronal function (Komiya et al., 2014).

In reference to angiogenesis, considering our finding that cortical microvessels of p17-hippocampal injected mice retain and express p17 concomitant with CD105 (a marker of activation and angiogenesis in endothelial cells) in addition to CD31, our *in vitro* experiments went on to investigate how p17 might influence the angiogenic process.

Previously, studies suggested a link between p17 and angiogenesis in lymphatic endothelial cells. The study showed that p17 promoted lymphangiogenesis by binding to chemokine (C-X-C motif) receptor-1 and chemokine (C-X-C motif) receptor-2 expressed on lymph node-derived lymphatic endothelial cells and activating the Akt/extracellular signal-regulated kinase signalling pathway (Caccuri et al., 2014). Therefore, a partial signalling mechanism was identified in these very specific EC.

In this study it was shown that in scratch wound migration assay with human brain endothelial cells, both p17 and S75X significantly increased cellular migration. The wound healing results demonstrated that both p17 and S75X stimulated cell migration after the scratch wound was made. S75X produced thinner, longer, organised and polar grouping of migrating cells comparing with p17/FGF-2. Polarised cell migration is a conserved regulated process that takes place in tissue development and wound healing (Fukata et al., 2003). Differences in cell signalling processes could account for polarization in S75X-treated cells and this needs to be investigated in more detail since it could relate to different pathology induced by different p17 isoforms.

Tube-like structure formation assay showed p17 and S75X increased the number of tubes compared to control with those of S75X appearing to be thinner (as stated previously). Formation of normal and functional blood vessels require complex cell signalling processes (Helfrich and Schadendorf, 2011), which if interrupted leads to formation of abnormal vessels that may not function correctly, for example it could lead to leakage of blood from the vessels or prevent the passage of blood through them. Therefore, it is possible that S75X has an effect on this process leading to formation of abnormal looking and functional vessels.

Blocking of EGFR-1-Y1172, with a specific blocking peptide was able to significantly perturb EGFR1 phosphorylation by p17 (Fig. 45), down-stream cell signalling via ERK1/2 and tube-like-structure formation/angiogenesis, whilst not affecting FGF-2-induced angiogenesis. This identified a major signalling pathway through which p17 stimulated angiogenesis.

The endothelial cell spheroid assay provides a suitable *in vitro* model to study (lymph) angiogenesis and test pro- and anti-(lymph) angiogenic factors or drugs (Blacher et al., 2014). The spheroid assay demonstrated cells and sprouts were more strongly chemo-attractive in S75X compared to p17. These findings may suggest that S75X produces chemokines that causes the chemo attraction between sprouts emanating from adjacent spheroid. Moreover, the signalling pathways involving Rac and its downstream effector the p21-activated serine/threonine kinase (PAK) are recognised to modulate endothelial cell biology, such as sprouting, migration, polarity, proliferation, lumen formation, and maturation (Moya et al., 2009).

p17 strongly stimulated migration, sprouting, chemotaxis and tube-like-structure formation in HcMEC with a similar potency to FGF-2 a known angiogenic mitogen. So far, we are not sure of the physiological relevance of activating brain microvessels nor how this could impact upon a possible neurodegenerative process, although excessive improper vascularization could result

in none-patent vasculature, haemorrhage and neuronal hypoxia through abnormal remodelling (Zlokovic, 2005). In addition, vascular activation is now considered a critical player in establishment of neurodegenerative progression. For example, two separate transgenic murine models AD, the cerebro-vasculature was studied in detail and was found to be activated with overexpression of amyloid beta, thrombin, tumour necrosis factor alpha, interleukin-1 beta, interleukin-6, and matrix metalloproteinase 9 (Grammas et al., 2014).

I have identified a novel signalling pathways in this study, operating in both brain microvessel endothelial cells and neurons via p17. Cell signalling in endothelial cells seems to operate primarily through the EGFR-1 pathway, whilst in neurons, IRS-1 and FAK appear to be important intermediates. In consideration of our findings above, aberrant EGFR signalling could predispose brain microvessels towards vascular accelerated angiogenesis and dysfunction, and has been identified recently as part of a network cluster within the CSF and plasma proteome-as a significant gene associated with AD risk (Li et al., 2012).

In addition, EGFR-Aβ expression fusion constructs dramatically enhanced neuronal cell death via ASK1/JNK signalling pathways implicating it in a role under these circumstances linked to neurodegeneration (A. Sandberg et al., 2010).

Aβ also induced apoptosis of rat PC12 cells via FAK stimulation through NF-kB and ERK1/2, (Cinzia Giagulli et al., 2011) -suggesting this pathway activation through p17 could damage the hippocampal and cortical neurons we observed staining positive-although these processes require further detailed investigation.

Phosphorylated type 1 insulin receptor substrate, p-IRS-1, (the phosphorylated/activated form; whose expression is linked to insulin resistance, diabetes and neuro-inflammation in dementia) was found in sporadic cortical neurons of mouse sections injected with p17 but not in normal control mouse sections.

Brain tissue studies suggested that dysfunctionally p-IRS1 in neural-derived blood exosomes is associated with preclinical Alzheimer's disease (Kapogiannis et al., 2015).

Both animal and human studies also revealed that deregulation of IRS1 pathway is linked to diabetic complications associated with dementia and de-regulation of insulin production and signalling pathways (Ma et al., 2015).

Alpha-synuclein (α-Syn) is a major component of neurodegenerative diseases including AD. Evidence suggests that α-Syn-mediated neurotoxicity is connected to insulin signalling via IRS-1 and then downstream signalling pathways such as phosphatidylinositol 3-kinase/Akt and mammalian target of rapamycin (mTOR)/ribosomal protein S6 kinase (S6K)1 known to be linked to AD (Gao et al., 2015). Hence p17 activated IRS-1 signalling could have an impact on the neurodegenerative process.

In addition, p-EGFR (epidermal growth factor receptor) which is a prime receptor stimulating cell growth in both neurons and EC, and p-FAK (focal adhesion kinase), a cell signalling intermediate again, associated with correct focal adhesion and cell spreading, required for effective co-ordinated cell growth and tissue regeneration during growth phases, it was also observed in cortical neurons of some of the p-17-injected animals. (These have been discussed earlier in the chapter).

Conclusion

The most striking finding was to highlight the presence of p17 in amyloid-like structures in the brain parenchyma and to show a possible co-localization of the viral protein with Aβ. This finding, together with p17 expression in ECs and in activated cortical neurons, opened the way to further study the possible involvement of p17 in promoting neuropathological degeneration.

We also found that p17 stimulated angiogenesis through the EGFR1 pathway with potency similar to FGF-2, a known angiogenic mitogen. So far, the pathobiological and physiological relevance of activating brain microvessels and its impact upon a possible neurodegenerative process is not known. However, excessive improper vascularization is known to result in non-patent vasculature and haemorrhage, which may cause neuronal hypoxia through abnormal remodelling (Zlokovic, 2005).

Cell signalling in neurones seems to operate primarily through IRS-1 and FAK – since Aβ also induced apoptosis of rat PC12 cells, a clone of a rat pheochromocytoma, via FAK stimulation through NF-kB and ERK1/2 (Wang et al., 2012), this suggests a pathway activation through p17 could damage the hippocampal and cortical neurons we observed staining positive, although these processes require further detailed investigation.

Other data generated from our murine injected model showed that direct injection of p17 into the hippocampus resulted in both behavioural and cognitive deficiency, similar to that seen in Tg animals that showed symptoms of dementia. Histology of brain sections confirmed evidence of neurological damage in p17-injected animals with strong co-localization between p17 and pTau in hippocampal neurons which appeared swollen and abnormally-irregularly orientated, although cell number was not decreased.

Startlingly, we (and our collaborators) showed that in vitro, p17 was able to polymerise into 'amyloid-like' fibrils which often combined to form parallel helical twisted fibres. The presence of these fibres was also seen in p17-injected animals providing strong evidence for a role in mediating neurodegeneration. Deposition of α-helical oligomeric aggregates of amyloid fibrils consisting of Aβ1-40 and Aβ1-42 in the extracellular matrix ECM of the brain is a major feature of dementia, and is linked to neuronal toxicity and apoptosis (Li et al., 2012).

Further studies should confirm and detail these findings in a larger cohort of patients and determine if either circulating p17 and its variants can predict the risk of cognitive decline and HAND in HIV patients or in addition if 'clearing' of the protein could form the basis of a potential therapeutic to prevent neurodegenerative disease.

Future work

- Investigating more details of the differences between the native p17 and variant isoforms in terms of the effects on angiogenesis and neurodegeneration *in-vitro* and *in-vivo*.

- To determine if inhibition of p17 could reduce or prevent HAND/dementia using the murine model of dementia.

- To identify whether p17 and its variants could be used as biomarkers to predict a risk of developments of HAND in HIV patients (measured as RNA from blood samples or in CSF)

- To identify a potential therapeutic that may protect HIV patients from developing HAND.

- To determine if p17 might be responsible for developments of other HIV associated illness, for example, early onset cardiovascular disease or tumours associated with HIV.

- In individuals who died with HIV, we were limited in only being able to obtain 3 patients samples, however these were sufficient to be able to identify strong p17 staining mimicking conventional neurodegenerative protein (Aβ/tau) expression in regions identified with plaques/inflammation and or neuronal cell death. Further studies should confirm and detail these findings in a larger cohort of patients and determine if either circulating p17 and its variants can predict the risk of cognitive decline and HAND in HIV patients or in addition if 'clearing' of the protein could form the basis of a potential therapeutic to prevent neurodegenerative disease.

References

Afonso, P. V., Ozden, S., Prevost, M. C., Schmitt, C., Seilhean, D., Weksler, B., Couraud, P. O., Gessain, A., Romero, I. A. and Ceccaldi, P. E. (2007) 'Human blood–brain barrier disruption by retroviral-infected lymphocytes: role of myosine light chain kinase in endothelial tight-junction disorganization.' *J Immunol*, 179

Allen, N., Robinson, AC., Snowden, J., Davidson, YS., Mann, DM.. (2014). Patterns of cerebral amyloid angiopathy define histopathological phenotypes in Alzheimer's disease. *Neuropathol Appl Neurobiol*. 10.1111 (2), 136-148.

Baker, J. V., Peng, G., Rapkin, J., Abrams, D. I., Silverberg, M. J., MacArthur, R. D., Cavert, W. P., Henry, W. K. and Neaton, J. D. (2008) 'CD4+ count and risk of non-AIDS diseases following initial treatment for HIV infection.' *AIDS*, 22(7), Apr 23, pp. 841-848.

Basta, D., Latinovic, O., Lafferty, M. K., Sun, L., Bryant, J., Lu, W., Caccuri, F., Caruso, A., Gallo, R. and Garzino-Demo, A. (2015) 'Angiogenic, lymphangiogenic and adipogenic effects of HIV-1 matrix protein p17.' *Pathog Dis*, 73(8), Nov, p. ftv062.

Bhatia, M., Karlenius, T. C., Trapani, G. D. and K., T. (2013) *In* Tonissen, K. (ed.) *Carcinogenesis*.

Birbrair, A., Zhang, T., Wang, Z.-M., Messi, M. L., Olson, J. D., Mintz, A. and Delbono, O. (2014) 'Type-2 pericytes participate in normal and tumoral angiogenesis.' *American Journal of Physiology - Cell Physiology*, 307(1), 2014-07-01 00:00:00, pp. C25-C38.

Blacher, S., Erpicum, C., Lenoir, B., Paupert, J., Moraes, G., Ormenese, S., Bullinger, E. and Noel, A. (2014) 'Cell Invasion in the Spheroid Sprouting Assay: A Spatial Organisation Analysis Adaptable to Cell Behaviour.' *Plos One*, 9(5), May 7,

Bloom, G. S. (2014) 'Amyloid-beta and Tau The Trigger and Bullet in Alzheimer Disease Pathogenesis.' *Jama Neurology*, 71(4), Apr, pp. 505-508.

Bonsor, K. and Curran, O. (2016) How AIDS Works. Science | Cellular & Microscopic Biology ed.: HowStuffWorks

Brechtl, J. R., Breitbart, W., Galietta, M., Krivo, S. and Rosenfeld, B. (2001) 'The use of highly active antiretroviral therapy (HAART) in patients with advanced HIV infection: Impact on medical, palliative care, and quality of life outcomes.' *Journal of Pain and Symptom Management*, 21(1), Jan, pp. 41-51.

Brown, R. M., Meah, C. J., Heath, V. L., Styles, I. B. and Bicknell, R. (2016) 'Tube-Forming Assays.' *Methods Mol Biol*, 1430 pp. 149-157.

Budson, A. E. and Solomon, P. R. (2012) 'New diagnostic criteria for Alzheimer's disease and mild cognitive impairment for the practical neurologist.' *Practical Neurology*, 12(2), April 1, 2012, pp. 88-96.

Bukrinskaya, A. (2007) 'HIV-1 matrix protein: A mysterious regulator of the viral life cycle.' *Virus Research*, 124(1-2), Mar, pp. 1-11.

Bukrinsky, M. (2004) 'A hard way to the nucleus.' *Molecular Medicine*, 10(1-6), Jan-Jun, pp. 1-5.

Caccuri, F., Rueckert, C., Giagulli, C., Schulze, K., Basta, D., Zicari, S., Marsico, S., Cervi, E., Fiorentini, S., Slevin, M., Guzman, C. A. and Caruso, A. (2014) 'HIV-1 matrix protein p17 promotes lymphangiogenesis and activates the endothelin-1/endothelin B receptor axis.' *Arterioscler Thromb Vasc Biol*, 34(4), Apr, pp. 846-856.

Caccuri, F., Giagulli, C., Bugatti, A., Benetti, A., Alessandri, G., Ribatti, D., Marsico, S., Apostoli, P., Slevin, M. A., Rusnati, M., Guzman, C. A., Fiorentini, S. and Caruso, A. (2012) 'HIV-1 matrix protein p17 promotes angiogenesis via chemokine receptors CXCR1 and CXCR2.' *Proceedings of the National Academy of Sciences of the United States of America*, 109(36), Sep 4, pp. 14580-14585.

Canobbio, I., Abubaker, A. A., Visconte, C., Torti, M. and Pula, G. (2015) 'Role of amyloid peptides in vascular dysfunction and platelet dysregulation in Alzheimer's disease.' *Frontiers in Cellular Neuroscience*, 9, Mar 3,

Castellani, R. J., Perry, G. and Smith, M. A. (2004) 'Prion disease and Alzheimer's disease: pathogenic overlap.' *Acta Neurobiol Exp (Wars)*, 64(1) pp. 11-17.

Chan, G. K. Y., Kleinheinz, T. L., Peterson, D. and Moffat, J. G. (2013) 'A Simple High-Content Cell Cycle Assay Reveals Frequent Discrepancies between Cell Number and ATP and MTS Proliferation Assays.' *Plos One*, 8(5), May 17,

Cockerham, L., Scherzer, R., Zolopa, A., Rimland, D., Lewis, C. E., Bacchetti, P., Grunfeld, C., Shlipak, M. and Tien, P. C. (2010) 'Association of HIV infection, demographic and cardiovascular risk factors with all-cause mortality in the recent HAART era.' *J Acquir Immune Defic Syndr*, 53(1), Jan, pp. 102-106.

Cohen, M. S., Chen, Y. Q., McCauley, M., Gamble, T., Hosseinipour, M. C., Kumarasamy, N., Hakim, J. G., Kumwenda, J., Grinsztejn, B., Pilotto, J. H. S., Godbole, S. V., Mehendale, S., Chariyalertsak, S., Santos, B. R., Mayer, K. H., Hoffman, I. F., Eshleman, S. H., Piwowar-Manning, E., Wang, L., Makhema, J., Mills, L. A., de Bruyn, G., Sanne, I., Eron, J., Gallant, J., Havlir, D., Swindells, S., Ribaudo, H., Elharrar, V., Burns, D., Taha, E. T., Nielsen-Saines, K., Celentano, D., Essex, M., Fleming, T. R. and Team, H. S. (2011) 'Prevention of HIV-1 Infection with Early Antiretroviral Therapy.' *New England Journal of Medicine*, 365(6), Aug 11, pp. 493-505.

Conant, K., St Hillaire, C., Anderson, C., Galey, D., Wang, J. and Nath, A. (2004) 'Human immunodeficiency virus type 1 Tat and methamphetamine affect the release and activation of matrix-degrading proteinases.' *Journal of Neurovirology*, 10(1) pp. 21-28.

Cunningham, E. L., McGuinness, B., Herron, B. and Passmore, A. P. (2015) 'Dementia.' *Ulster Med J*, 84(2), May, pp. 79-87.

Dauchy, S., Miller, F., Couraud, P. O., Weaver, R. J., Weksler, B., Romero, I. A., Scherrmann, J. M., De Waziers, I. and Decleves, X. (2009) 'Expression and transcriptional regulation of ABC transporters and cytochromes P450 in hCMEC/D3 human cerebral microvascular endothelial cells.' *Biochemical Pharmacology*, 77(5), Mar 1, pp. 897-909.

Davis, G. E., Koh, W. and Stratman, A. N. (2007) 'Mechanisms controlling human endothelial lumen formation and tube assembly in three-dimensional extracellular matrices.' *Birth Defects Res C Embryo Today*, 81(4), Dec, pp. 270-285.

De Francesco, M. A., Caruso, A., Fallacara, F., Canaris, A. D., Dima, F., Poiesi, C., Licenziati, S., Corulli, M., Martinelli, F., Fiorentini, S. and Turano, A. (1998) 'HIV p17 enhances lymphocyte proliferation and HIV-1 replication after binding to a human serum factor.' *AIDS*, 12(3), Feb 12, pp. 245-252.

De Francesco, M. A., Baronio, M., Fiorentini, S., Signorini, C., Bonfanti, C., Poiesi, C., Popovic, M., Grassi, M., Garrafa, E., Bozzo, L., Lewis, G. K., Licenziati, S., Gallo, R. C. and Caruso, A. (2002) 'HIV-1 matrix protein p17 increases the production of proinflammatory cytokines and counteracts IL-4 activity by binding to a cellular receptor.' *Proc Natl Acad Sci U S A*, 99(15), Jul 23, pp. 9972-9977.

DEMENTIA-CARE-NOTES. (2016) *How dementia impacts behavior*. [Online] [Accessed on 2016] http://dementiacarenotes.in/dementia/dementia-behaviour/

Desai, B. S., Schneider, J. A., Li, J. L., Carvey, P. M. and Hendey, B. (2009) 'Evidence of angiogenic vessels in Alzheimer's disease.' *Journal of Neural Transmission*, 116(5), May, pp. 587-597.

Dong, X., Li, H., Derdowski, A., Ding, L., Burnett, A., Chen, X., Peters, T. R., Dermody, T. S., Woodruff, E., Wang, J.-J. and Spearman, P. (2005) 'AP-3 Directs the Intracellular Trafficking of HIV-1 Gag and Plays a Key Role in Particle Assembly.' *Cell*, 120(5), 3/11/, pp. 663-674.

Douek, D. C., Roederer, M. and Koup, R. A. (2009) 'Emerging Concepts in the Immunopathogenesis of AIDS.' *Annual Review of Medicine*, 60 pp. 471-484.

Dzamba, D., Harantova, L., Butenko, O. and Anderova, M. (2016) 'Glial cells - the key elements of Alzheimer s disease.' *Curr Alzheimer Res*, Jan 28,

Elbirt, D., Mahlab-Guri, K., Bezalel-Rosenberg, S., Gill, H., Attali, M. and Asher, I. (2015) 'HIV-associated neurocognitive disorders (HAND).' *Isr Med Assoc J*, 17(1), Jan, pp. 54-59.

Enciu, A. M., Constantinescu, S. N., Popescu, L. M., Muresanu, D. F. and Popescu, B. O. (2011) 'Neurobiology of vascular dementia.' *J Aging Res*, 2011 p. 401604.

Fiorentini, S., Marini, E., Caracciolo, S. and Caruso, A. (2006) 'Functions of the HIV-1 matrix protein p17.' *New Microbiol*, 29(1), Jan, pp. 1-10.

Folkman, J. (1971). Tumor angiogenesis: therapeutic implications. *The New England Journal of Medicine* . 18;285 (21), 1182-1186.

Fukata, M., Nakagawa, M. and Kaibuchi, K. (2003) 'Roles of Rho-family GTPases in cell polarisation and directional migration.' *Curr Opin Cell Biol*, 15(5), Oct, pp. 590-597.

Gao, S., Duan, C., Gao, G., Wang, X. and Yang, H. (2015) 'Alpha-synuclein overexpression negatively regulates insulin receptor substrate 1 by activating mTORC1/S6K1 signaling.' *Int J Biochem Cell Biol*, 64, Jul, pp. 25-33.

Garcia-Mesa, Y., Lopez-Ramos, J. C., Gimenez-Llort, L., Revilla, S., Guerra, R., Gruart, A., LaFerla, F. M., Cristofol, R., Delgado-Garcia, J. M. and Sanfeliu, C. (2011) 'Physical Exercise Protects Against Alzheimer's Disease in 3xTg-AD Mice.' *Journal of Alzheimers Disease*, 24(3) pp. 421-454.

Gavalas, N., Liontos, M., Trachana, S.-P., Bagratuni, T., Arapinis, C., Liacos, C., Dimopoulos, M. and Bamias, A. (2013) 'Angiogenesis-Related Pathways in the Pathogenesis of Ovarian Cancer.' *International Journal of Molecular Sciences*, 14(8) p. 15885.

Giagulli, C., Marsico, S., Magiera, A. K., Bruno, R., Caccuri, F., Barone, I., Fiorentini, S., Andò, S. and Caruso, A. (2011) 'Opposite Effects of HIV-1 p17 Variants on PTEN Activation and Cell Growth in B Cells.' *PLoS ONE*, 6(3), 03/14. 09/29/received. 02/15/accepted, p. e17831.

Giagulli, C., Marsico, S., Magiera, A. K., Bruno, R., Caccuri, F., Barone, I., Fiorentini, S., Ando, S. and Caruso, A. (2011) 'Opposite Effects of HIV-1 p17 Variants on PTEN Activation and Cell Growth in B Cells.' *Plos One*, 6(3), Mar 14,

Giagulli, C., Magiera, A. K., Bugatti, A., Caccuri, F., Marsico, S., Rusnati, M., Vermi, W., Fiorentini, S. and Caruso, A. (2012) 'HIV-1 matrix protein p17 binds to the IL-8 receptor CXCR1 and shows IL-8–like chemokine activity on monocytes through Rho/ROCK activation.' *Blood*, 119(10), 2012-03-08 00:00:00, pp. 2274-2283.

Goel, S., Duda, D. G., Xu, L., Munn, L. L., Boucher, Y., Fukumura, D. and Jain, R. K. (2011) 'Normalization of the vasculature for treatment of cancer and other diseases.' *Physiol Rev*, 91(3), Jul, pp. 1071-1121.

Gottfries, C. G., Blennow, K., Karlsson, I. and Wallin, A. (1994) 'The Neurochemistry of Vascular Dementia.' *Dementia*, 5(3-4), May-Aug, pp. 163-167.

Grammas, P., Martinez, J., Sanchez, A., Yin, X., Riley, J., Gay, D., Desobry, K., Tripathy, D., Luo, J., Evola, M. and Young, A. (2014) 'A new paradigm for the treatment of Alzheimer's disease: targeting vascular activation.' *J Alzheimers Dis*, 40(3) pp. 619-630.

Hashimoto, Y., Niikura, T., Chiba, T., Tsukamoto, E., Kadowaki, H., Nishitoh, H., Yamagishi, Y., Ishizaka, M., Yamada, M., Nawa, M., Terashita, K., Aiso, S., Ichijo, H. and Nishimoto, I. (2003) 'The Cytoplasmic Domain of Alzheimer's Amyloid-β Protein Precursor Causes Sustained Apoptosis Signal-Regulating Kinase 1/c-Jun NH2-Terminal Kinase-Mediated Neurotoxic Signal via Dimerization.' *Journal of Pharmacology and Experimental Therapeutics*, 306(3), September 1, 2003, pp. 889-902.

Helfrich, I. and Schadendorf, D. (2011) 'Blood vessel maturation, vascular phenotype and angiogenic potential in malignant melanoma: one step forward for overcoming anti-angiogenic drug resistance?' *Mol Oncol*, 5(2), Apr, pp. 137-149.

Heneka, M. T., Carson, M. J., El Khoury, J., Landreth, G. E., Brosseron, F., Feinstein, D. L., Jacobs, A. H., Wyss-Coray, T., Vitorica, J., Ransohoff, R. M., Herrup, K., Frautschy, S. A., Finsen, B., Brown, G. C., Verkhratsky, A., Yamanaka, K., Koistinaho, J., Latz, E., Halle, A., Petzold, G. C., Town, T., Morgan, D., Shinohara, M. L., Perry, V. H., Holmes, C., Bazan, N. G., Brooks, D. J., Hunot, S., Joseph, B., Deigendesch, N., Garaschuk, O., Boddeke, E., Dinarello, C. A., Breitner, J. C., Cole, G. M., Golenbock, D. T. and Kummer, M. P. (2015) 'Neuroinflammation in Alzheimer's disease.' *Lancet Neurol*, 14(4), Apr, pp. 388-405.

Hermida-Matsumoto, L. and Resh, M. D. (2000) 'Localization of human immunodeficiency virus type 1 Gag and Env at the plasma membrane by confocal imaging.' *J Virol*, 74(18), Sep, pp. 8670-8679.

Hu, W. T., Chen-Plotkin, A., Arnold, S. E., Grossman, M., Clark, C. M., Shaw, L. M., McCluskey, L., Elman, L., Karlawish, J., Hurtig, H. I., Siderowf, A., Lee, V. M., Soares, H. and Trojanowski, J. Q. (2010) 'Biomarker discovery for Alzheimer's disease, frontotemporal lobar degeneration, and Parkinson's disease.' *Acta Neuropathol*, 120(3), Sep, pp. 385-399.

Iadecola, C. (2004) 'Neurovascular regulation in the normal brain and in Alzheimer's disease.' *Nature Reviews Neuroscience*, 5(5), May, pp. 347-360.

Iadecola, C. (2013) 'The pathobiology of vascular dementia.' *Neuron*, 80(4) p. 10.1016/j.neuron.2013.1010.1008.

Ivey, N. S., MacLean, A. G. and Lackner, A. A. (2009) 'AIDS and the blood-brain barrier.' *Journal of neurovirology*, 15(2) pp. 111-122.

Jellinger, K. A. (2008) 'The pathology of "vascular dementia": A critical update.' *Journal of Alzheimers Disease*, 14(1) pp. 107-123.

Kapogiannis, D., Boxer, A., Schwartz, J. B., Abner, E. L., Biragyn, A., Masharani, U., Frassetto, L., Petersen, R. C., Miller, B. L. and Goetzl, E. J. (2015) 'Dysfunctionally phosphorylated type 1 insulin receptor substrate in neural-derived blood exosomes of preclinical Alzheimer's disease.' *FASEB J*, 29(2), Feb, pp. 589-596.

Ke, Q. and Costa, M. (2006) 'Hypoxia-Inducible Factor-1 (HIF-1).' *Molecular Pharmacology*, 70(5), November 1, 2006, pp. 1469-1480.

Kelleher, R. J. and Soiza, R. L. (2013) 'Evidence of endothelial dysfunction in the development of Alzheimer's disease: Is Alzheimer's a vascular disorder?' *Am J Cardiovasc Dis*, 3(4) pp. 197-226.

Koh, W., Mahan, R. D. and Davis, G. E. (2008) 'Cdc42- and Rac1-mediated endothelial lumen formation requires Pak2, Pak4 and Par3, and PKC-dependent signaling.' *Journal of Cell Science*, 121(7), 2008-04-01 00:00:00, pp. 989-1001.

Koh, W., Mahan, R. D. and Davis, G. E. (2008) 'Cdc42-and rac1-mediated endothelial lumen formation requires Pak2, Pak4 and Par3, and PKC-dependent signaling.' *Journal of Cell Science*, 121(7), Apr, pp. 989-1001.

Komiya, E., Sato, H., Watanabe, N., Ise, M., Higashi, S., Miyagi, Y. and Miyazaki, K. (2014) 'Angiomodulin, a marker of cancer vasculature, is upregulated by vascular endothelial growth factor and increases vascular permeability as a ligand of integrin alphavbeta3.' *Cancer Med*, 3(3), Jun, pp. 537-549.

Kovari, E., Charidimou, A., Herrmann, F. R., Giannakopoulos, P., Bouras, C. and Gold, G. (2015) 'No neuropathological evidence for a direct topographical relation between microbleeds and cerebral amyloid angiopathy.' *Acta Neuropathologica Communications*, 3, Aug 14,

Krupinski, J., Kaluza, J., Kumar, P., Kumar, S. and Wang, J. M. (1993) 'Some remarks on the growth-rate and angiogenesis of microvessels in ischemic stroke. Morphometric and immunocytochemical studies.' *Patol Pol*, 44(4) pp. 203-209.

Krupinski, J., Kaluza, J., Kumar, P., Kumar, S. and Wang, J. M. (1994) 'Role of angiogenesis in patients with cerebral ischemic stroke.' *Stroke*, 25(9), Sep, pp. 1794-1798.

Lamalice, L., Le Boeuf, F. and Huot, J. (2007) 'Endothelial cell migration during angiogenesis.' *Circulation Research*, 100(6), Mar 30, pp. 782-794.

Li, J., Duan, Y., Liu, R. W., Lam, K. S. and Jin, L. W. (2012) 'Alzheimer's disease drug candidates stabilize A-beta protein native structure by interacting with the hydrophobic core.' *Abstracts of Papers of the American Chemical Society*, 244, Aug 19,

Li, S. and Li, Q. (2014) 'Cancer stem cells and tumor metastasis (Review).' *International Journal of Oncology*, 44(6), Jun, pp. 1806-1812.

Lindl, K. A., Marks, D. R., Kolson, D. L. and Jordan-Sciutto, K. L. (2010) 'HIV-Associated Neurocognitive Disorder: Pathogenesis and Therapeutic Opportunities.' *Journal of Neuroimmune Pharmacology*, 5(3), 04/16

12/09/received

03/05/accepted, pp. 294-309.

Liuzzo, J. P., Ambrose, J. A. and Coppola, J. T. (2005) 'Sirolimus- and taxol-eluting stents differ towards intimal hyperplasia and re-endothelialization.' *J Invasive Cardiol*, 17(9), Sep, pp. 497-502.

Ma, L., Shao, Z., Wang, R., Zhao, Z., Dong, W., Zhang, J., Zhang, X., Sheng, S., Ji, Z. and Zhang, J. (2015) 'Rosiglitazone improves learning and memory ability in rats with type 2 diabetes through the insulin signaling pathway.' *Am J Med Sci*, 350(2), Aug, pp. 121-128.

Massiah, M. A., Starich, M. R., Paschall, C., Summers, M. F., Christensen, A. M. and Sundquist, W. I. (1994) 'Three-dimensional structure of the human immunodeficiency virus type 1 matrix protein.' *J Mol Biol*, 244(2), Nov 25, pp. 198-223.

Meadows, K. N., Bryant, P. and Pumiglia, K. (2001) 'Vascular endothelial growth factor induction of the angiogenic phenotype requires Ras activation.' *Journal of Biological Chemistry*, 276(52), Dec 28, pp. 49289-49298.

Minagar, A., Shapshak, P., Fujimura, R., Ownby, R., Heyes, M. and Eisdorfer, C. (2002) 'The role of macrophage/microglia and astrocytes in the pathogenesis of three neurologic disorders: HIV-associated dementia, Alzheimer disease, and multiple sclerosis.' *Journal of the Neurological Sciences*, 202(1-2), Oct 15, pp. 13-23.

Moya, E. M. G., Le Guelte, A. and Gavard, J. (2009) 'PAKing up to the endothelium.' *Cellular Signalling*, 21(12), Dec, pp. 1727-1737.

Munoz-Chapuli, R. (2011) 'Evolution of angiogenesis.' *Int J Dev Biol*, 55(4-5) pp. 345-351.

Nicosia, R. F. and Tuszynski, G. P. (1994) 'Matrix-Bound Thrombospondin Promotes Angiogenesis *in-Vitro*.' *Journal of Cell Biology*, 124(1-2), Jan, pp. 183-193.

Oddo, S., Caccamo, A., Shepherd, J. D., Murphy, M. P., Golde, T. E., Kayed, R., Metherate, R., Mattson, M. P., Akbari, Y. and LaFerla, F. M. (2003) 'Triple-transgenic model of Alzheimer's disease with plaques and tangles: Intracellular A beta and synaptic dysfunction.' *Neuron*, 39(3), Jul 31, pp. 409-421.

Olyslaegers, D. A. J., Desmarets, L. M. B., Dedeurwaerder, A., Dewerchin, H. L. and Nauwynck, H. J. (2013) 'Generation and characterization of feline arterial and venous endothelial cell lines for the study of the vascular endothelium.' *Bmc Veterinary Research*, 9, Aug 29,

Pfisterer, L. and Korff, T. (2016) 'Spheroid-Based *In Vitro* Angiogenesis Model.' *Methods Mol Biol*, 1430 pp. 167-177.

Popovic, M., Tenner-Racz, K., Pelser, C., Stellbrink, H. J., van Lunzen, J., Lewis, G., Kalyanaraman, V. S., Gallo, R. C. and Racz, P. (2005) 'Persistence of HIV-1 structural proteins and glycoproteins in lymph nodes of patients under highly active antiretroviral therapy.' *Proceedings of the National Academy of Sciences of the United States of America*, 102(41), Oct 11, pp. 14807-14812.

Prasansuklab, A. and Tencomnao, T. (2013) 'Amyloidosis in Alzheimer's Disease: The Toxicity of Amyloid Beta (Aβ), Mechanisms of Its Accumulation and Implications of Medicinal Plants for Therapy.' *Evidence-Based Complementary and Alternative Medicine*, 2013 p. 10.

Rambaran, R. N. and Serpell, L. C. (2008) 'Amyloid fibrils Abnormal protein assembly.' *Prion*, 2(3), Jul-Sep, pp. 112-117.

Revilla, S., Suñol, C., García-Mesa, Y., Giménez-Llort, L., Sanfeliu, C. and Cristòfol, R. (2014) 'Physical exercise improves synaptic dysfunction and recovers the loss of survival factors in 3xTg-AD mouse brain.' *Neuropharmacology*, 81, 6//, pp. 55-63.

Ryan, L. A., Zheng, J., Brester, M., Bohac, D., Hahn, F., Anderson, J., Ratanasuwan, W., Gendelman, H. E. and Swindells, S. (2001) 'Plasma Levels of Soluble CD14 and Tumor Necrosis Factor-α Type II Receptor Correlate with Cognitive Dysfunction during Human Immunodeficiency Virus Type 1 Infection.' *Journal of Infectious Diseases*, 184(6), September 15, 2001, pp. 699-706.

Sacharidou, A., Stratman, A. N. and Davis, G. E. (2012) 'Molecular mechanisms controlling vascular lumen formation in three-dimensional extracellular matrices.' *Cells Tissues Organs*, 195(1-2) pp. 122-143.

Sacktor, N. (2002) 'The epidemiology of human immunodeficiency virus-associated neurological disease in the era of highly active antiretroviral therapy.' *J Neurovirol*, 8 Suppl 2, Dec, pp. 115-121.

Sadowski, M., Pankiewicz, J., Scholtzova, H., Li, Y. S., Quartermain, D., Duff, K. and Wisniewski, T. (2004) 'Links between the pathology of Alzheimer's disease and vascular dementia.' *Neurochemical Research*, 29(6), Jun, pp. 1257-1266.

Sandberg, A., Luheshi, L. M., Söllvander, S., Pereira de Barros, T., Macao, B., Knowles, T. P. J., Biverstål, H., Lendel, C., Ekholm-Petterson, F., Dubnovitsky, A., Lannfelt, L., Dobson, C. M. and Härd, T. (2010) 'Stabilization of neurotoxic Alzheimer amyloid-β oligomers by protein engineering.' *Proceedings of the National Academy of Sciences of the United States of America*, 107(35), 08/16, pp. 15595-15600.

Sandberg, A., Luheshi, L. M., Sollvander, S., Pereira de Barros, T., Macao, B., Knowles, T. P., Biverstal, H., Lendel, C., Ekholm-Petterson, F., Dubnovitsky, A., Lannfelt, L., Dobson, C. M. and Hard, T. (2010) 'Stabilization of neurotoxic Alzheimer amyloid-beta oligomers by protein engineering.' *Proc Natl Acad Sci U S A*, 107(35), Aug 31, pp. 15595-15600.

Sanmarti, M., Ibanez, L., Huertas, S., Badenes, D., Dalmau, D., Slevin, M., Krupinski, J., Popa-Wagner, A. and Jaen, A. (2014) 'HIV-associated neurocognitive disorders.' *J Mol Psychiatry*, 2(1) p. 2.

Scaltriti, M. and Baselga, J. (2006) 'The epidermal growth factor receptor pathway: A model for targeted therapy.' *Clinical Cancer Research*, 12(18), Sep 15, pp. 5268-5272.

Smith, E. (2016) 'Vascular Cognitive Impairment.' *Continuum (Minneap Minn)*, 22(2 Dementia), Apr, pp. 490-509.

Spudich, S. and Gonzalez-Scarano, F. (2012) 'HIV-1-Related Central Nervous System Disease: Current Issues in Pathogenesis, Diagnosis, and Treatment.' *Cold Spring Harbor Perspectives in Medicine*, 2(6), Jun,

Talwar, P., Silla, Y., Grover, S., Gupta, M., Agarwal, R., Kushwaha, S. and Kukreti, R. (2014) 'Genomic convergence and network analysis approach to identify candidate genes in Alzheimer's disease.' *BMC Genomics*, 15 p. 199.

Tanzi, R. E. (2012) 'The Genetics of Alzheimer Disease.' *Cold Spring Harbor Perspectives in Medicine*, 2(10), October 1, 2012,

Tarasoff-Conway, J. M., Carare, R. O., Osorio, R. S., Glodzik, L., Butler, T., Fieremans, E., Axel, L., Rusinek, H., Nicholson, C., Zlokovic, B. V., Frangione, B., Blennow, K., Menard, J., Zetterberg, H., Wisniewski, T. and de Leon, M. J. (2015) 'Clearance systems in the brain-implications for Alzheimer disease.' *Nature Reviews Neurology*, 11(8), Aug, pp. 457-470.

Tian, J., Shi, J. and Mann, D. M. (2004) 'Cerebral amyloid angiopathy and dementia.' *Panminerva Med*, 46(4), Dec, pp. 253-264.

Tycko, R. and Wickner, R. B. (2013) 'Molecular Structures of Amyloid and Prion Fibrils: Consensus versus Controversy.' *Accounts of Chemical Research*, 46(7), Jul 16, pp. 1487-1496.

van Norden, A. G., van Dijk, E. J., de Laat, K. F., Scheltens, P., Olderikkert, M. G. and de Leeuw, F. E. (2012) 'Dementia: Alzheimer pathology and vascular factors: from mutually exclusive to interaction.' *Biochim Biophys Acta*, 1822(3), Mar, pp. 340-349.

Versaevel, M., Riaz, M., Corne, T., Grevesse, T., Lantoine, J., Mohammed, D., Bruyere, C., Alaimo, L., De Vos, W. H. and Gabriele, S. (2016) 'Probing cytoskeletal pre-stress and nuclear mechanics in endothelial cells with spatiotemporally controlled (de-)adhesion kinetics on micropatterned substrates.' *Cell Adh Migr*, Apr 25, p. 0.

Vieira, R. T., Caixeta, L., Machado, S., Silva, A. C., Nardi, A. E., Arias-Carrion, O. and Carta, M. G. (2013) 'Epidemiology of early-onset dementia: a review of the literature.' *Clin Pract Epidemiol Ment Health*, 9 pp. 88-95.

Vu, K., Weksler, B., Romero, I., Couraud, P. O. and Gelli, A. (2009) 'Immortalized Human Brain Endothelial Cell Line HCMEC/D3 as a Model of the Blood-Brain Barrier Facilitates *In Vitro* Studies of Central Nervous System Infection by Cryptococcus neoformans.' *Eukaryotic Cell*, 8(11), Nov, pp. 1803-1807.

Wang, X., Chen, Q. and Xing, D. (2012) 'Focal adhesion kinase activates NF-kappaB via the ERK1/2 and p38MAPK Pathways in amyloid-beta25-35-induced apoptosis in PC12 cells.' *J Alzheimers Dis*, 32(1) pp. 77-94.

Warren, J. D., Fletcher, P. D. and Golden, H. L. (2012) 'The paradox of syndromic diversity in Alzheimer disease.' *Nature Reviews Neurology*, 8(8), Aug, pp. 451-464.

Webster, S. J., Bachstetter, A. D., Nelson, P. T., Schmitt, F. A. and Van Eldik, L. J. (2014) 'Using mice to model Alzheimer's dementia: an overview of the clinical disease and the preclinical behavioral changes in 10 mouse models.' *Frontiers in Genetics*, 5, 04/23

02/21/received

04/01/accepted, p. 88.

Weksler, B., Romero, I. A. and Couraud, P.-O. (2013) 'The hCMEC/D3 cell line as a model of the human blood brain barrier.' *Fluids and Barriers of the CNS*, 10(1) pp. 1-10.

Wilson, S. L., Ahearne, M. and Hopkinson, A. (2015) 'An overview of current techniques for ocular toxicity testing.' *Toxicology*, 327, Jan 2, pp. 32-46.

Wolfe, M. S. (2012) 'The Role of Tau in Neurodegenerative Diseases and Its Potential as a Therapeutic Target.' *Scientifica*, 2012 p. 20.

Zhao, X. and Guan, J. L. (2011) 'Focal adhesion kinase and its signaling pathways in cell migration and angiogenesis.' *Adv Drug Deliv Rev*, 63(8), Jul 18, pp. 610-615.

Zhou, L. and Saksena, N. K. (2013) 'HIV Associated Neurocognitive Disorders.' *Infect Dis Rep*, 5(Suppl 1), Jun 6, p. e8.

Zlokovic, B. V. (2005) 'Neurovascular mechanisms of Alzheimer's neurodegeneration.' *Trends Neurosci*, 28(4), Apr, pp. 202-208.

APPENDIX 1.

HIV patient's clinical information

ICTUS	AGE	SEX	CARDIOVASCULAR RISK FACTORS	CT-SCAN	Origin	Treatments
A-29-94	60	M	SMOKING, VHC, VIH DETECTED ONLY 3 MONTHS PRIOR TO DEATH, PNEUMONIA, BRAIN OEDEMA, TOXOPLASMOSIS	THALAMIC HIPODENSE MASS	caucasian	no HIV treatment
A-35-08	31	M	NONE	ABCESS RIGHT BASAL GANGLIA	african	no HIV treatment
A-11-59	49	M	HTA, DIABETES, ISHAEMIC HEART DISEASE, CAROTID ATEROMATOSIS, STENT RIGHT INTERNAL CAROTID	MRI: FRONTO-TEMPORO-PARIETAL STROKE	caucasian	combivir, reyataz, norvir

APPENDIX 2.

Brief description of the major behavioural testing

Animals are normally tested for changes of non-cognitive and cognitive behaviour from 2 weeks after hippocampal injections on a daily basis for around 2 weeks.

Sensorimotor responses: Visual reflex and posterior legs extension reflex can be determined by holding an animal by the tail and lowering it vertically towards a black surface. Motor coordination and equilibrium are then assessed by measuring the distance covered and the time taken to fall from a horizontal wooden rod or a metal wire rod. Prehensility and motor coordination are measured by the wire hang test, - distance covered from the middle of a horizontal wire using its forepaws for 5-60 second trials.

Corner test: Neophobia of a new home-cage is often used to assess this and involves placing the animal in the centre of a square cage (35 x 35 x 25 cm) and counting the number of corners visited and rearings over a period of 30 s. The latency of the first rearing is also recorded.

Open field test: Rodents can be placed in the centre of a home-made, white, box approximate dimensions-55 x 55 x 25 cm high, and observed for 5 min. Horizontal locomotor activity (distance covered and direction patterns) and vertical movement (rearings) are then analysed throughout the test. Note is usually taken of specifics such as initial freezing, self-grooming behaviour and the number of urination events/ defecation boli.

Dark and light box test: Anxiety can be measured in a dark-light box. The apparatus consists of two compartments connected by an opening (approximately 7 x 7 cm). The rodents would be introduced into the black compartment and observed for 5 min. The time taken to enter the lit compartment, and in addition, the time spent within the lit compartment and the number of rearing's is recorded.

Boissier's four hole-board test: Exploration of the rodent is measured here e.g. by the number of head-dips and time spent head-dipping on each of four holes spaced equally in the floor of the board. The time taken for movement, first dipping and four hole dipping is measured.

Tail suspension test: Mice are suspended by the tail 30cm above a surface to assess depression-like behaviour. The tail is fixed with adhesive tape approximately 1 cm from its tip. The duration of immobility (no movement only respiration) is then scored during 6 min.

Object recognition test: Animals are placed in the middle of a black maze and objects to be discriminated - usually made of wood (5-6 cm high, brightly coloured) shown to them. A 10 min acquisition trial is firstly carried out during which the mouse is placed in the maze in the presence of two identical novel objects one on each side. Retentive ability is carried out 2 h later, replacing object A' in the maze by object B. Later object A in the maze is replaced with object C. The time that the mouse spends exploring the new objects and the old objects is recorded. The maze and the objects are usually cleaned with ethanol between experiments to eliminate olfactory cues.

Morris water maze test: Animals can be tested here for spatial learning and memory using the Morris water maze (MWM). Mice are taught the location of a hidden underwater platform over a six day period (10 cm diameter, located 20 cm from the wall and 0.5 cm below the water surface) in a circular pool using opaque water, and enclosed with black curtains. The mouse will find the platform by relying on distinctive landmarks as visual cues on day seven, the platform will be removed and the mice undergo a 60 second trial to test for retention of learning. A computerized tracking system – video analysis enables the measurement of distance covered during the learning tasks etc.